Modeling pathological consequences of astrocytic tauopathy

Dissertation der Fakultät für Biologie

der Ludwig-Maximilians-Universität München

Vorgelegt von

Katrin Pratsch

geboren in Wien

München, 2022

Diese Dissertation wurde angefertigt
unter der Leitung von Prof. Dr. Jochen Herms
im Bereich der translationalen Hirnforschung
an der Ludwig-Maximilians-Universität München
und von Prof. Dr. Heinrich Leonhardt
an der Fakultät für Biologie vertreten.

Erstgutachter:	Prof. Dr. Heinrich Leonhardt
Zweitgutachterin:	Prof. Dr. Anja Horn-Bochtler
Tag der Abgabe:	15.06.2022
Tag der mündlichen Prüfung:	30.01.2023

EIDESSTATTLICHE VERSICHERUNG

Ich versichere hiermit an Eides statt, dass meine Dissertation selbständig und ohne unerlaubte Hilfsmittel angefertigt worden ist. Die vorliegende Dissertation wurde weder ganz, noch teilweise bei einer anderen Prüfungskommission vorgelegt. Ich habe noch zu keinem früheren Zeitpunkt versucht, eine Dissertation einzureichen oder an einer Doktorprüfung teilzunehmen.

München, den 15.06.2022

_____

Katrin Pratsch

Declaration

All experiments for this thesis were conducted at the Ludwig-Maximilians-University Munich under the supervision of Prof. Dr. Jochen Herms.

For the project, Katrin Pratsch performed the experimental procedures. Gian Marco Calandra was involved in the analysis of the astrocytic Ca^{2+} transients. The viral vector production department of EPFL Lausanne was involved in the production of the experimental tau virus.

Gewidmet meinem Großvater

Johann Pratsch Sen.

Index

Summary

Tau is a microtubule-associated protein that interacts, stabilizes and promotes the assembly of microtubules. In the healthy brain it undergoes several post-translational modifications, including phosphorylation. During neurodegeneration, misfolding and hyperphosphorylation lead to aberrant aggregation of tau filaments in the brain, which is a pathological hallmark of tauopathies. Tau is highly expressed in neurons but also to a lesser extent in astrocytes. Astrocytes, along with neurons, are an important cell type in the central nervous system and exert various functions in maintaining brain homeostasis. One important role includes the regulation and modulation of synaptic function, mediated by the fine processes of astrocytes which form connections with thousands of neuronal synapses. Astrocytes are also implicated to play a role in the development of tauopathies. Several tauopathies are characterized by astrocytic inclusions of tau. While the toxic effects of tau aggregation in neurons have been extensively studied, much less is known about the pathological mechanisms of astrocytic tau inclusions. Therefore, this thesis focuses on the investigation of pathophysiological consequences of an astrocytic tauopathy. A virus-inducible mouse model of astrocytic tauopathy was developed and characterized, that expresses the human P301S tau mutation of frontotemporal dementia in Aldh1l1 astrocytes throughout the central nervous system. The first aim of this thesis involved an *in vivo* approach to investigate Ca^{2+} signaling in cortical astrocytes. Two-photon astrocytic Ca^{2+} imaging revealed a hyperactive phenotype of Ca^{2+} transients in astrocytic microdomains. The increased firing frequency indicates that astrocytic Ca^{2+} levels in the fine processes are disrupted in mice with astrocytic tauopathy. The second aim of this thesis was to elucidate the effect on neuronal synapses. By using a quantitative immunohistochemical approach, an overall excitatory synapse loss could be observed in both pre- and postsynaptic compartments of somatosensory cortical neurons. These results imply a contribution of tau in astrocytes to the pathophysiology and progression of tauopathies. Therapeutic interventions should therefore also take into account the aspect of astrocytic influence on

neurodegenerative processes and may consider astrocytic tau as a potential target for future treatment approaches.

Zusammenfassung

Tau ist ein Protein, welches verantwortlich für den Aufbau und die Stabilität von Mikrotubuli ist. Im gesunden Gehirn durchläuft dieses Protein posttranslationale Modifikationen, darunter die Phosphorylierung. Bei neurodegenerativen Prozessen führen jedoch eine Fehlfaltung und Hyperphosphorylierung zu einer abnormen Aggregation von Tau Filamenten im Gehirn, welches ein pathologisches Merkmal von so genannten Tauopathien ist. Tau wird in hohem Maße in Neuronen, aber auch zu geringem Umfang in Astrozyten exprimiert. Astrozyten sind neben Neuronen ein wichtiger Zelltyp im Zentralnervensystem und üben verschiedene Funktionen zur Aufrechterhaltung der Gehirnhomöostase aus. Eine wichtige Rolle ist die Regulierung und Modulation der synaptischen Transmission, da ihre feinen Ausläufer Verbindungen mit Tausenden von neuronalen Synapsen bilden. Astrozyten spielen demnach auch eine Rolle bei der Entstehung von Tauopathien. Einige Tauopathien sind durch astrozytäre Einschlüsse von Tau gekennzeichnet. Während die toxischen Auswirkungen einer Tau Aggregation in Neuronen umfassend erforscht werden, ist über die pathologischen Mechanismen astrozytärer Tau-Einschlüsse weit weniger bekannt. Daher konzentriert sich diese Thesis auf die Untersuchung der pathophysiologischen Folgen einer astrozytären Tauopathie. Dazu wurde ein virusinduzierbares Mausmodell der Astrotauopathie entwickelt und charakterisiert, welches die P301S-Tau Mutation der frontotemporalen Demenz in Aldh1l1-Astrozyten im zentralen Nervensystem exprimiert. Das erste Ziel dieser Studie umfasste einen *in vivo* Ansatz zur Untersuchung der Ca^{2+} Transienten in kortikalen Astrozyten. Die Ca^{2+} Bildgebung mittels 2-Photonen Fluoreszenzmikroskopie zeigte einen hyperaktiven Phänotyp von Ca^{2+} Transienten in astrozytären Mikrodomänen. Die erhöhte Frequenz deutet darauf hin, dass Ca^{2+} Signale in den feinen astrozytären Fortsätzen bei Mäusen mit

astrozytärer Tauopathie gestört sind. Das zweite Ziel dieser Studie war es, den Einfluss auf neuronale Synapsen aufzuklären. Durch Immunfluoreszenzuntersuchungen an Gehirnschnitten der Mäuse wurde ein umfassender Verlust an exzitatorischen Prä- und Postsynapsen im somatosensorischen Kortex festgestellt.

Diese Ergebnisse deuten auf eine Beteiligung von Tau in Astrozyten zum Fortschreiten von Tauopathien hin. Zukünftige therapeutische Ansätze sollten daher auch den Aspekt des astrozytären Einflusses auf neurodegenerative Prozesse berücksichtigen und könnten astrozytäres Tau als potenzielles Ziel für neue therapeutische Interventionen in Betracht ziehen.

1 Introduction

1.1 Microtubule-associated protein tau

1.1.1 Tau structure and expression

First described in 1975, tau is a microtubule-associated protein (MAPT) that plays an essential role in the stabilization of microtubules in axons [1]. The human *MAPT* gene is located on the long arm of chromosome 17 (17q21) and contains 16 exons [2]. During the transcription process, the pre-mRNA undergoes alternative splicing, giving rise to different isoforms. In the central nervous system (CNS) splicing events happen on exon 2, 3 and 10. Those isoforms can be distinguished depending on the number of N-terminal inserts from splicing exons 2 and 3 (0N,1N,2N) and the repeat sequences in the microtubule binding region (MTBR), from splicing exon 10 (3R, 4R) (Figure 1) [3], [4]. The expression of those isoforms is highly regulated during development. In the adult human CNS all six tau isoforms are expressed, ranging from 352 to 441 amino acids (aa) [5]. In the fetal brain, only the smallest isoform of 352 aa (N0R3) is expressed.

Unlike humans, the tau gene in mice is located on chromosome 11 and slightly shorter in length. In contrast to the human brain, the adult murine brain solely contains tau including exon 10, resulting in the presence of only three isoforms (0N4R, 1N4R, 2N4R) [6]–[8]. Differences in the protein structure are mainly found in the N-terminal region, which contains 11 aa less in mice than in humans. The lack of this sequence may imply to influence some tau related functions [9].

In recent decades, through the development of more sensitive detection methods, tau mRNA has been found also in other tissues but it is most abundant in the CNS [10], [11].

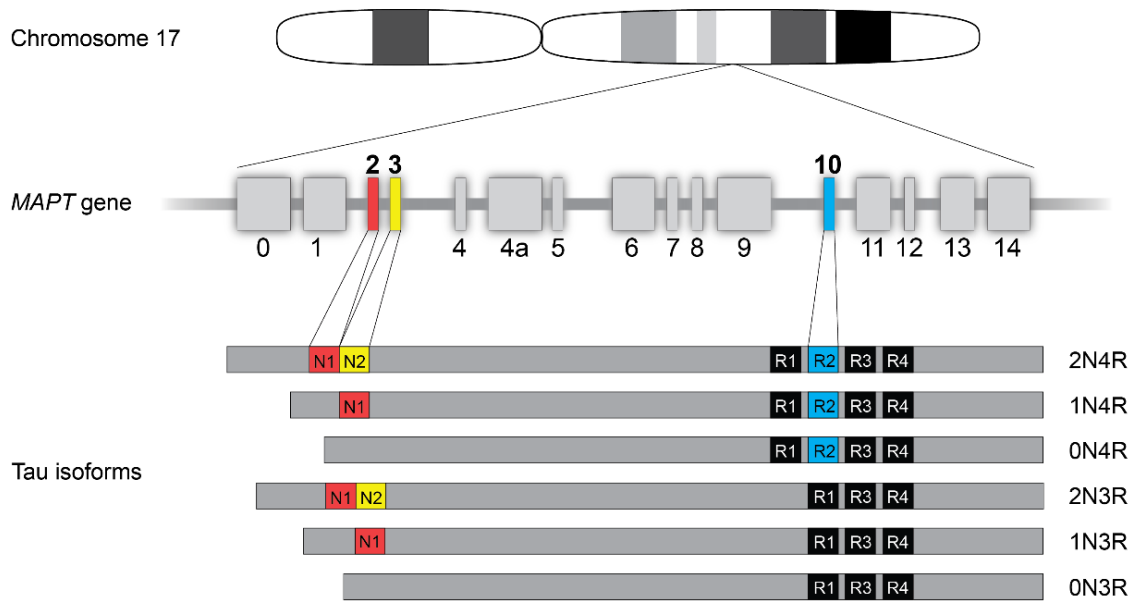

Figure 1. Human *MAPT* gene and generation of tau isoforms. In the human central nervous system, the *MAPT* gene is located on Chromosome 17 and contains 16 exons. Through alternative splicing of exons 2 (red box), 3 (yellow box) and 10 (blue box), six different isoforms can be generated. They contain three or four repeats (3R or 4R) with either zero, one or two inserts (0N-2N). All six isoforms exist in the adult human brain, whereas in the fetal brain, only the shortest isoform 0N3R is expressed.

In the brain, tau is mainly expressed in the axonal compartment of neurons, but also to a small extent in oligodendrocytes and astrocytes [12]–[15]. Tau is an intrinsically disordered protein with the propensity to change conformation upon interaction with other proteins. Besides its natively unfolded character, a study using fluorescence resonance energy transfer (FRET) found that tau monomers in solution preferably form a so called “paperclip” conformation, where the C- and N-terminal domains approach each other by folding on the repeat region [16]. Upon binding to microtubules, tau adopts an open conformation, in which the C-terminus strongly binds to the microtubule while the N-terminal end projects away, suggesting a role in spacing between microtubules (Figure 2) [17], [18].

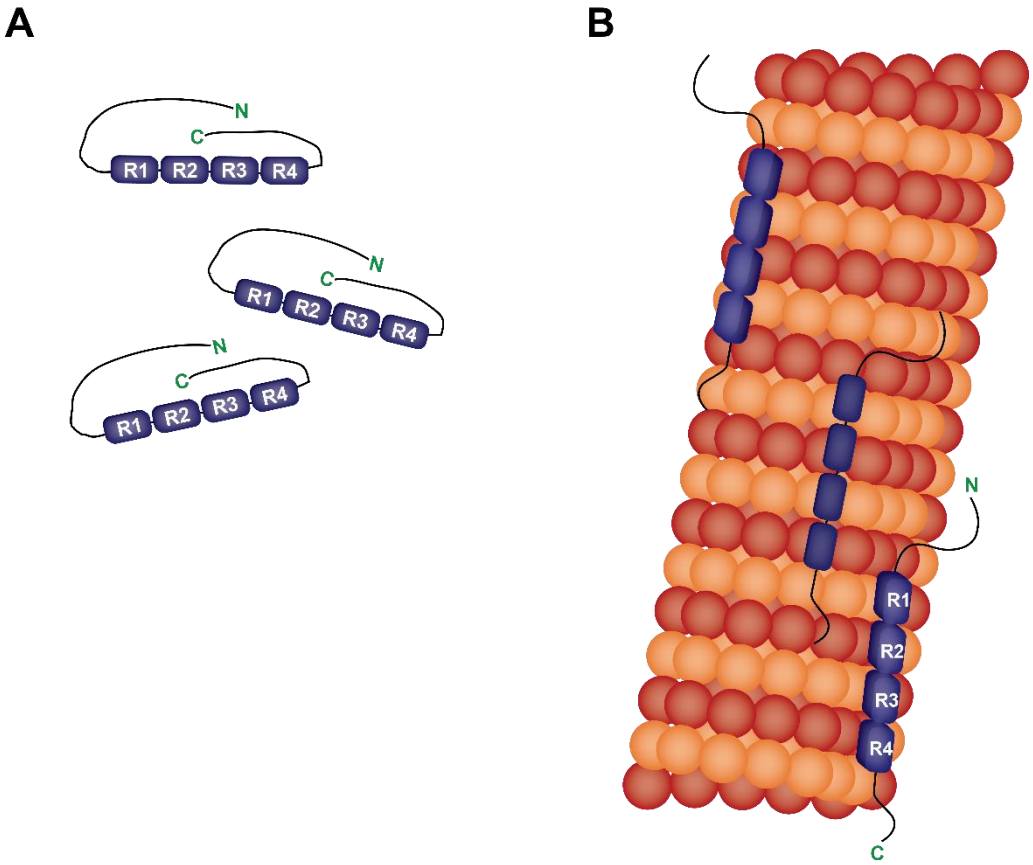

Figure 2. Tau in solution and bound to microtubules. A) Tau in solution adopts a so called "paperclip" formation. The C-terminus folds close to the MTBR and the N-terminus folds onto the C terminal portion, bringing both ends close together. B) Tau changes to an open conformation when bound to microtubules.

1.1.2 Function in normal physiology

Tau is mainly involved in the stabilization of microtubule bundles in axons. The protein prevents depolymerization processes of microtubules by hindering tubulin rings on both ends to dissociate [19]. Microtubules are part of the cellular cytoskeleton, maintaining cell integrity and motility by dynamic assembly and disassembly of tubulin dimers (so called "dynamic instability"). In neurons, tau tightly binds to microtubules through the C-terminal located MTBR, promoting their assembly by tubulins, stabilization, and dynamic processes [4], [20], [21]. The MTBR also contains the four repeat sequences. 4R tau has a higher binding affinity to microtubules compared to 3R tau, therefore those isoforms prevent

disassembly of microtubules more effectively [22], [23]. Another functional aspect is the involvement of tau in axonal transport. A study of mice overexpressing P301L tau showed that this mutation leads to a reduced binding ability to microtubules, which results in a faster anterograde axonal transport of mitochondria. Therefore, destabilization of microtubules might be the cause for changes in mitochondria transport [24]. In contrast, elevated tau levels are postulated to disrupt axonal vesicle trafficking, implying a role of tau for regulation of axonal transport [25]. Studies suggest that tau also has a functional role in synaptic physiology [26], [27]. A knock down of endogenous tau in the hippocampus of adult mice with AAV-ShRNATau showed a reduction of synaptic spine density, leading to an impairment in spatial learning and memory, as well as deficits in motor coordination. By halting the expression of the ShRNA, those effects could be reversed [28]. These results support the assumption that tau plays a role in physiological synaptic function.

Studies in tau deficient mice further showed altered cerebral oscillation patterns, suggesting a role of tau for maintaining synchronization between brain regions and for the sleep-wake cycle [29], [30]. Chronic sleep deprivation in humans increases tau levels in the CSF [31], reinforcing the statement that tau has a role in sleep. Other physiological roles of tau are still under investigation. Because tau undergoes multiple alternative splicing events and occurs in different isoforms, these could play specific roles for different cell types and brain regions, but this remains to be elucidated [32].

1.1.3 Tau phosphorylation and implications in pathophysiology

After translation, tau undergoes several modifications, including phosphorylation, ubiquitination or oxidation [33]. Tau can be phosphorylated at over 80 different serine, threonine and tyrosine residues by multiple kinases, most of them in physiological conditions, but several are only found in neurodegenerative diseases. A major tau kinase is the cycline-dependent kinase 5 (Cdk5). Cdk5 preferentially phosphorylates Ser/Thr-Pro sequences [34], from which 16 exist in tau [35].

In the healthy brain, a balance is maintained between kinases and phosphatases to regulate phosphorylation. A disruption of this equilibrium is thought to be a predecessor for neurodegeneration, starting with increased phosphorylation (hyperphosphorylation) of tau and followed by the formation of aggregates [36]. Most of the phosphorylation residues are found in regions flanking the microtubule-binding domains [37]. The phosphorylation status of tau plays therefore an important role for regulating microtubule stability and assembly [38]. Newer studies further determined that phosphorylation at different sites can also affect tau conformation and promoting activation of distinct signaling pathways that modulate fast axonal transport of organelles [39]. Further, phosphorylation at Ser199, Ser202, and Thr205 was shown to increase the space between microtubules and affect mitochondrial transport along the axon [40]. Those residues are found to be hyperphosphorylated in neurodegenerative diseases, like Alzheimer's disease (AD) and can be recognized by the monoclonal antibody AT8 [41].

Although tau is also found in dendrites, a massive accumulation and mislocalization to the cell body and dendritic compartments is an early pathological event in neurodegeneration. A study has shown that treatment with amyloid-beta (Aβ) oligomers leads to missorting of tau into dendritic regions and increased phosphorylation, ultimately resulting in synapse loss *in vitro* [42]. Thus, tau phosphorylation may also determine its cellular localization, but this needs to be further explored.

Over the past years, extensive research has been made to investigate the pathophysiological role of tau in the CNS. Tau is involved in the development of several neurodegenerative and psychological diseases. Although tau diseases vary greatly in their appearance, a common trait is the hyperphosphorylation of tau, leading to the formation and accumulation of insoluble filaments in the brain [38]. Yet, it is still unclear which phosphorylation sites are responsible for the formation of aggregates and their specific role for disease development [43]. A certain class of such neurodegenerative diseases are even named after its causing protein – the tauopathies.

1.2 Tauopathies

Neurodegenerative diseases comprise a group of disorders that are characterized by an inevitable degeneration of the nervous system, ultimately leading to nerve cell death. A clinically heterogeneous class of neurodegenerative disorders are tauopathies, which can be classified by a massive neuronal and/or glial accumulation of misfolded filaments of tau. Diseases with that phenotype can be categorized into either a primary or a secondary tauopathy. In primary tauopathies, intracellular tau inclusions are the predominant feature. In secondary tauopathies, massive accumulation of another protein in addition to tau pathology is significant for the progression of neurodegenerative processes. A prominent example from the latter is AD, whose pathological hallmarks include the extracellular deposition of Aβ in the brain, as well as the formation of neurofibrillary tau tangles.

As this thesis focuses on aspects of primary tauopathies, the neuropathological phenotypes of this particular class are described in greater detail in the following chapter.

1.3 Primary tauopathies

1.3.1 Classification and clinical heterogeneity

The most characteristic feature of primary tauopathies is the substantial accumulation of fibrillized tau in neurons and/or glial cells. Primary tauopathies can occur sporadically, but can also be hereditary [44]. In the late nineties, mutated tau was identified as the first gene for being the causative agent for a hereditary form of Frontotemporal Dementia (FTD) with parkinsonism linked to chromosome 17 (FTDP-17) [7], [45]–[47]. To date, over 60 different mutations in the tau gene were identified causing FTD syndromes [48], [49]. Other tauopathies like progressive nuclear palsy (PSP), Corticobasal degeneration (CBD), Pick’s

Disease (PiD) and globular glial tauopathy (GGT) typically occur spontaneously, but rare cases have been found in family members carrying *MAPT* mutations [50].

The clinical manifestations of primary tauopathies are very heterogeneous. The symptoms often involve dysfunctions in movement, language, cognition/behavior and memory [51]. As the disease profiles are phenotypically so diverse, an accurate diagnosis can be difficult. It is important to differentiate which cell types are affected, the distribution of tau inclusions in different brain areas, the predominating tau isoform, as well as the co-occurrence of other pathological proteins [52]. In families with a history of *MAPT* mutations, the pathophenotype can vary between and even within families with the same mutation, which further complicates the diagnosis process [53].

Tauopathies can be further classified in 3R and 4R tauopathies. In the healthy brain both isoforms are expressed in equal amounts. This equilibrium can be disturbed in some diseases. In a pathological state, 3R or 4R tau can be predominating. 3R tau is mainly found in PiD, whereas 4R is outweighing the 3R isoform in PSP, CBD, GGT and argyrophilic grain disease (AGD) [54]. It is implicated that the haplotype of tau may contribute to that imbalance. Two different haplotypes of tau exist (H1 and H2), which differ in the inversion of a 900 kb sequence in chromosome 17 (including the tau sequence) and the deletion of a base pair sequence upstream of exon 10 in H2 [55]. The H1c subhaplotype is postulated to preferentially express 4R tau [56], and this subtype is found predominately in patients with 4R tauopathies, suggesting that the haplotype may be another risk factor for the development of 4R tauopathies. Also, mutations in exon 10 in the tau gene were found to be responsible for a disturbed equilibrium of 3R and 4R tau by altering its splicing ability, leading to an increased production of 4R tau [57].

1.3.2 Mutations in the *MAPT* gene

In the healthy brain, phosphorylation at serine and threonine sites in the MTBR modulates binding dynamics to microtubules [58]. Mutations in those regions can

lower the ability of tau to bind to microtubules and lead to a loss/altered protein function [59], [60]. Free tau species have a higher propensity to hyperphosphorylate, making them more prone to form β-sheet conformations, which leads to an aggregation into neurofibrillary tangles (NFT) [61]. Missense, deletion, intronic or silent mutations are described to appear in different tauopathies [44]. In particular, the missense mutations P301L and P301S that are found in FTD patients have become of scientific interest. They are located in Exon 10, thus only affecting 4R tau isoforms [62]–[64].

Clinically, patients carrying a P301S mutation develop a more aggressive form of FTD and have an earlier disease onset than carriers of P301L. The mean age of disease onset is 33.7 years in P301S patients, with an average duration of 4.2 years. Patients with a P301L mutation have a later disease onset and a longer disease duration (52.6 years and 6.7 years, respectively) [65], [66]. For this thesis the P301S mutation is of interest, therefore it is described in more detail in the following chapter.

1.3.3 P301S *MAPT* mutation

The P301S mutation is the result of an amino acid substitution from Proline to Serine through a change at codon 301 from CCG to TCG. As the mutation appears in exon 10, it increases the propensity of tau to aggregate and reduces the ability to bind to microtubules [67]–[69]. This mutation was first described in a Dutch family that suffered from a hereditary, early-onset FTD (~20-30 years of age) with parkinsonian features. The patients developed a rapidly progressive degeneration in the frontal lobe with early onset dementia, language disturbances and a rapid decline in motor movement [70]. The same mutation was also described in other families, with varying clinical symptoms [71], [72]. One family is described carrying a P301S mutation, but resulting in different disease diagnosis, either FTD or CBD. Hyperphosphorylated tau inclusions were observed in neurons, astrocytes and oligodendrocytes of these patients [71].

Because of its aggressive character and the ability to form filaments, this mutation is widely used in *in vitro* and *in vivo* animal models for dementia research [73]–[77]. Transgenic mice overexpressing P301S tau develop a neuropathological phenotype with tau hyperphosphorylation subsequently formation of filaments that resemble the neurodegenerative processes in cases of FTD [73], [78]. A newer study with a mouse model expressing P301S, but lacking the hexapeptide motifs - which are needed for heparin-induced filament formation - exhibited a normal life span and showed no signs of neurodegeneration. P301S tau with those deletions did not form β-sheet structures after heparin incubation, suggesting that preceded β-sheet assembly of P301S tau is necessary to form filaments, followed by neurodegeneration [79].

Yet still unclear is the impact of different cell types for the development and progression of tauopathies. In some tauopathies, tau inclusions are predominately observed in neurons, others are described with varying amounts of additional glial tauopathy. Familial cases of FTD with a *MAPT* mutation were described with tau deposits in neurons, but also in astrocytes [7], [62]. One case study presented two sisters with a behavior variant of FTD exhibiting a predominant Astrotauopathy, with only minor amounts of neuronal tau inclusions [80]. Therefore, the contribution of astrocytes for disease development of tauopathies should not be underestimated.

1.4 Astrocytes

Astrocytes, besides microglia, oligodendrocytes, and ependymal cells, belong to the class of glial cells and are found in the CNS. Glia were historically first described by pathologist Rudolf Virchow in the 1850s as “nerve glue” (“Nervenkitt”), a connective tissue, that solely maintains nerve cell structure [81]. In the late 19th century Camillo Golgi investigated glial cells for the first time in more detail, and was the first to describe astrocytic end feet [82]. Finally, the term astrocyte (“star-shaped cell”) was described in 1891 [83] and researchers began to decipher more and more functions of this cell type.

Traditionally, astrocytes were classified into two morphological classes: protoplasmic and fibrous astrocytes. Protoplasmic astrocytes have an extensive amount of fine processes and are abundant in the cortical gray matter, whereas fibrous astrocytes are less ramified with long processes and mainly found in white matter tracts [84], [85]. But also several other specialized astrocytes were described, like radial glia (e.g. Bergmann glia in the cerebellum), vellate astrocytes or surface-associated astrocytes [86], [87]. Newer research suggests a high heterogeneity in astrocytes with specific intra-regional cellular functions within and between different brain regions in the human and mouse brain [88], [89].

Mature astrocytes are highly ramified cells with numerous thin processes that occupy certain non-overlapping domains in the brain [90]. Astrocytes carry out many different functions in the healthy brain, including the maintenance of the blood-brain-barrier [91], the formation and regulation of synaptic connections [92]–[94], the regulation of extracellular neurotransmitters and ions [95] and guiding mechanisms [96], [97].

One specific role of astrocytes is the interaction with neuronal synapses. They mainly function through their peripheral astrocytic processes (PAP), where they preferentially enwrap the pre- and postsynaptic connections of neurons [98]. Those processes are extremely fine (<50 nm) therefore they are smaller than

microscopic resolution, and account for around 75 % of the cell volume [90], [99], [100]. Only the advances of electron microscopy (EM) in recent years made it possible to uncover more details about their synaptic connections [101], [102]. Not only PAPs are enwrapping neuronal synaptic terminals but also primary astrocytic processes and the soma can form connections with synapses [103]. In addition, not all processes are covering synapses, but connecting or withdrawing from them depending on activity, which makes them highly plastic structures [98], [104]. The whole concept of the connection of astrocytic processes with both synaptic compartments is also termed the "tripartite synapse" [105].

1.4.1 The concept of the Tripartite synapse

The name tripartite synapse refers to the concept of the close structural and functional association between astrocytes and the pre- and postsynaptic compartments of neurons. In addition to the bilateral information exchange between the neuronal pre- and postsynapse, astrocytic processes also form a close connection with both synaptic terminals (Figure 3) [106]. It is estimated that one astrocyte in the human cerebral cortex can cover up to two million synapses [107]. Through their close synaptic proximity, they maintain neurotransmitter and ion homeostasis, they release neuromodulators to regulate synaptic function [108], [109] and they provide lactate as an energy source to neurons [110], [111].

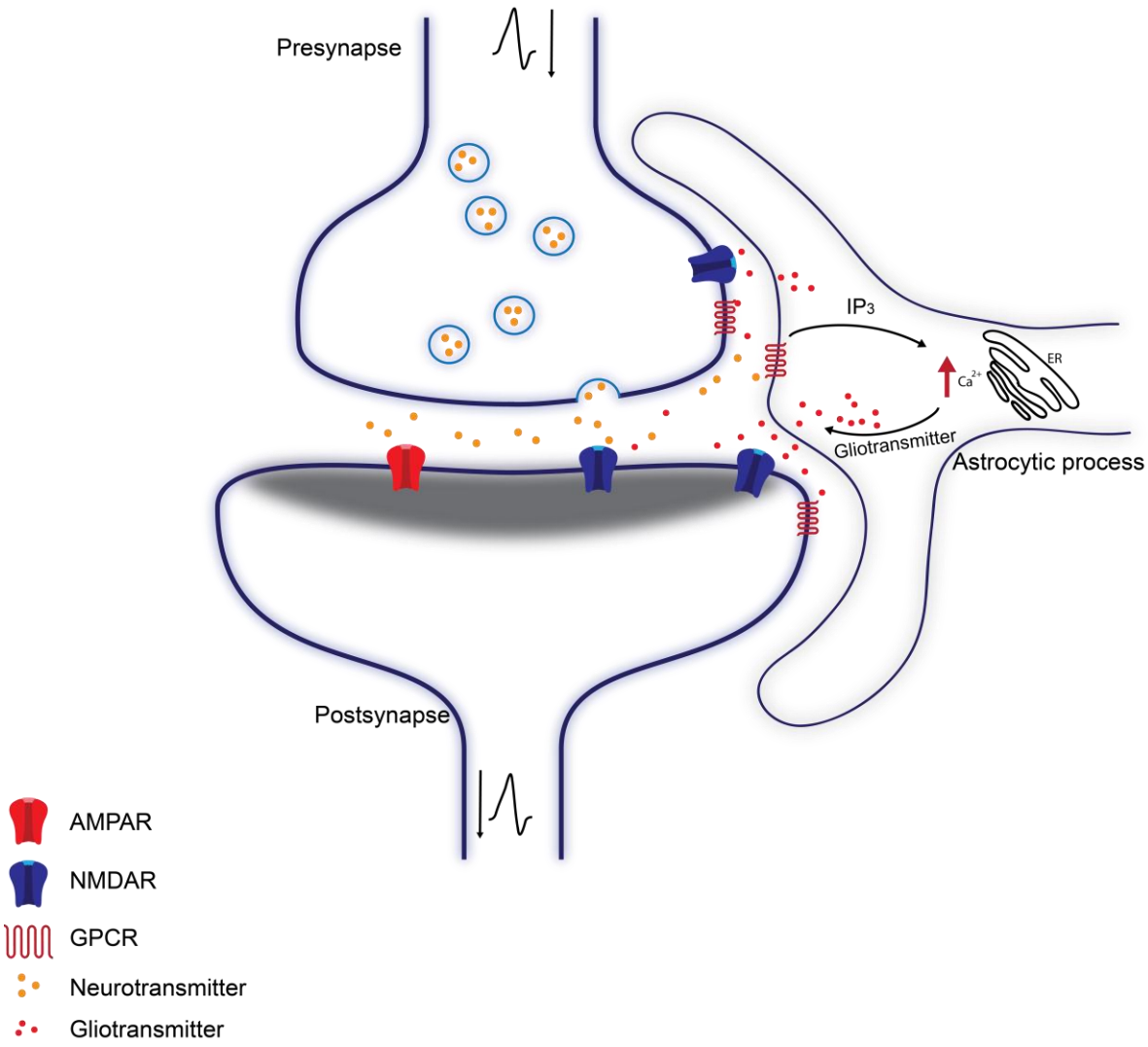

Figure 3. Simplified schematic of the tripartite synapse: Bidirectional communication between the pre- and postsynapse with astrocytic processes. Upon neurotransmission synaptic vesicles are released from the presynaptic terminal. Released neurotransmitters (orange) bind to receptors in the postsynaptic membrane but can also bind to receptors located on the astrocytic processes. Upon binding to G-protein coupled receptors (GPCRs) on the astrocytes, internal IP_3 leads to an increase of internal astrocytic Ca^{2+} from the endoplasmic reticulum (ER). The elevated Ca^{2+} levels trigger the release of gliotransmitters (red) via different pathways, which - when bound to their respective synaptic receptors - modulate synaptic transmission.

Upon synaptic activity, astrocytes are stimulated by neurotransmitters via metabotropic or ionotropic receptors located in perisynaptic processes. Astrocytes express specific receptors for neurotransmitters such as adenosine

triphosphate (ATP), gamma-Aminobutyric acid (GABA), glutamate or endocannabinoids [112]–[115]. Glutamate is a major excitatory neurotransmitter in the brain and an important signal molecule in astrocytes [116]. Glutamate released from the presynapse stimulates metabotropic glutamate receptors (mGluR), which upon activation stimulates phospholipase C activity and the formation of inositol 1,4,5-triphosphate (IP_3). IP_3 in turn binds to respective intracellular receptors located in the membrane of the endoplasmic reticulum (ER), leading to a release of Ca^{2+} from internal stores [117]–[119]. The elevated astrocytic Ca^{2+} levels trigger the release of neuroactive substances, so called gliotransmitters [120]. These gliotransmitters, including glutamate, GABA, ATP or D-serine among others, can bind to their corresponding receptors on the neuronal synapse and modulate synaptic transmission and firing frequency [121]–[123].

Gliotransmitter release can take place through different pathways, like vesicular exocytosis, channel-mediated diffusion or through plasma membrane transporters [124]–[126]. Each gliotransmitter acts on different neuronal pathways. Released glutamate binds to NMDA receptors, which elicits inward membrane currents and synchronizes action potential firing [127]–[129]. GABA, glutamate and ATP regulates synaptic vesicle release in the presynapse, therefore controlling synaptic strength [113], [130], [131].

1.4.2 Calcium signaling in astrocytes

Unlike neurons, astrocytes are not electrically excitable, their cellular activity depends on internal fluctuations of calcium levels [132]. Since the discovery that glutamate evokes a rise in astrocytic internal Ca^{2+} concentrations [133], [134], it is believed that astrocytic Ca^{2+} transients are another factor influencing neuronal signaling in the CNS. In earlier years, research focused only on Ca^{2+} transients happening in the astrocytic soma and main processes [135], later the development of genetically encoded calcium indicators (GECIs) made it possible to investigate also spatially restricted near-membrane Ca^{2+} transients in the PAPs, so called microdomains, in greater detail [136], [137]. Microdomain events occur more frequently than somatic events and may arise through IP_3 dependent

as well as IP_3 independent pathways [138], [139]. Ca^{2+} microdomains are very heterogeneous and can occur in response to synaptic activity but also in absence of it. Different signaling pathways may underlie the mediation of microdomain transients, which may lead to distinct astrocyte functions. Newer findings show that astrocytic Ca^{2+} microdomains can exhibit fast kinetics in a similar timescale as neurons, which are evoked by local synaptic activity [140]. Those confined transients in the PAPs may play a role in the localized delivery of gliotransmitters to influence neuronal transmission [141]. Astrocytic Ca^{2+} generated in single cells can also propagate between the astrocytic network in Ca^{2+} waves, enabling an activation of a large population of cells [142], [143]. One way this propagation of Ca^{2+} waves can be achieved is by gap junctions. These gap junctions between astrocytes thus allow an intercellular communication and the formation of a complex network in the CNS.

1.4.3 Astrocytic influence on brain functions

The development of cutting-edge techniques made it possible to investigate astrocytic functions in greater detail. Through targeted genetic manipulation of astrocytes, their impact on other cell types and higher brain functions can be elucidated [120].

Astrocytes play an important role for regulating synaptic function. Several astrocyte secreted factors are reported to be essential for synapse formation and stabilization [144]. This includes the control of presynaptic release probability of neurotransmitters and postsynaptic strength. For the latter it was found that the modulation of glutamatergic NMDA and AMPA receptor abundance in the postsynapse can be achieved via the secretion of factors like tumor necrosis factor-α or thrombospondins [145], [146]. Therefore astrocytes also play a role in long term potentiation (LTP) and long term depression (LTD) in neurons by regulating synaptic strength in response to neuronal activity [94].

Astrocytes were also found to be involved in cholinergic processing of visual inputs, hippocampal oscillatory activity and whisker stimulation, suggesting they may play a role in higher cognitive functions and memory processing [147], [148].

Studies with mice lacking AMPA receptors in Bergmann glia of the cerebellum show deficits in fine motor coordination, indicating a role of glutamatergic gliotransmission for the functional integrity of cerebellar networks and for adjusting neuronal processes underlying motor behavior [149]. Other gliotransmitters such as D-serine, ATP and adenosine are implicated to play a role in sleep homeostasis by modulating slow brain oscillations. Mice with inhibited gliotransmission exhibited longer periods of wakefulness through a decrease of cortical slow oscillations and an accumulation of sleep pressure [150], [151].

Astrocytes also play a role in brain energy metabolism. They take up glucose, store it either as glycogen or metabolize it to lactate, which can then be released into the extracellular space, fueling neuronal energy demands in an activity-dependent manner. Glucose can also travel intercellularly through the vast astrocytic network by gap junctions. This process is disrupted upon AMPA receptor inhibition, suggesting an involvement of postsynaptic mechanisms in recruiting astrocytic metabolic coupling [110], [152]. Especially under high neuronal activity this coupling mechanism is important for maintaining glutamatergic synaptic transmission.

1.5 Astrocytes in primary tauopathies

Astrocytes not only perform certain tasks in the healthy brain. They also undergo changes in pathological conditions. In case of an injury or a disease in the CNS, astrocytes can enter a reactive state (reactive gliosis) in which they change their morphology, alter gene expression and their metabolism [153]–[155]. Astrocytes are a key element in the pathogenesis of primary tauopathies. Reactive gliosis and neuroinflammation are common in tauopathy patients [156], [157]. However, the most characteristic element is the abundance of aberrant astrocytes in primary tauopathies. Disease-specific types can be distinguished, such as tufted astrocytes (TA) in PSP, astrocytic plaques in CBD, ramified astrocytes in PiD, granular-fuzzy astrocytes in age related tau astrogliopathy and several other unnamed types common in FTD-tau [158]. A common trait of those astrocyte types is the massive intracellular accumulation of hyperphosphorylated AT8 positive tau, also referred to as astrotauopathy.

1.5.1 Astrotauopathy

In the brain, tau is predominantly expressed by neurons and localized in the axonal compartment, where it contributes to the assembly and stabilization of microtubules. Under pathological conditions aberrant tau is aggregating and forming NFTs that accumulate in neurons. However, in primary tauopathies mutated and hyperphosphorylated tau inclusions are also or predominantly found in astrocytes [158].

Astrocytic tau inclusions found in brains of patients with most sporadic primary tauopathies are composed of 4R tau isoforms. In contrast, astrocytes of PiD patients contain mainly 3R tau [159]. In FTLD-tau cases, most of the astrocytic tau inclusions are of 4R isoforms, depending on the tau mutation [51].

In recent years, researchers could recapitulate several tauopathies with distinct astrocytic tau inclusions by using different mouse models. Studies with a mouse model expressing P301S under a neuron specific Thy1.2 promoter found not only phospho-tau accumulation on neuronal cells [160], but also in astrocytes at

12 months of age [161]. Another study found that intracerebral injection of pathological tau extracted from brains of patients with different tauopathies into WT mice recapitulates the corresponding human disease. Inoculation with different tau strains induced unique cellular tau distribution. Accumulation of tau in neurons as well as glial tau inclusions were found, depending on the specific seed used [162]. A follow-up experiment of the same group revealed that the formation of glial tau aggregates does not depend on neuronal tau, suggesting that glial tau pathology has functional consequences, independent of neuronal tau [163].

Astrotauopathy ultimately leads to functional consequences in neurons, as astrocytes closely engage with neuronal synaptic terminals. In the pathological human brain, astrocytic tau pathology can contribute to synapse loss in CBD, suggesting a possible role of astrocytes for cognitive decline in patients [164]. *In vitro* studies show that astrocytes derived from P301S mice lack molecules to regulate glutamate homeostasis and lose the capacity to support neuronal survival which may explain neuronal loss in this mouse model [165]. Another study using mice expressing the same tau mutation, but under the astrocyte-specific glial fibrillary acidic protein (GFAP) promoter revealed an age dependent accumulation of glial tau with similar astrocytic morphology as seen in human tauopathies. Transgenic mice exhibited TAs, astrocytic plaques and thread pathology that resemble PSP and CBD astrocyte morphology. Further, astrocytic tau pathology led to axonal degeneration with myelin disruption [166].

However, still unknown are functional effects of astrocytic tau inclusions *in vivo*, especially for astrocytic Ca^{2+} signals, the influence on neuronal synapses and their overall contribution to pathophysiological mechanisms in the brain.

1.6 Two-photon *in vivo* imaging

The advance of microscopy techniques brought researchers to a whole new dimension of imaging structures to understand complex biological processes. Traditional optical microscopy uses a single-photon of a particular wavelength to excite a fluorophore [167]. However, this technique is limited due to a poor tissue penetration depth (<100 µm), phototoxicity and light scattering which blurs the image [168], making it unsuitable to image living systems. With the development of two-photon excited fluorescence laser scanning microscopy, the disadvantages of single-photon microscopy have been drastically improved.

1.6.1 Principles

Using this technique, fluorophore excitation arises from absorbing two photons near-simultaneously in one single event. These photons are of a longer wavelength and have half the energy as compared to a corresponding single photo event, so they are only sufficient to elicit a photon by exciting simultaneously [169].

Those photons need to arrive in a timescale of an attosecond (10^{-18} seconds) [170]. To increase the probability that two photons get absorbed at the same time, an immense photon flux is needed. Therefore sample illumination is provided by an ultra-short pulsed laser, like a mode-locked titanium-sapphire (Ti:Sapphire) laser. Such lasers can achieve pulses of around 100 femtosecond with a pulsing rate of ~80-100 MHz [171], [172].

1.6.2 Advantages

Two-photon laser excitation has several advantages over single-photon microscopy. First, a deeper imaging depth can be reached through the use of longer excitation wavelengths (deep red and near infrared), for example >400 µm for imaging mouse brains *in vivo* [173]. Longer wavelengths are scattered and absorbed less by living tissue [174], as compared to conventional confocal microscopy where scattered emitted photons lead to a higher tissue background

in the sample, thus making it unsuitable to reach a deeper tissue depth. Second, fluorescence excitation is limited to the plane of focus, due to the generation of an optical section of a sample. Without out-of-plane fluorescence, there is no phototoxicity of surrounding tissue and therefore no need of a pinhole as commonly used in confocal microscopy [175]. All those advantages make two-photon microscopy perfectly suitable to image biological samples *in vivo*.

1.6.3 *In vivo* astrocytic Ca^{2+} imaging

Calcium is a ubiquitous second messenger for mediating intracellular processes. Astrocytes exhibit a certain excitability to interact with other cells by an increase in intracellular Ca^{2+} levels in response to synaptic activity [176], [177]. The development of genetically encoded calcium indicators (GECIs) opened a whole new spectrum to measure Ca^{2+} dynamics in the brain [178], [179]. GCaMPs are a family of GECIs that are comprised of a single circularly permutated enhanced green fluorescent protein (cpEGFP), flanked by the M13 peptide from myosin light-chain kinase and calmodulin (CaM). Ca^{2+} binds with a high affinity to CaM, leading to intramolecular conformational changes in the cpEGFP, which in turn affects the fluorophore intensity (dim and bright state) (Figure 4) [180]–[182].

Over the past years, constant improvements in sensitivity, fluorescence intensity and specific subcellular targeting were made, creating enhanced GECIs like GCAMP6f with fast rise and decay dynamics [183]–[185]. GECIs can be genetically targeted to specific tissues by using viral vectors [186] or in transgenic mice [187], [188].

Advances in two-photon microscopy made it possible to study astrocytic Ca^{2+} transients *in vivo*. By using a cranial window, Ca^{2+} signals can be investigated in cortical layers in the living organism [189], [190]. To study distinct Ca^{2+} signals in astrocytic intracellular compartments, new GCamPs were developed, either targeted to the cytosol (cyto-GCamP) to detect somatic Ca^{2+} signals or with a membrane-tethered domain (lck-GCamP) for detecting Ca^{2+} fluctuations in microdomains [136], [137], [191].

Most of the Ca^{2+} transients occur in the microdomains of very fine processes [192]–[194] and are rather short (<2 s) [195], [196], therefore a membrane-targeted lck-GCamP6f was used in this thesis to study Ca^{2+} dynamics in the astrocytic microdomains.

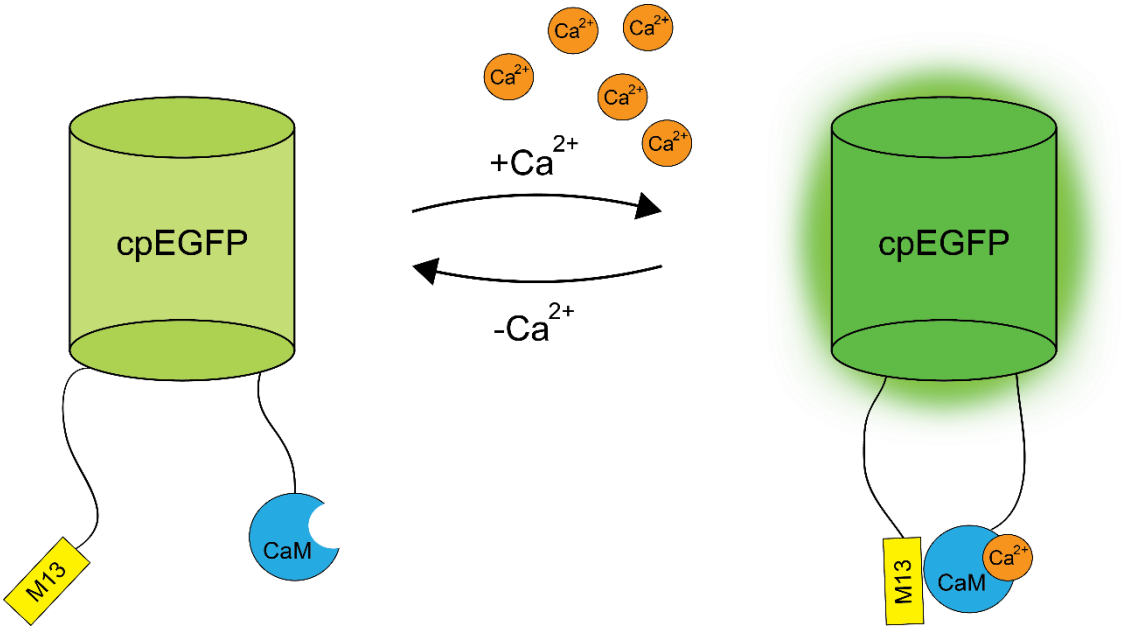

Figure 4. Schematic representation of the GCamP signaling cascade. A circularly permutated enhanced green fluorescent protein (cpEGFP) is connected to a Ca^{2+} binding protein calmodulin (CaM) and a CaM binding M13 fragment of myosin light chain kinase. Ca^{2+}-dependent intramolecular conformational changes lead to the binding of CaM to the M13 domain, which is followed by changes in the spectral properties of the cpEGFP chromophore and thus modifying its fluorescence intensity to a bright state.

1.7 Aim of thesis

The aim of this thesis is to elucidate the pathophysiological role of tau in astrocytes. While the toxic effects mediated by pathological neuronal tau deposits have been extensively studied, the implications of astrocytes carrying pathological tau and the effects on surrounding cells are still poorly understood. Astrocytes are important cells that actively contribute to neuronal transmission and higher brain functions, and abundant astrocytic tau inclusions in several neurodegenerative diseases raises the question whether astrocytic tau deposits contribute to the progression of those diseases. To answer this question a mouse model was generated, expressing mutated tau selectively in astrocytes by utilizing a viral approach. *In vivo* two-photon functional Ca^{2+} imaging and immunohistochemical approaches were applied to decipher the impact of mutated tau on astrocytic function and consequences on surrounding cells.

2 Material and Methods

2.1 Transgenic mouse lines and husbandry

All experiments were performed with the mouse (*mus musculus*) as model system.

2.1.1 Aldh1l1-cre/ERT2

Aldh1l1-cre/ERT2 mice express a ligand dependent Cre recombinase (CreERT), which is targeted to the majority of Aldh1l1 astrocytes. [188] (Stock No 029655; Jackson Laboratory, USA). After application of the synthetic estrogen receptor ligand tamoxifen, Cre recombinase is translocated into the nucleus and activated, therefore allowing temporal and tissue specific control of Cre activation. Once translocated, Cre recombines DNA sequences flanked by LoxP sequences (flox), which leads to an expression, excision or exchange of any transgene exclusively in Cre positive astrocytes. This mouse line was maintained as a heterozygous colony.

2.1.2 Husbandry

Mice were bred in the in-house mouse facility at the Center for Neuropathology and Prion Research, Munich. Mice were housed in individually ventilated cages with a floor area of 530 cm^2 (Ehret) under specific and opportunistic pathogen free (SOPF) conditions, with a 12 hour light/dark cycle. The animals were provided *ad libitum* with standard food pellets (Ssniff, Germany) and water. At three weeks of age, the mice were given unique identification numbers by ear punches, and the removed tissue biopsies were stored for later genotyping purposes. They were housed in small groups until cranial window surgery, after which they were housed separately to avoid damage on the surgery site. All experiments were conducted in accordance with the animal welfare guidelines of the government of upper Bavaria and were approved under the animal experiment application number 55.2-2532.Vet_02-19-114.

2.2 Genotyping

The mouse DNA was extracted from ear biopsies and samples were amplified by polymerase chain reaction (PCR) to detect the respective genotype.

2.2.1 DNA extraction

First, the DNA was extracted with a mouse genotyping kit (Quanta Biosciences) regarding the manufacturers protocol. Briefly, 50 µl of Extraction Reagent was mixed with the tissue samples and heated to 95°C for 30 minutes on a Thermomixer heating block (Eppendorf). After a short cooling step, 50 µl of Stabilization Buffer was added. The DNA extracts were stored at 4°C until further processing.

2.2.2 PCR amplification

After the extraction step, the mouse DNA was amplified by PCR. Extracted template DNA samples were mixed with specific primers (Merck) and amplified in a thermocycler (Eppendorf). Mouse line specific PCR mixtures and thermocycler programs are listed below. Subsequently, 8 µl of DNA ladder (NEB, New England BioLabs) and amplified sample DNA were loaded onto an agarose gel mixed with SYBR™ Safe DNA Gel Stain (Invitrogen) and fragments were separated by gel electrophoresis (120 V, ~1 h). The separated DNA bands were then visualized under UV light to identify the right mouse genotypes.

Cre recombinase (Aldh1l1-cre/ERT2)

Transgene detected at **200 bp** and **350 bp**

	NAME	LENGTH (BP)	TEMPERATURE (°C)
PRIMERS	Cre-F	21	68,4
	Cre-R	20	68,4
	MT3-F	23	71,6
	MT3-R	23	76,9

	PRODUCT	VOLUME (µl)
MASTER MIX (25 µL STOCK)	OneTaq HotStart Quickload, (Neb) (x2 mm)	12,5
	Cre-f	1
	Cre-r	1
	MT3-F	1
	MT3-R	1
	Template DNA	2
	H_2O	6,5

	STEP	TEMPERATURE (°C)	TIME	REPEAT
PCR CYCLING	1	94	2 min	1x
	2	94	30 sec	35x
	3	58	40 sec	35x
	4	72	40 sec	35x
	5	72	3 min	1x
	6	10	unlimited	

2.3 Viral Vectors and production

2.3.1 pAAV hMAPT P301S

A custom-designed viral vector was purchased from Vectorbuilder (USA). The vector has floxed inserts for recombinant human microtubule-associated protein tau (hMAPT) carrying the P301S mutation and mKate2 far-red fluorophore reporter (derived from *Entacmaea quadricolor*) under a ubiquitous chicken β-actin hybrid (CBh) promoter. The virus was produced and evaluated *in vitro* at the EPFL Lausanne in scope of a collaboration.

2.3.2 Control Vector

The same vector, only expressing the mKate2 fluorophore served as control. Vector and ready-to-use virus were purchased from Vectorbuilder (USA).

2.3.3 GCamP6f calcium indicator

For astrocytic Ca^{2+} imaging, a membrane tethered GCAMP6f virus was used (AAV2/5.GfaABC1D.Lck-GCaMP6f, #52924, Penn Vector, Philadelphia, PA).

2.3.4 Adeno-associated virus (AAV) production and *in vitro* validation

Plasmid DNA of the pAAV hMAPT P301S was amplified in *Escherichia coli* (DH10B) and the AAV was generated by plasmid transfection of HEK293 cells. Briefly, HEK293 cells were plated in DMEM (Gibco) + 10 % FBS, 1 % ampicillin. On the next day they were transfected using the CaPO4 method with the transgene of interest, the pRepCap and the pHelper. After incubation of six hours the media was replaced by serum free media Episerf (Gibco). After three days, cells were harvested by trypsinization (Trypsine-EDTA, Gibco) and lysed. The virus was finally purified using an iodixanol gradient and ion exchange chromatography according to standard procedures, viral particle concentration was determined using qPCR and the virus was frozen down in 10 µl aliquots at - 80°C until needed. For *in vitro* validation, a western blot was performed of the

HEK293 cells transfected with either virus construct and Cre transgene, Cre only, construct only or non-transfected cells. 30 µg of protein was loaded in each lane. HT7 antibody at a dilution of 1:2500 was used to detect total human tau and β-tubulin antibody at a dilution of 1:10.000 was used as loading control.

2.4 Intravenous Virus injection

The virus was administered via injection into the lateral tail vein. Briefly, 2-3 months old mice were restrained in a custom made restrainer from a 50 ml Falcon tube. The lateral tail vein was detected using a fiber optic illuminator lamp. The virus suspension was diluted in 1x phosphate buffered saline (PBS) and injected into the blood stream with a 30G needle, at a concentration of either $1x10^{11}$ vector genomes (vg) or $1x10^{12}$ vg.

2.5 Tamoxifen administration

To induce cell-specific activation of Cre recombinase in Aldh1l1-cre/ERT2 mice, Tamoxifen was administered. Mice were injected intraperitoneal (i.p.) with Tamoxifen (Sigma) dissolved in Miglyol (Caesar & Loretz) at a dose of 75 mg/kg body weight for five consecutive days.

2.6 Surgery procedures

2.6.1 Cranial window implantation

Mice were deeply anesthetized with a combination of Ketamine (0,13 mg/g body weight, bela-pharm GmbH & co.KG) and Xylazine (0,01 mg/g body weight, Bayer) i.p.. After a waiting period of around 10 minutes, the toe was firmly pinched to evaluate the anesthesia depth (toe pinch reflex). To prevent postoperative

infections and pain, Enrofloxacin (Baytril, 5mg/kg body weight, Bayer) and Carprofen (Rimadyl, 4mg/kg body weight, Zoetis) were administered subcutaneously (s.c.). After an appropriate anesthesia depth was reached (absence of toe pinch reflex), the head was fixed in a stereotactic frame (World Precision Instruments), and placed on a heating pad to maintain body temperature during the whole procedure. The eyes were prevented from drying out by applying a drop of Bepanthen ointment (Bayer). All surgery tools were sterile and disinfected prior to surgery.

First, the head was shaved and the scalp was disinfected thoroughly with 70 % Ethanol (EtOH) (Figure 5 and Table 1). A small piece of scalp was removed with scissors. Remaining connective tissue was scratched off and the skull was roughened with a scalpel (Swann-Morton). To prevent the later applied dental cement from falling off, the skull was further roughened by applying iBond® self etch adhesive (Kulzer). The etching reaction was stopped after 20 seconds with a polymerization lamp (Kerr Demi Plus, Kerr Corporation). A circle with a diameter of four mm was marked over the somatosensory region with a Biopsy Punch (KAI Medical). The marking was then drilled into the skull with a dental drill (Schick). The bone flap was removed and a drop of PBS was applied on top of the skull opening to prevent the brain from drying out. Then, the dura mater was gently removed with a sharp forceps (Fine science tools, FST) and any occurring bleedings were stopped immediately using Gelfoam (Pfizer). Afterwards, a round cover glass with a diameter of four mm (VWR) was placed on top of the skull opening and sealed with Vetbond tissue adhesive (3M). The surrounding skin was also sealed with tissue adhesive, to prevent inflammation. The skull was then covered with dental composite (Ivoclar Vivadent) and a custom built metal z-bar was placed and sealed onto the skull, using the same composite. The dental cement was hardened with a polymerization lamp. After surgery, the mice were placed back into their home cage, resting on a heating pad until they recovered from the anesthesia. Mice were allowed to have a recovery period of around one month to ensure that the cranial window is clear before imaging sessions started.

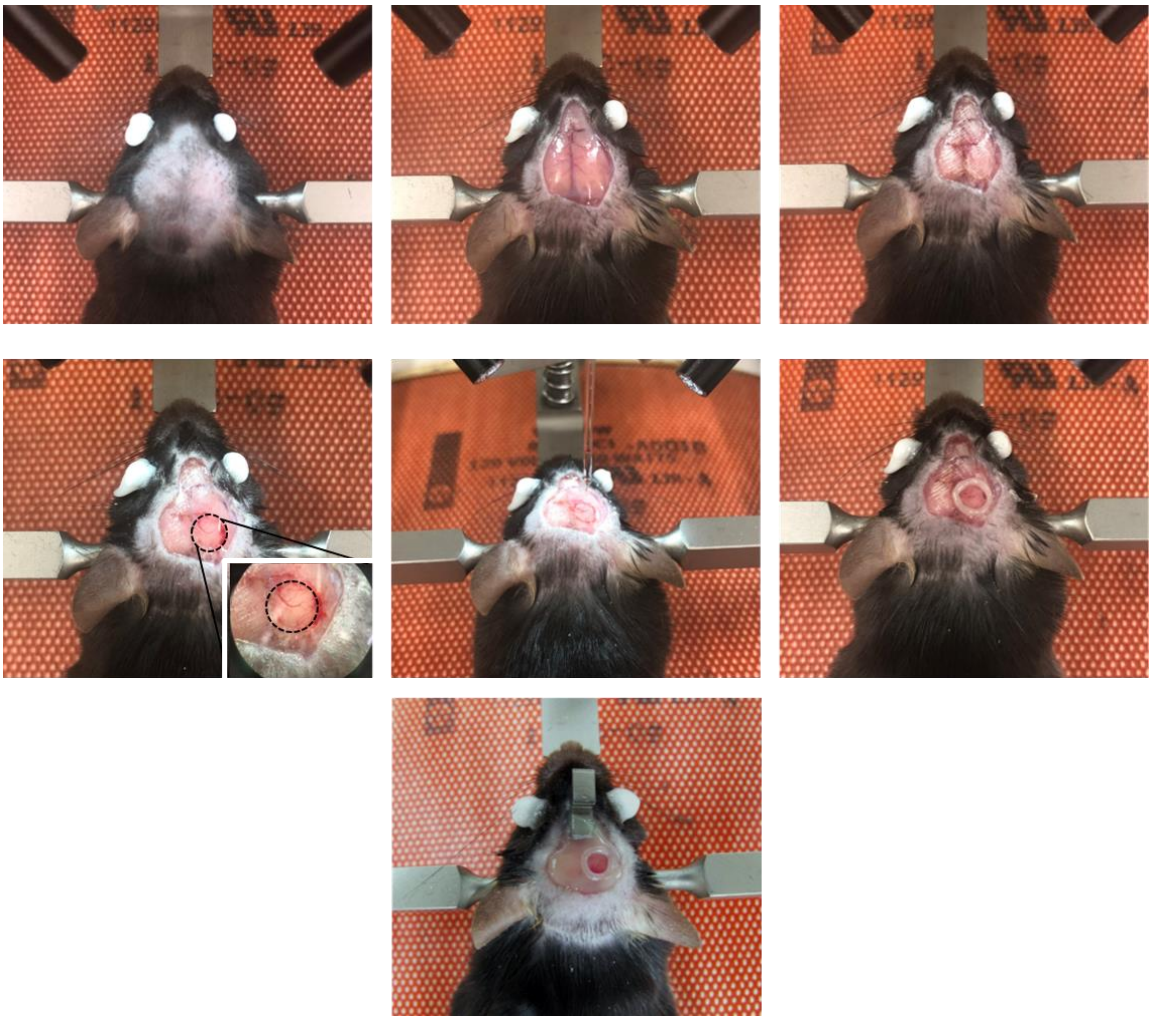

Figure 5. Mouse cortex surgery procedure and intracranial virus injection. After reaching appropriate anesthesia depth, the mouse head was shaved and a piece of scalp was removed. The skull surface was roughened and a circular window was drilled into the skull (small inset). After opening the skull, the dura mater was carefully removed. For stereotactic virus injections, a small glass needle filled with virus suspension was inserted into the cortex. The hole was sealed with a cover glass and covered with dental composite. A small metal z-bar was attached to the skull for head repositioning in subsequent imaging sessions.

Table 1. List of tools used for the cranial window surgery.

TOOL	MANUFACTURER
1x PBS	Gibco
70 % EtOH	Sigma
Sterile cotton tip applicators	NeoLab
Sugi eyespear pointed tip	Kettenbach
Bepanthen eye ointment	Bayer
Gelfoam absorbable gelatin sponge	Pfizer
Vetbond tissue adhesive	3M
IBond® self etch	Kulzer
Pasteur pipette	A. Hartenstein
Tetric evoflow dental cement	Ivoclar Vivadent
Pulled glass capillary	World Precision Instruments
Dental drill	Henry Schein
Sterile single use scalpel	Swann Morton
Round glass window Ø4 mm	WPI (custom order)
Biopsy Punch Ø4 mm	KAI Medical
Sterile scissors	FST
Forceps with sharp tip	FST
Forceps with bent tip	FST
Blunt forceps	FST
Metal z-bar	Custom-made
Stereotaxic frame	Neurostar
Nanoliter Injector	WPI
Stereodrive Software	Neurostar

2.6.2 Stereotactic virus injection

For stereotactic injections, after opening the skull (as previously described) a pulled glass needle (World Precision Instruments, WPI) was inserted into the brain (~300 µm below the cortex surface) (Figure 5, middle panel). 300 nl of an astrocyte specific GCAMP6f virus suspension (1:10 dilution in PBS) was slowly injected into the brain at two to three different positions with a rate of 30 nl per minute, using a nanoliter injector (Neurostar). After injection, the cranial window implantation was continued, as described previously.

2.7 Two-photon *in vivo* astrocytic Ca^{2+} imaging

The imaging sessions started one month after cranial window surgery and stereotactic virus injection (Figure 6). Mice were imaged using a LSM 7MP two-photon microscope, equipped with a femtosecond laser (Mai Tai DeepSee, Spectra Physics) and a water-immersion objective (20x, NA = 1.0, Carl Zeiss Microscopy). The astrocytic Ca^{2+} imaging was performed under light anesthesia. Mice were sedated with Medetomidin (Domitor, 0,5 mg/kg, Orion Corporation), positioned in a custom made head holder by using the metal z-bar and placed on a heating pad to maintain body temperature. Then, the eyes were covered in Bepanthen eye ointment to prevent from drying out. The left leg was shaved and a pulse oximeter sensor (MouseOx Plus, Starr Life Sciences Corp., Oakmont, PA, USA) was attached to the thigh, providing a strong signal from the femoral artery to monitor vital sings. Throughout the imaging session mice received 0,5 % Isoflurane in 95 % O_2 and 5 % CO_2. The average breath and heart rate were monitored with the pulse oximeter attached to the left thigh. Only images acquired under the same anesthesia depth were taken for further analysis, in order to compare between the groups (breath rate between 80-100 breaths per minute, brpm, and heart rate between 150-250 beats per minute, bpm). The laser was tuned to 920 nm and time-lapse image series were acquired from GCaMP6f positive regions of interest (ROIs) in layers I-II of the somatosensory cortex. Each ROI (75 x 75 µm) was recorded for four minutes at a rate of 4,17 Hz and contained

spontaneous Ca^{2+} transients from microdomains. After each imaging session, which lasted maximum one hour, mice were brought back into their home cage on a heating pad until they recovered.

2.7.1 Analysis of Ca^{2+} transients

Prior to analysis, the *in vivo* Ca^{2+} signals were pre-processed. First, the image series were motion corrected to remove moving artifacts by using the NoRMCorre algorithm in Python [197]. Afterwards background noise was subtracted. Then, the Ca^{2+} transients, size, area and activity from individual microdomains were detected and extracted by using FASP software in Image J/FIJI [198]. For baseline alignment of Ca^{2+} transients, python based software Scipy was used. Then the extracted traces were analyzed with python based software Stimfit and Ca^{2+} kinetics and frequency were calculated [199].

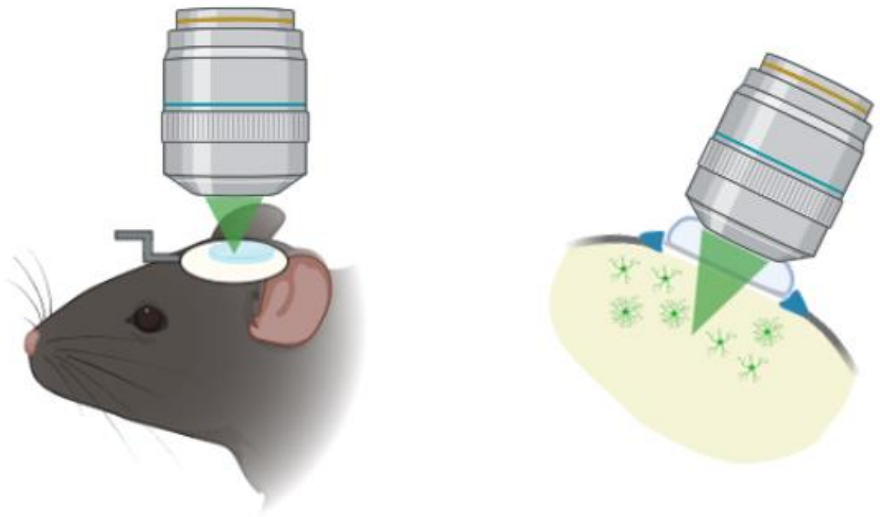

Figure 6. *In vivo* imaging scheme with a cranial window. Mice were imaged through a cranial window placed over the somatosensory cortex. Mice were positioned in a custom made head holder and different ROIs containing GCaMP expressing astrocytes were imaged subsequently. Schematic was created with BioRender.com.

2.8 Transcardial perfusion

For perfusions, mice were deeply anesthetized with a combination of Ketamine (0,13 mg/g body weight) and Xylazine (0,01 mg/g body weight) diluted in NaCl. After reaching appropriate anesthesia depth, mice were fixed on a Styrofoam plate and the abdomen was opened until reaching the diaphragm. The diaphragm and thorax were then opened. A butterfly needle was inserted into the left heart ventricle and the right auricle was cut to let the blood flow out. Mice were first perfused using 1x PBS for 5 min to clean the blood circuit from remaining blood cells, following 4 % paraformaldehyde (PFA) solution (Roti Histofix, Carl Roth) for five min to fix the tissue. After perfusion, the skull was opened carefully with scissors and the brain was removed. The brain was post-fixed with 4 % PFA overnight at 4°C, then transferred in 1x PBS with 0,05 % NaN_3 and stored at 4°C until further processing.

2.9 Immunofluorescence on mouse brain tissue

For immunofluorescence stainings, PFA fixed brains were cut into 50 µm coronal sections using a Vibratome (VT1200 S, Leica). First, an antigen retrieval step was applied for 20 min at 95°C in Citrate Buffer (pH 6.0). After cooling down to room temperature they were permeabilized with 2 % Triton X-100 (Sigma) in 1x PBS overnight at 4°C. Sections were then blocked with Blocking Reagent (10 % goat serum, Invitrogen) for one hour at room temperature, and incubated with primary antibodies (Table 2), 10 % goat serum and 0,3 % Triton X-100 in 1x PBS overnight or two days at 4°C. Sections were then washed three times with 1x PBS and incubated with secondary antibodies coupled to Alexa fluorophores (1:1000, Invitrogen) for three hours, or one hour with goat anti mouse secondary antibody (Invitrogen) for tau HT7 and AT8 stainings. For sensitive detection of tau, a signal amplification step was performed after secondary antibody incubation, by using an Alexa Fluor 555 Tyramide SuperBoost Kit (Invitrogen, #B40913). Sections

were washed three times with 1x PBS and mounted on a cover slide with DAKO fluorescent mounting medium (Agilent) for subsequent confocal imaging.

2.10 Immunofluorescence on human brain tissue

Formalin-fixed and paraffin-embedded post mortem cortical brain samples of one PSP and one CBD case were used for illustration and comparison purpose. Prior to staining, 10 µm thick tissue sections were deparaffinized and subjected to an antigen retrieval step. The sections were incubated in citrate buffer (pH 6.0) for 20 min in a pressure cooker. After antigen retrieval, autofluorescence was quenched by photobleaching with a quenching solution (1x PBS, 30 % H_2O_2, 1M NaOH). Sections were submerged in the solution and sandwiched between two broad spectrum LED light sources (20.000-25.000 Lux). After 45 min of incubation, the solution was replaced by fresh reagent and sections were incubated for another 45 min between the LED light sources. Afterwards sections were washed four times with 1x PBS and blocked with blocking solution (5 % goat serum and 0,3 % Triton-X-100 in 1x PBS) for one hour at room temperature. Then they were incubated with primary antibodies against AT8 and GFAP (Table 2) overnight at 4°C. On the next day, sections were washed three times with 1x PBS and incubated with corresponding secondary antibodies coupled to Alexa fluorophores (1:1000, Invitrogen) for one hour at room temperature. After three times washing with 1x PBS, sections were mounted with Roti Mount FluorCare containing DAPI (Roth) for subsequent imaging.

2.11 Confocal microscopy

Mouse brain images were acquired with a Zeiss LSM 780 confocal microscope. Z-stack images were obtained with a Plan Apochromat 40x/NA 1.4 Oil DIC M27 objective. For synaptic stainings, high resolution tile scan images were obtained from the somatosensory cortex layers (2048 x 8192 pixels, z-stack: 20 µm, z-resolution 1 µm). For the virus evaluation experiment, tile scan images of the somatosensory region were obtained (1024 x 3072 pixels).

Images from human brain samples were acquired with a Leica Stellaris 5 confocal microscope. Cortical regions with tufted astrocytes and astrocytic plaques were chosen and z-stacks were acquired, using a HC Plan Apochromat CS2 63x/NA 1.40 Oil objective (2048 x 2048 pixels).

Table 2. Primary Antibody list.

1°Antibody	Species	Dilution	Manufacturer	Cat. No
Tau HT7	Mouse	1:1000	Invitrogen	MN1000
Tau AT8	Mouse	1:1000	Invitrogen	MN1020
Anti-tRFP(mKate2)	Rabbit	1:500	Evrogen	AB233
s100β	Guinea Pig	1:500	SYSY	287 004
HOMER1	Guinea Pig	1:500	SYSY	160 004
VGLUT1	Guinea Pig	1:500	SYSY	135 304
Anti GFP	Chicken	1:1000	Abcam	ab13970
GFAP	Guinea Pig	1:500	SYSY	173004

2.12 **Synaptic Data analysis**

Acquired images from HOMER1 and VGLUT1 synaptic stainings were analyzed with a custom written macro in Image J/FIJI. A small rectangle (400 x 400 pixels) was chosen and laid over mKate2 positive astrocytes, then synapses were quantified on a single plane with the SynQuant Image J/FIJI plugin [200]. The same rectangle was then laid over a mKate2 negative neighbor region and another synaptic quantification step was applied on the same single plane. Detected synaptic puncta containing total synaptic number and size per ROI were exported into an excel file and marked with the corresponding ROI (with astrocyte, without astrocyte). MKate2 positive astrocytes from the somatosensory cortex of all layers were taken into account for analysis.

2.13 **Statistical Analysis**

For statistical analysis, the software GraphPad PRISM 7.01 (GraphPad Software Inc.) was used. Data was first tested for Gaussian distribution by using Shapiro-Wilk-test. Depending on the normal distribution of the data, parametric or non-parametric tests were used (two-tailed Students *t*-test and two-way ANOVA or Mann-Whitney U test and Kruskal-Wallis test). When effects in the virus treatment, time or interaction were found, a Bonferroni *post-hoc* analysis was performed. $F_{treatment}$ refers to the groups injected with P301S virus or control virus. The data represent the mean ± SEM. An alpha level of 0,05 was chosen to be of statistical significance with a confidence interval of 95 %.

3 Results

3.1 Viral strategy to selectively express P301S tau in Aldh1l1 astrocytes

Extensive research has been made on the effect of toxic tau species on neurons and its implications for the progression of neurodegenerative diseases. However, also astrocytes are affected by tau in several sporadic and familial tauopathies and are shown to have tau inclusions in various amounts, depending on disease.

So far, numerous mouse models have been developed, but most of them carrying mutant tau in neurons, either by using transgenic, seeding, or viral approaches [74], [201]–[207] and only few that selectively address astrocytic tau [161], [166], [208]. In particular, there is a lack of knowledge about the role of astrocytic tau deposition in tauopathies and its contribution to neurodegenerative processes [209].

3.1.1 Experimental Design

To address this, a viral approach was developed to selectively overexpress P301S mutant tau in astrocytes in the Aldh1l1-cre/ERT2 mouse line. This mouse line has a tamoxifen-inducible Cre recombinase targeted to Aldh1l1 astrocytes [188]. For this study, an AAV was designed, carrying transgenes for the P301S human tau mutation, and the far-red mKate2 fluorophore reporter under the strong CBh promoter (Figure 7A). As control, a virus only carrying the fluorophore reporter transgene was used (Figure 7B). The transgenes in both viruses are flanked by two pairs of LoxP sites (FLEX Cre-On switch) that, upon interaction with active Cre recombinase, invert the initially antisense oriented sequences and turn on the expression of the transgenes only in cells with active Cre. The use of a PHP.eB capsid that can cross the blood-brain barrier (BBB) opened the possibility for a systemic, non-invasive AAV delivery by simply injecting the virus into the bloodstream of the mice [210]. Viruses with that capsid efficiently target neurons and astrocytes in the CNS [210].

For all following experiments, the virus was injected into the lateral tail vein of 2-3 months old Aldh1l1-cre/ERT2 mice. The virus transduced neurons and astrocytes in the CNS but the transgene expression was halted due to the lack of active Cre recombinase. After i.p. application of Tamoxifen for five consecutive days, Cre recombinase activation in Aldh1l1 astrocytes led to the expression of virus transgenes selectively in astrocytes (Figure 7C). For all following experiments the term Aldh1l1/P301S is used for this mouse model.

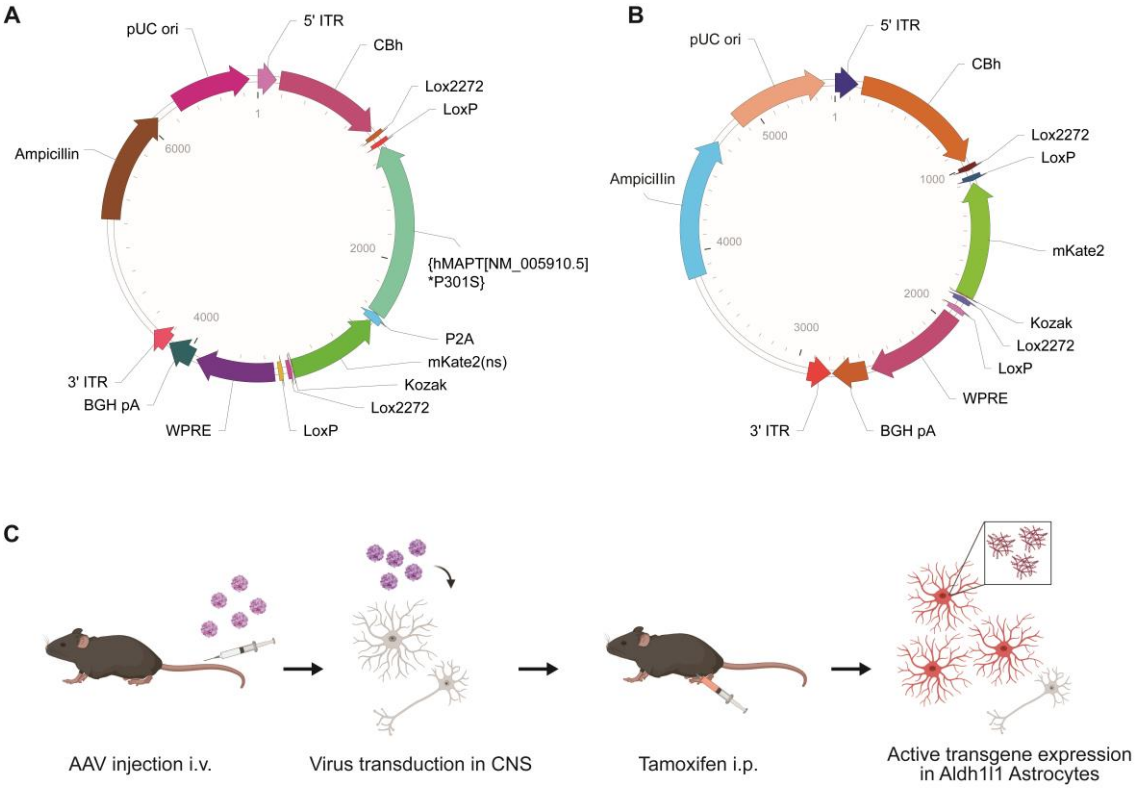

Figure 7. Virus plasmids and schematic illustration of the experimental approach. (A) Plasmid of the experimental virus carrying the P301S mutant tau transgene and mKate2 fluorophore flanked by LoxP sites. **(B)** Plasmid of the control virus carrying the fluorescent mKate2 reporter gene only. **(C)** The virus was injected intravenously into the lateral tail vein of mice and transduced cells in the CNS. Only after tamoxifen application, viral transgenes start expressing in Cre positive Aldh1l1 astrocytes. Image A and B were created with Vectorbuilder.com. Image C was created with BioRender.com.

3.2 Astrocytes express transgenes only upon Cre activation *in vitro* and *in vivo*

To validate the specificity and functionality of the virus and DNA construct, *in vitro* and *in vivo* experiments were carried out. To investigate the dependence of transgene expression of Cre recombinase *in vitro*, a western blot analysis of transfected HEK293 cells was performed. The tau transgene was only expressed in HEK293 cells when Cre was present. In cells where only the virus construct was present, no tau expression was visible (Figure 8A). Next, the function was tested *in vivo* by injecting the virus via the tail vein, followed by five days application of tamoxifen. The virus transduction and transgene expression efficiency were determined one month later. Efficient gene expression was only observable in the group treated with tamoxifen, compared to the control group lacking tamoxifen treatment (Figure 8B). These results show that the astrocytes efficiently express the transgenes only after activation of Cre recombinase through tamoxifen.

3.2.1 Vector dose evaluation

Typical viral doses used for applications with AAV-PHP.eB range from 1 x 10^{11} and 3 x 10^{12} vg in adult mice [211]. However, optimal dose varies depending on the target cell population and desired expression levels. Therefore, the vector dose required for gaining a sufficiently high expression level of the transgene in astrocytes was determined. Two different doses were injected into the lateral tail vein of mice (1 x 10^{11} vg and 1 x 10^{12} vg) and the level of transgene expression was evaluated one month later with immunofluorescence stainings. The lower dose transduced few astrocytes only, while the higher dose markedly transduced astrocytes throughout the whole brain (Figure 8C and D). Particularly in the cortical regions, a high efficiency of virus transduction was observed. Based on these observations, all further experiments were carried out using 1 x 10^{12} vg to obtain robust astrocytic transduction.

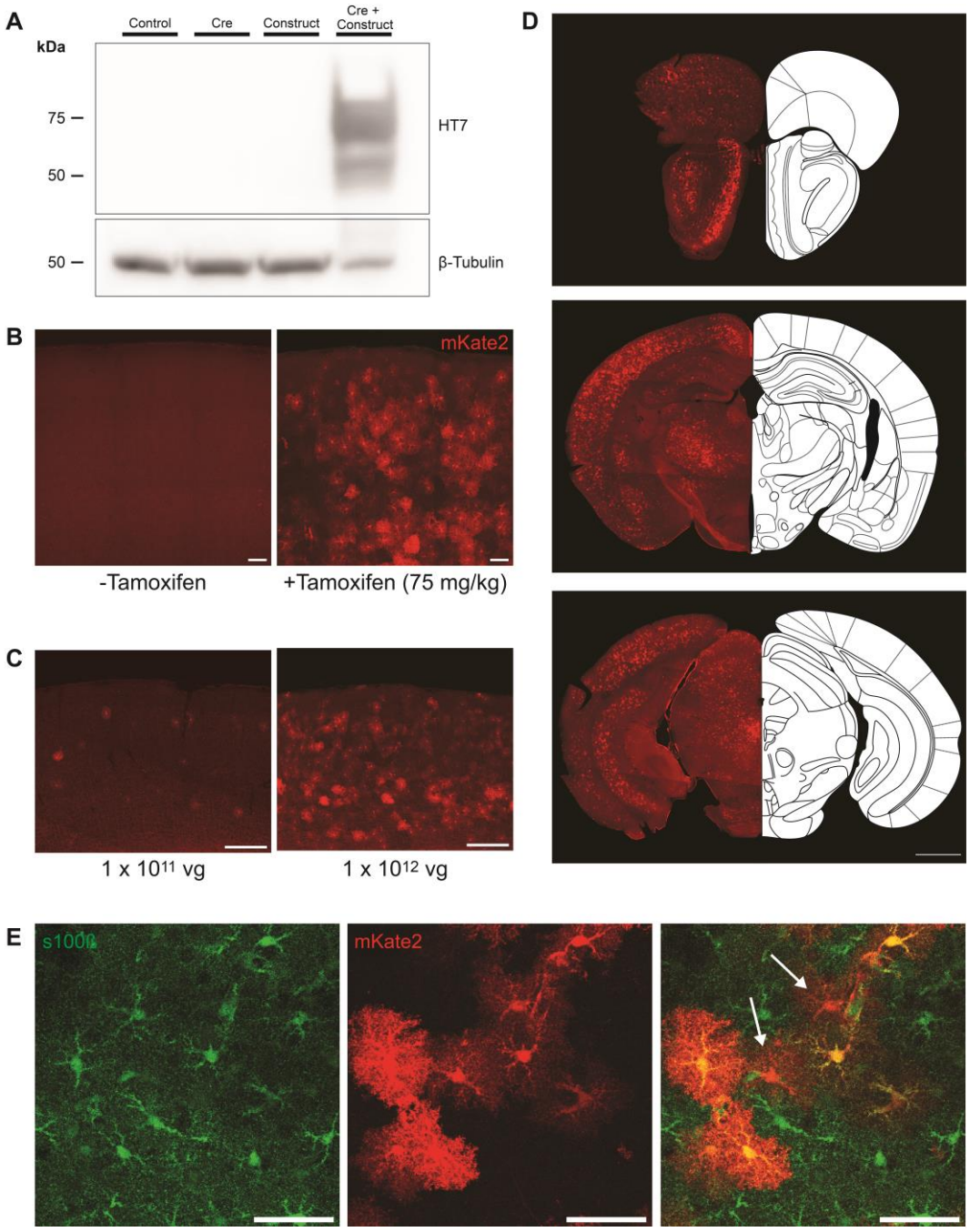

Figure 8. *In vitro* and *in vivo* validation. (A) and **(B)** *In vitro* and *in vivo* validation experiments revealed an expression of the transgenes only upon presence of Cre recombinase. Scale bar = 50 µm. **(C)** Virus load was evaluated based on two different doses of vg injected. When the lower dose was administered (1 x 10^{11} vg), only few astrocytes expressed the transgene. The higher dose (1 x 10^{12} vg) showed an efficiently high transduction of astrocytes, as observed with the reporter fluorophore mKate2, and was then utilized for further experiments. Scale bar = 200 µm. **(D)** The higher dose was evaluated among regions of the anterior (top panel), mid and posterior (bottom panel) part of the brain, in coronal sections. Scale bar = 1 mm. **(E)** MKate2 positive signal colocalizes with s100β and has astrocytic, bushy morphology, confirming cell type specificity. Some astrocytes did not colocalize with s100β (white arrows), but had the same astrocytic morphology. Scale bar = 50 µm.

3.3 Virus expresses in astrocytes in the somatosensory cortex

Based on the high virus expression in the neocortex of Aldh1l1/P301S mice, all following experiments were carried out in that region. In order to confirm the expression specificity of the virus in astrocytes and to investigate the infection efficacy in that region, Aldh1l1/P301S and control mice were sacrificed one or three months post injection (p.i.). Coronal sections including the somatosensory cortex were prepared and stained for the astrocytic marker s100β and mKate2 reporter fluorophore. Tile scans including all somatosensory cortical layers were obtained by confocal imaging.

Immunofluorescence staining with mKate2 revealed a spongiform and extensively ramified morphology, characteristic of astrocytes. Co-localization with s100β confirmed the cell type specificity (Figure 8E). Noteworthy, not all mKate2 positive astrocytes were found to colocalize with s100β but still shared the same morphological attributes typical for that cell type (Figure 8E, white arrows). To further evaluate the amount of s100β astrocytes that were expressing the virus, a ratio was calculated from the total number of s100β astrocytes per ROI and astrocytes found to colocalize with mKate2.

In the mouse cohort 1 month p.i., ~28 % (Control) and ~43 % (Aldh1l1/P301S) of s100β positive astrocytes were colocalizing with mKate2 (mean colocalization % ± SEM: Control = 27,89 ± 3,498; Aldh1l1/P301S = 43,17 ± 5,305, p >0,05). In the cohort that was sacrificed 3 month p.i. significantly more astrocytes colocalized for both markers in Aldh1l1/P301S animals (55 %), compared to control cohort (22 %) (mean colocalization % ± SEM: Control = 22,41 ± 9,473; Aldh1l1/P301S = 54,73 ± 2,544, p <0,05).

3.4 Astrocytic phospho-tau in Aldh1l1/P301S mice has morphological similarities to PSP tufted astrocytes

Several primary tauopathies are characterized by the accumulation of phospho-tau in astrocytes. These astroglial inclusions exhibit distinct morphologies between different tauopathies. In PSP brains, tau positive fibrils form so called tufts around the nucleus in astrocytes (tufted astrocytes) [159]. In contrast, CBD is characterized by astrocytic plaques that are comprised of spindle-shaped tau aggregates, arranged in a ring like manner.

To address whether hyperphosphorylated tau can be found in the cortex of Aldh1l1/P301S mice, brain sections were obtained and stained for HT7 total human tau and AT8 phospho-tau in animals 1, 3, 6 and 8 months p.i. To confirm the expression of the tau transgene, HT7 was shown to be expressed in mKate2 positive astrocytes (Figure 9A upper panel).

Staining with AT8 revealed different morphological appearances of astrocytes in the cortex. Several astrocytes exhibited AT8 positivity in the cell soma and primary processes and were found in mice from three months p.i. on (Figure 9A lower panel). Also, in brains of mice three months p.i., AT8 positive tau inclusions could be found in the cell body of astrocytes, in conjunction with morphological atrophy (Figure 9B upper panel). MKate2 staining revealed an abnormal astrocytic morphology that appear to have lost its spongiform structure with only some branches remaining, emerging from the soma. In mouse brains six months p.i., several AT8 positive star-shaped structures were found, which are reminiscent of astrocytes but negative for mKate2 (Figure 9B lower panel).

These ramified, fibrillary structures appear to be of very similar morphology to AT8 positive tufted astrocytes in brains of human PSP patients (Figure 9C left). Both structures seem to be denser in the core with pericentral branched AT8 tau positive tufts. In contrast, astrocytic plaques in brains of CBD patients show a more dispersed circular tau pattern without a dense core (Figure 9C right). These results suggest that phospho-tau can be found in astrocytes in the Aldh1l1/P301S mouse model and are reminiscent of human primary tauopathies.

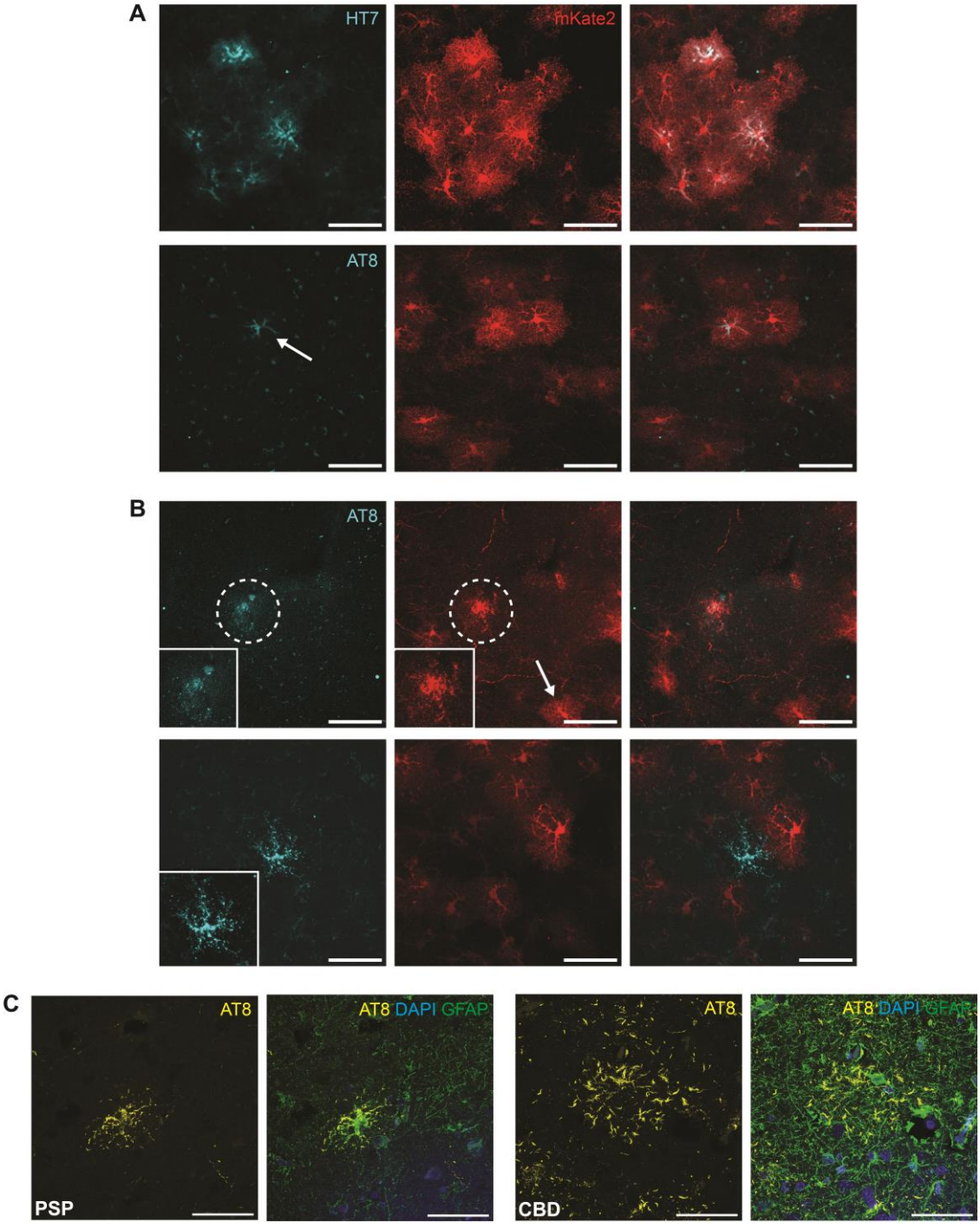

Figure 9. Total human tau and hyperphosphorylated AT8 tau is found in astrocytes in Aldh1l1/P301S mice. (A) Immunofluorescence staining with total human tau (HT7) revealed an expression of the tau transgene in astrocytes, colocalized with mKate2. Phospho-tau was observable in mice of different age p.i., based on AT8 positivity. **(B)** Different phospho-tau positive structures could be observed in several mice. The upper panel shows a tau inclusion like dense structure in an astrocyte (dashed circle), with beginning atrophy of the cell. The white arrow points to a ramified mKate2 astrocyte in contrast to the morphologically aberrant cell. The lower panel shows a phospho-tau positive star shaped structure, resembling an astrocyte, but negative for mKate2. **(C)** Comparison with AT8 positive TAs from PSP brains and astrocytic plaques from CBD brains of patients. Scale bar = 50 µm.

3.5 Spontaneous astrocytic Ca^{2+} transients in microdomains are altered in Aldh1l1/P301S mice

Changes in astrocytic intracellular Ca^{2+} concentrations can occur spontaneously or be evoked in response to neuronal activity. In turn, astrocytic Ca^{2+} transients regulate the release of gliotransmitters to modulate synaptic activity [106]. Thus, astrocytes and neurons interact bidirectionally in a finely tuned manner as active partners in the “tripartite synapse” [105].

Studies with animal models show clear evidence that astrocytic Ca^{2+} activity is disturbed in neurodegenerative diseases, like AD [208], [212]–[214]. Astrocytes with internalized oligomeric tau also show alterations in gliotransmitter release and intracellular Ca^{2+} signaling, which affects pre- and postsynapses *in vitro* in astrocyte-neuron co-cultures, suggesting that tau alters astrocytic functions and further affects neighboring neurons [215]. Isolated astrocytes from P301S mice also acquire early functional deficits, leading to a loss of neurosupportive functions [165]. These *in vitro* studies bring up evidence that tau may affect the physiological function of astrocytes, which extends to their trisynaptic partners.

In order to understand if astrocytes in the Aldh1l1/P301S model show abnormal Ca^{2+} activity *in vivo*, astrocytic Ca^{2+} transients of microdomains, where the contact points between PAPs and neuronal synapses reside, were investigated. To this end, a cranial window was implanted over the somatosensory cortex in mice two months after administration of tamoxifen for Tau expression, and a virus encoding a membrane tethered GCaMP Ca^{2+} sensor (AAV2/5.GfaABC1D.Lck-GCaMP6f) was stereotactically injected into the brain. *In vivo* two-photon imaging of astrocytic Ca^{2+} transients was performed in mice three months p.i.

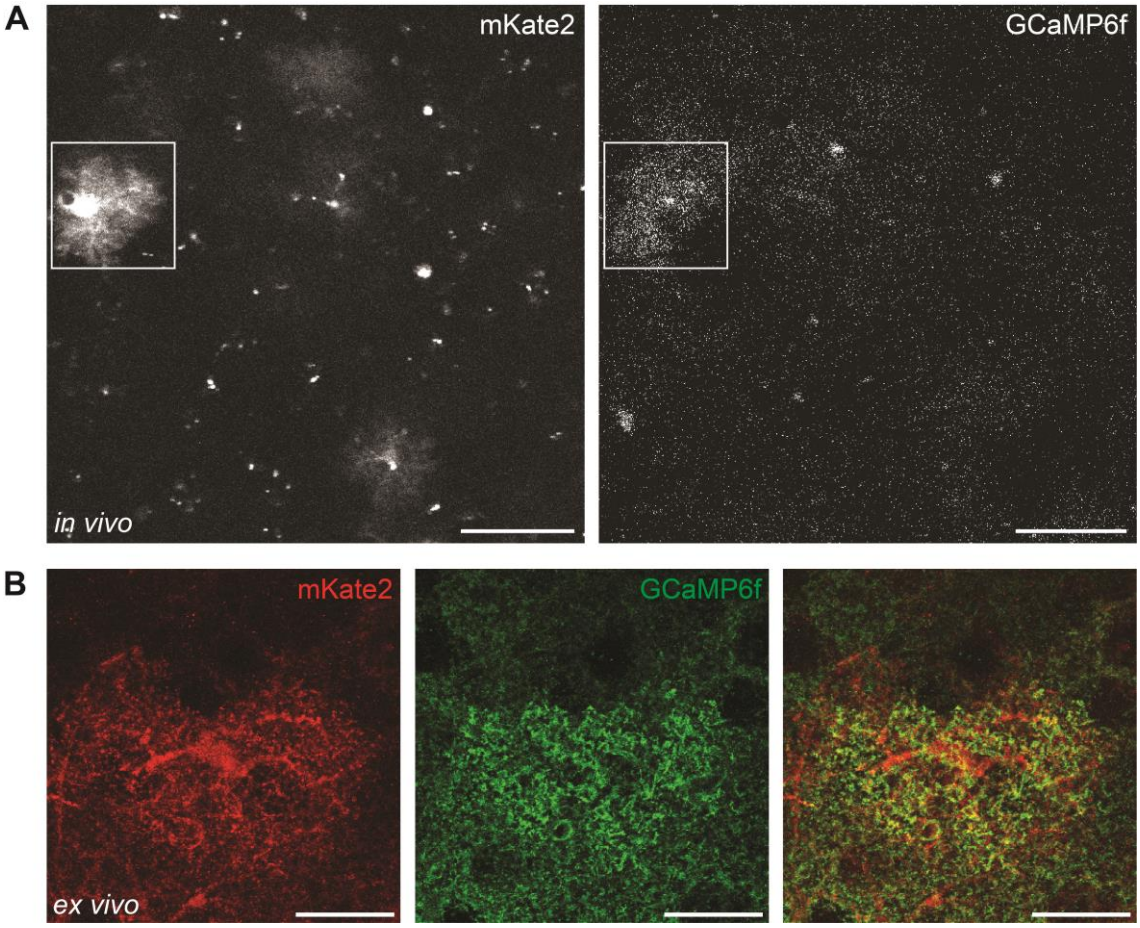

Figure 10. *In vivo* and *ex vivo* GCaMP6f signal. (A) *In vivo* two-photon example image of a ROI in the somatosensory cortex of an mKate2 fluorescent astrocyte with overlapping GCamP6f Ca^{2+} indicator. Image was acquired through a cranial window one month post-surgery. Scale bar = 50 µm **(B)** *Ex vivo* confocal example image of a cortical astrocyte with overlapping mKate2 and GFP staining from GCamP6f. Scale bar = 20 µm.

Imaging was carried out under light anesthesia. Mice were sedated with Medetomidine (0,5 mg/kg) and received 0,5 % Isoflurane in 95 % O_2 and 5 % CO_2 throughout the imaging session. Breathing and heart rate was monitored with a pulse oximeter probe. Only images acquired under the same anesthesia depth were taken for further analysis (breath rate between 80-100 brpm and heart rate between 150-250 bpm).

Time-lapse image series of ROIs (75 x 75 µm) with astrocytic microdomain Ca^{2+} transients from GCaMP6f signal were acquired from cortical layers I-II (Figure 10A). In order to confirm the astrocytic origin of Ca^{2+} transients, astrocytes were later on stained for mKate2 and anti-GFP to reveal GCamP6f signal (Figure 10B).

Ca^{2+} transients of active astrocytic microdomains obtained from *in vivo* time-lapse image series were analyzed using a ROI-based analysis pipeline, as described in the methods section. No significant differences were found in the microdomain size and in the total number of active domains (mean microdomain size in μm^2 ± SEM: Control = 7,182 ± 2,729; Aldh1l1/P301S = 7,961 ± 4,456, p >0,05), (mean number active domains ± SEM: Control = 23,75 ± 6,199; Aldh1l1/P301S = 47,58 ± 8,837, p >0,05) (Figure 11A-D). When analyzing Ca^{2+} events (Figure 11E) a significant increase in astrocytic Ca^{2+} transients per minute was observed in Aldh1l1/P301S animals, compared to control group (mean frequency/min ± SEM: Control = 2,085 ± 0,4367; Aldh1l1/P301S = 2,941 ± 0,435, p <0,05) (Figure 11E,H). Regarding rise and decay time kinetics, no significant differences were found between both groups (mean rise time in ms ± SEM: Control = 3142 ± 330; Aldh1l1/P301S = 2581 ± 246,8, mean decay time in ms ± SEM: Control = 3692 ± 457,3; Aldh1l1/P301S = 2824 ± 236, p >0,05) (Figure 11F,G).

Taken together, these results indicate that astrocytes of Aldh1l1/P301S mice show alterations in astrocytic microdomain Ca^{2+} signaling. An increased firing frequency per minute could be observed, which suggests a hyperactive signaling of microdomains in the astrocytes of Aldh1l1/P301S mice.

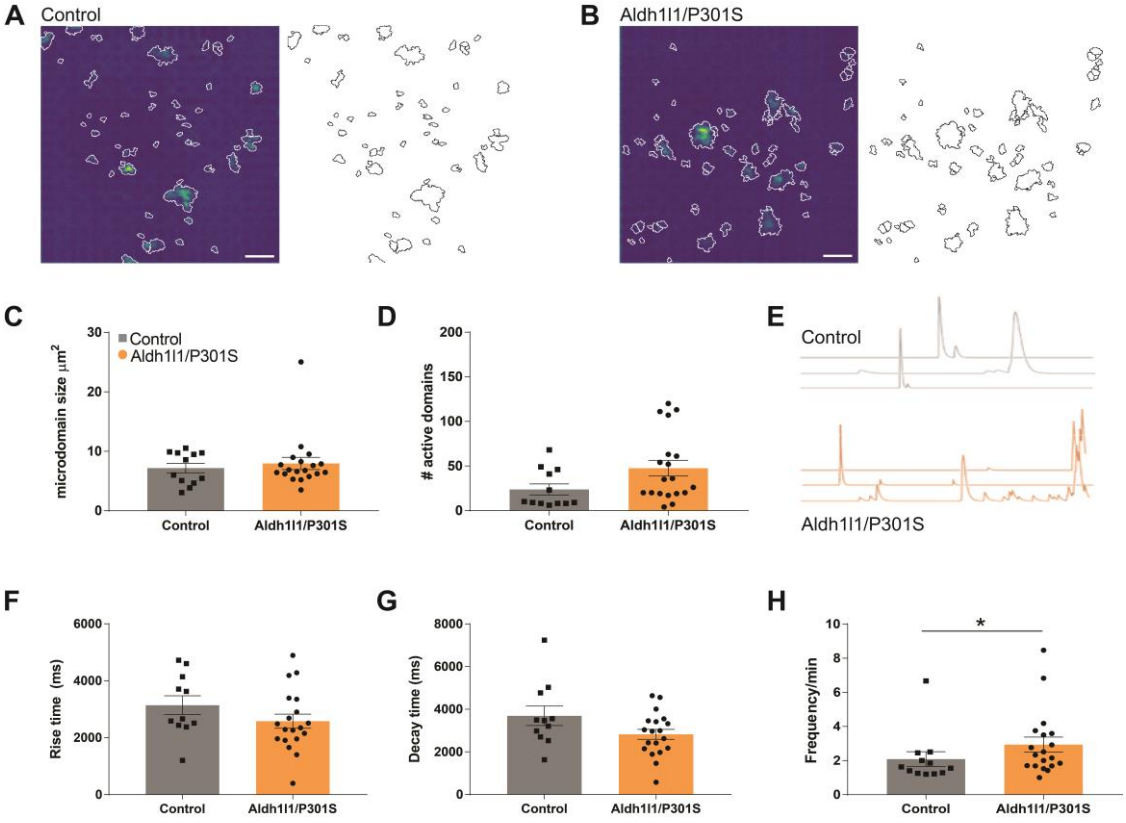

Figure 11. Frequency of astrocytic Ca^{2+} transients is increased in Aldh1l1/P301S animals. **(A)** and **(B)** Example images of active microdomains and detected microdomain outlines from control and Aldh1l1/P301S animals. Scale bar = 10 µm. **(C)** The area of microdomains (Mann-Whitney test: p = 0,8574; U = 109) as well as the number of active microdomains **(D)** are unchanged in both groups (Mann-Whitney test: p = 0,0688; U = 69). **(E)** Examples of extracted Ca^{2+} traces from control and Aldh1l1/P301S animals. **(F)** The rise time (two-tailed students t-test: p = 0,1809; t(28) = 1,372) and decay time **(G)** are not altered in Aldh1l1/P301S mice (two-tailed students t-test: p = 0,0720; t(28) = 1,87). **(H)** The frequency per minute is significantly increased in Aldh1l1/P301S animals (Mann-Whitney test: p = 0,0362; U = 62,5). **p* <0,05. Data presented as mean ± SEM; n = 4-5 animals, 2-5 ROIs/mouse.

3.6 Excitatory postsynapses are reduced in Aldh1l1/P301S mice

Two hallmarks found in neurodegenerative disease, namely deposition of phospho-tau in astrocytes and aberrant Ca^{2+} signaling, were observed in Aldh1l1/P301S mice. Thus, such a deregulation may further affect neuronal synapses. Synapse loss is a key feature of primary tauopathies and precedes overt neurodegeneration. Abnormal tau accumulates in synapses, leading to a disruption of synaptic function and further to synaptic loss [216]–[219]. However, those studies focused on accumulated tau in neurons and its consequences on synaptic function. A previous study from our laboratory found a loss of synapses in postmortem brains of PSP and CBD patients, in the latter a correlation between synapse loss and the spatial domain of astrocytic plaques could be observed [164]. Yet, it is still unclear whether astrocytes alone can contribute to synaptic degeneration, or if this effect can be rather traced to other adverse events in tauopathies.

To address this, the synaptic density of excitatory pre- and postsynapses was evaluated in the somatosensory cortex of Aldh1l1/P301S mice and control animals one and three months p.i. Brain sections were obtained and stained for pre- and postsynaptic markers. VGLUT1 was used as a marker for presynaptic excitatory synapses and HOMER1 was used for postsynaptic excitatory synapses. Confocal images of the somatosensory cortex including all layers were obtained. Then, an Image J macro including SynQuant synapse quantification plugin was used to quantify synaptic puncta. To quantify whether a loss of synaptic density could be observed in the individual astrocytic spatial domain, ROIs of 400 x 400 pixels were chosen and laid over mKate2 positive astrocytic domains and neighboring mKate2 negative ROIs (Figure 12A and B, left images). Total synaptic puncta per ROI were obtained from both areas and used for subsequent analysis. Astrocytes of all somatosensory cortical layers were taken into consideration.

One month p.i. a trend to a reduction of VGLUT1 presynapses could be observed in the Aldh1l1/P301S group, however the effect was not significant (Figure 12A) (mean synapses/10 µm^2 mKate2+ area ± SEM: Control = 4,377 ± 0,07167; Aldh1l1/P301S = 4,153 ± 0,08259, mKate2- area ± SEM: Control = 4,359 ± 0,09566; Aldh1l1/P301S = 4,183 ± 0,09068, *p* >0,05). Three months p.i. a significant overall decrease in presynapses could be observed in the Aldh1l1/P301S group, compared to control (mean synapses/10 µm^2 mKate2+ area ± SEM: Control = 4,672 ± 0,04693; Aldh1l1/P301S = 4,52 ± 0,04558, mKate2- area ± SEM: Control = 4,683 ± 0,0536; Aldh1l1/P301S = 4,549 ± 0,04684, *p* <0,01). Interestingly, the synaptic reduction was not restricted to areas occupied by mKate2 positive astrocytes, but also evident in mKate2 negative neighboring areas.

In contrast, HOMER1 postsynapses were found to be affected more slowly by astrocytic tauopathy than VGLUT1 presynapses. No significant differences were found one month p.i. (Figure 12B) (mean synapses/10 µm^2 mKate2+ area ± SEM: Control = 4,038 ± 0,09952; Aldh1l1/P301S = 4,072 ± 0,07302, mKate2- area ± SEM: Control = 4,011 ± 0,1013; Aldh1l1/P301S = 4,1 ± 0,07035, *p* >0,05). Three months p.i. a significant reduction of HOMER1 postsynapses was evident in the Aldh1l1/P301S group, compared to control. Also here an overall reduction of synapses could be found that is not restricted to the astrocytic spatial domain. In total, a 24 % reduction in synaptic puncta was observed in the mKate2+ area, and an 18 % reduction was observed in mKate2 negative neighboring areas (mean synapses/10 µm^2 mKate2+ area ± SEM: Control = 3,965 ± 0,138; Aldh1l1/P301S = 3,015 ± 0,1299, mKate2- area ± SEM: Control = 3,798 ± 0,1449; Aldh1l1/P301S = 3,114 ± 0,1249, *p* <0,0001).

Lastly, the relationship between an overall change in synaptic density to viral load was investigated. In this way potential toxic effects of the PHP.eB virus per se could be assessed, and whether the synaptic pathology followed a simple linear relationship with the number of transfected astrocytes. For the control virus, the viral load and synaptic density showed no significant relationship (R^2 = 0,3103). Interestingly, also no clear relationship between the viral load and synaptic

density counts in the experimental virus could be observed (R^2 = 0,2291), suggesting that the effect mediated by the introduction of P301S tau into astrocytes may be modulated by unidentified sources of variability present between subjects. Indeed, a growing number of studies indicate that disease heterogeneity and severity of tauopathies can be influenced by other factors, such as chronic activation of the immune system, neuroinflammation or gender [220]–[222]. These findings open an interesting approach for future studies to investigate complementary factors for disease severity.

Taken together, these results show an overall phenotype characterized by loss of excitatory synapses in Aldh1l1/P301S animals three months p.i., regardless of astrocytic spatial domain, with slower kinetics for the loss at the postsynaptic level.

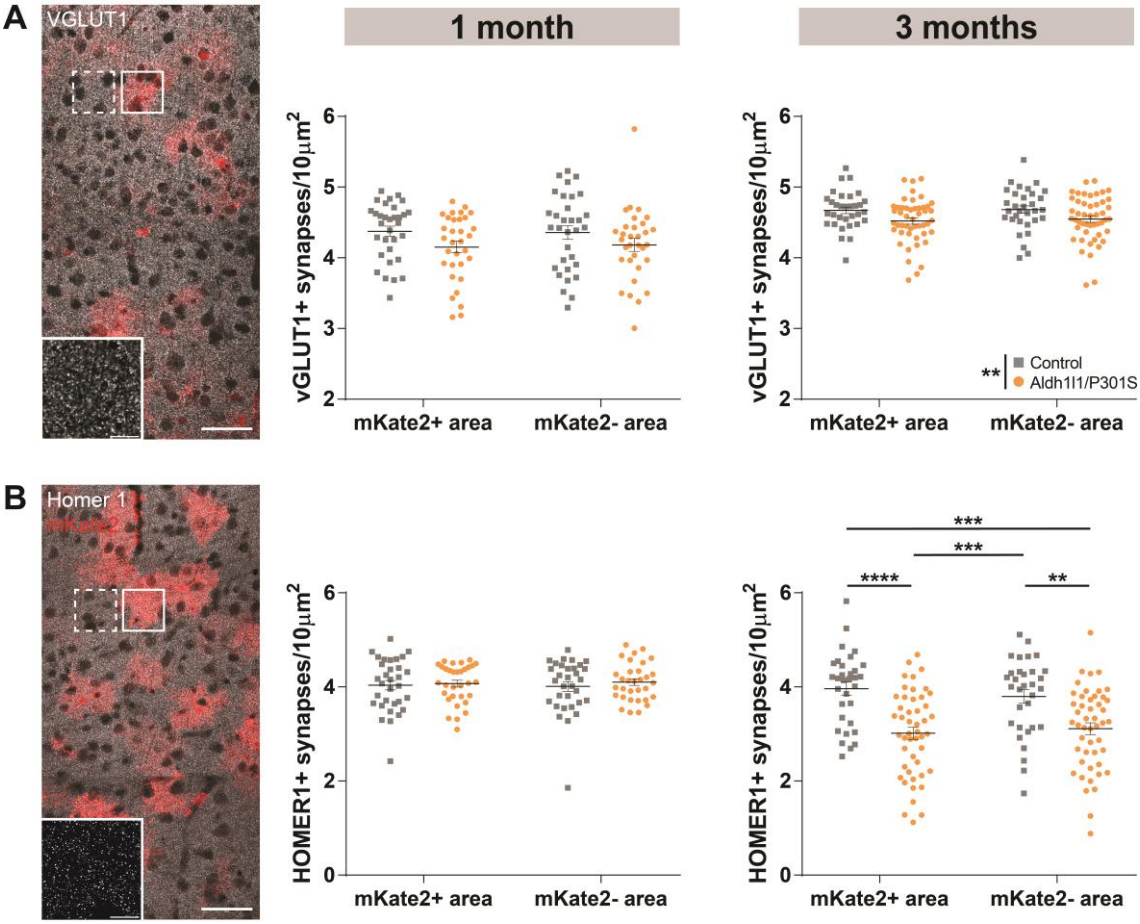

Figure 12. Excitatory bipartite synapses are reduced in Aldh1l1/P301S mice. (A) Example of VGLUT1 presynapses with overlaid ROIs of mKate2+ area (square) and mKate2- area (dashed square) in the somatosensory cortex. Scale bar = 50 µm. Quantification of VGLUT1 positive synapses/10 µm^2 revealed a non-significant trend in the reduction of synapses one month p.i. (Kruskal-Wallis test, p = 0,0832). Three months p.i. a significant decrease of presynaptic puncta was observable (Two-way ANOVA: $F_{treatment}$ (1, 156) = 8,297, p = 0,0045). **(B)** Example of HOMER1 postsynapses. Scale bar = 50 µm. No reduction of postsynapses was found one month p.i. (Kruskal-Wallis test, p = 0,9922). A significant reduction was observable three months p.i. in Aldh1l1/P301S mice, compared to control group (Two-way ANOVA, $F_{treatment}$(1, 156) = 35,33, p <0,0001; Bonferroni *post-hoc* test: **p<0,01, ***p<0,001, ****p<0,0001. Data presented as mean ± SEM; n = 4-6 animals, 8 ROI pairs/mouse.

4 Discussion

4.1 A virus-inducible mouse model for studying consequences of astrocytic tauopathy

Over the last decades researchers extensively investigated tau induced neurodegenerative processes, whereby the focus was placed on toxic effects of tau and cell death occurring in neurons [18]. However, several neurodegenerative diseases are characterized by an accumulation of tau in non-neuronal cells, like astrocytes. Under healthy conditions, astrocytes are an important key player in the brain network. Their tasks include the regulation of neuronal circuits, promotion of synapse formation, modulation of excitatory and inhibitory synapses and the maintenance of the BBB [223]–[226]. In contrast, the role of astroglia for neurodegenerative processes remains poorly explored. In several primary tauopathies, astrocytes are affected as they accumulate phospho-tau. In particular, the pathophysiological mechanisms involving tau in astrocytes for Ca^{2+} signaling and the influence on neighboring contacting synapses have only recently begun to be explored.

Therefore, this thesis focused on investigating pathophysiological consequences of phospho-tau in astrocytes. To achieve this, a virus-inducible mouse model of astrocytic tauopathy was developed. A custom designed virus that expresses a human tau mutation of FTD (P301S) in a Cre dependent manner was used. The virus was injected by systemic delivery into a mouse line with a tamoxifen-inducible Cre recombinase directed to Aldh1l1 astrocytes. This resulted in a mouse model, that expresses mutant P301S tau in Aldh1l1 astrocytes in the CNS (= Aldh1l1/P301S). The far-red fluorophore mKate2 was used as a reporter. By using this model, tau pathology induction and accumulation of phospho-tau could be investigated, and further functional consequences of pathological tau in astrocytes and a temporal effect on trisynaptic compartments in the somatosensory cortex.

As a first measure, tau pathology in astrocytes of Aldh1l1/P301S mice was evaluated, by using HT7 for total tau and AT8 for targeting pathological hyperphosphorylated tau. HT7 positive astrocytes could be observed throughout

the cortex, confirming expression of human total tau. Three months p.i. this model displayed hyperphosphorylated AT8 positive tau in several isolated astrocytes in the cortex.

Next, functional consequences of astrocytic tau were investigated *in vivo*. Spontaneous Ca^{2+} dynamics were measured in cortical astrocytic microdomains of Aldh1l1/P301S mice. The recent development of fast, membrane tethered AAV-GCaMP Ca^{2+} indicators [136], [185] enabled the examination of spontaneous Ca^{2+} transients in the very fine processes of astrocytes, the contact points to neuronal synapses. Through the use of advanced two-photon microscopy, astrocytic Ca^{2+} signals in the upper cortical layers could be reliably captured in the living mouse brain. Data analysis revealed that astrocytes in Aldh1l1/P301S mice have an increased frequency of Ca^{2+} transients in microdomains compared to the control group, whereas the area or number of microdomains remained unchanged.

The next question was if astrocytes in Aldh1l1/P301S mice have a pathological influence on neuronal synapse density. By using markers for excitatory pre- and postsynapses, it was investigated whether a change in synaptic density was observable in regions that are governed by mKate2 positive astrocytes compared to neighboring areas, that are negative for mKate2. The synaptic density was quantified in brain sections of Aldh1l1/P301S animal groups one month and three months p.i. and compared to the control group. Overall, a decrease of excitatory VGLUT1 presynapses could be observed three months p.i. in the Aldh1l1/P301S mouse, compared to control. Interestingly, the synapse loss was not confined to the astrocytic domain, but rather also evident in areas not governed by mKate2 positive astrocytes. A non-significant trend of synaptic decrease could be already seen one month p.i. in overall areas. In line with this result, a considerable reduction of excitatory HOMER1 postsynapses could be seen three months p.i., which was even more evident than the presynaptic synapse loss. One month p.i. no significant decrease was observed, in contrast to the presynaptic side. In other words, an overall loss of postsynapses seems to start more slowly than presynaptic degeneration in Aldh1l1/P301S mice.

4.2 Using a viral approach to induce astrocytic tauopathy

To study tauopathies *in vivo*, different approaches can be applied for modeling those diseases in rodents. For example, transgene constructs can be microinjected into a fertilized egg to generate a new transgenic mouse model [227]. Several different mouse models overexpressing tau have been developed so far. In early ages, MAPT transgenic mice have been studied which overexpress human wild-type tau isoforms [202], [228]. Later, research also focused on mice overexpressing tau mutations found in FTD patients. Especially mutations residing in exon 10 of the MAPT gene were applied to generate mouse models for studying pathological changes in tauopathies [229]–[232]. However, a disadvantage of using germline genetically engineered mice is that the transgene expression cannot be controlled in a time dependent manner, but rather is overexpressing from birth or early embryonic stages on, which may affect the normal development.

Another strategy is to use a genetically engineered virus to induce tau pathology [208], [233], [234]. However, viral approaches are often limited because of single localized injections into the brain, typically into the hippocampus. Such approaches may be insufficient for studying cell types which are widely distributed or for investigating the connection of circuits or between cell types. To overcome this issue, new virus capsids have been developed in recent years which opened up the possibility of transfecting cells throughout the CNS by systemic AAV administration through the vasculature. Those viruses are able to bypass the BBB and therefore provide efficient gene delivery to desired cells among the whole brain [210].

For this thesis, a viral approach with such capsids was employed. Thus, a transgene encoding the P301S tau mutation could be delivered into the CNS of Aldh1l1-cre/ERT2 mice and target the vast majority of astrocytes in a tamoxifen dependent manner. By creating an astrotauopathy model, pathophysiological mechanisms of tau in astrocytes and contacting synapses in the cortical tripartite

synapse environment could be investigated. As a first approach, this thesis showed that the virus infects a considerable number of astrocytes and reliably leads to expression of tau in the presence of Cre recombinase in those cells.

Interestingly, the control virus transfected less astrocytes as compared to the experimental virus, although both were injected at a dose of $1x10^{12}$ vg. While the experimental virus reached an infection rate of roughly 43 % and 55 % of s100β positive astrocytes, mice injected with control virus reached a rate of 28 % and 22 % of s100β astrocytes (one month and three months p.i. cohorts, respectively).

Although the injected viral titers, capsid, vector design and promoter were equal for both used viruses and the only difference was the inclusion of the P301S tau mutation in the experimental virus, those discrepancies were observed. A possible explanation of those variations in viral load could be different purification mechanisms or reagents used by the two virus production sites. Variabilities in final viral load may underlie those discrepancies. Nevertheless, those differences had no effect on the experiments. To account for these discrepancies, it was investigated whether total viral load affects synaptic density. As mentioned in the results part, there was no positive correlation between the synapse counts and number of affected astrocytes observable. In addition, the fluorophore mKate2, which is the only transgene inserted in the control virus, has been indicated to have low toxicity and is therefore suitable for use in living organisms [235].

4.3 Astrocytes in Aldh1l1/P301S mice show different states of phospho-tau formation

After translation, tau undergoes several post-translational modifications, including phosphorylation. In the healthy brain, tau can be phosphorylated and dephosphorylated at several sites, which is crucial for its stabilizing and binding ability to microtubules. Hyperphosphorylated tau has also been found in multimeric forms of the proteins including paired helical filaments (PHFs) and in the later stage NFTs, which are a characteristic sign of the pathogenesis of tauopathies [236], [237]. In secondary tauopathies like AD, those AT8 positive tau inclusions are mainly found in neurons, while in primary tauopathies, AT8 positive accumulations are also found in astrocytes. The P301S missense mutation used in this thesis causes the formation of NFTs in brains of patients as well as in P301S transgenic mice [74].

By staining for AT8 phospho-tau, pathological tau depositions in several cortical astrocytes in Aldh1l1/P301S mice at three months p.i. could be observed. AT8 positivity was mostly confined to the soma and the main processes. Several different morphologies could be seen. Some astrocytes were found to be positive for AT8 and still had a ramified astrocyte morphology. Others showed clumped-like tau depositions, with an aberrant astrocytic appearance, as seen by mKate2 staining. The highly ramified structure was lost, only the main processes remained. This may indicate an early pathological change in response to phospho-tau formation, and may show an early stage of pathology, as typically seen in several neurodegenerative diseases [238]. Six months p.i. phospho-tau positive astrocytes as well as several star-shaped AT8 tau deposits could be observed, which appear as a dense core with star-like arborizations that were negative for mKate2. The mKate2 negativity could be explained by phagocytic activity from microglia, however their ability to phagocytose and degrade the remaining phospho-tau may be impaired. Several studies showed that microglia can phagocytose tau and exocytose it again, releasing the protein in exosomes [61], [239]. Increased levels of tau in exosomes have been also found in the blood and cerebrospinal fluid of patients with FTD and AD [240], [241]. These results

suggest that phospho-tau can form in cortical astrocytes and lead to a pathological change in those cells, which may be an early sign of neurodegeneration. Astrocytic tau deposits may also take on a similar morphology reminiscent of human tauopathy. Given the endogenous expression of tau in astrocytes, although in a very small amount [15], astrocytes therefore may be able to hyperphosphorylate tau in the context of neurodegeneration, in addition to a postulated uptake from neurons [161].

4.4 Astrocytes exhibit increased Ca^{2+} signaling in Aldh1l1/P301S mice

Astrocytes mediate the release of gliotransmitters via elevations of intracellular Ca^{2+} transients to control synaptic function, thus astrocytes play a key role in the maintenance of cortical circuits. Under pathological conditions this finely tuned interplay is disturbed. Isolated astrocytes from post mortem brain sections of Alzheimer's disease patients showed that 32 genes related to Ca^{2+} signaling were dysregulated [242]. The recent improvements for astrocytic Ca^{2+} indicators made it possible to study Ca^{2+} signals *in vivo* in mouse models and elucidate their functions, especially during neurodegenerative processes. For example, aberrant Ca^{2+} signals have been found in reactive astrocytes [243]. Astrocytic hyperactivity was further observed *in vivo* in several mouse models of AD [212], [213]. Also, astrocytes derived from the P301S tau mouse model develop early functional deficiencies, suggesting an effect of tau on astrocyte function [165].

Therefore, the next aim was to investigate whether cortical astrocytes in Aldh1l1/P301S mice are functionally impaired. For this, an *in vivo* approach was applied by implanting a cranial window over the somatosensory cortex and a membrane tethered GECI to visualize Ca^{2+} signals of astrocytic microdomains was injected. Ca^{2+} transients from several ROIs in the somatosensory cortex in mice three months post injection were imaged. While no differences could be observed in general microdomain attributes, such as size and total number, time-

lapse imaging revealed an increased astrocytic activity. A significantly enhanced frequency of Ca^{2+} signaling events were observed in Aldh1l1/P301S mice, compared to control group. The hyperactive behavior of astrocytes in that model could be a sign of reactive astrocytes, and of early degenerative processes. These results go in line with previous published studies of astrocytic hyperactivity during neurodegeneration [212], [213] and tau mediated astrocytic dysfunctions [15], [165]. Thus, astrocytes alone might already be a predecessor or contributor to neurodegenerative processes in primary tauopathies. Consequently, pathological changes in astrocytic microdomain activity therefore might also impact neuronal synapses, which was addressed in the next experiment.

4.5 Excitatory bipartite synapse loss is an early event in Aldh1l1/P301S mice

Astrocytes are in close contact to synapses via their small PAPs, as postulated in the concept of the "tripartite synapse". Upon synaptic activation, neurotransmitters released into the synaptic cleft can not only be detected by the postsynaptic compartment, but also by small contacting PAPs which respond with intracellular elevations of Ca^{2+} and, in turn, a release of gliotransmitters [244], [245]. In other words, astrocytes are able to modulate synaptic function via uptake and secretion of neuroactive substances [14]. The major excitatory neurotransmitter in the human brain is glutamate, which can be secreted and transported by both neurons and astrocytes. Glutamate can be released from astrocytes in a Ca^{2+} dependent manner [246] and can take on fast modulatory actions on excitatory synaptic transmission [247]. Aberrant, elevated astrocytic Ca^{2+} signals are implicated in neurodegenerative processes [243].

Further, previous studies showed a reduction of excitatory synapses in post mortem brain tissue of tauopathy patients which is confined to the astrocytic domain [164].

Therefore, the next set of experiments aimed to resolve if excitatory synapse loss could also be observed in the Aldh1l1/P301S model. For this, brain sections were obtained and stained with synaptic markers for excitatory pre- (VGLUT1) and postsynapses (HOMER1) to investigate whether a synapse loss occurs within the domain of mKate2 positive astrocytes and neighboring areas in the somatosensory cortex. By using automated puncta quantification with SynQuant Image J plugin, pre- and postsynapses in the astrocytic domain and outside were quantified in animals one and three months p.i. A nonsignificant trend in reduction of presynaptic puncta one month p.i. could be observed in Aldh1l1/P301S animals, which became significant three months p.i., compared to control group. Regarding postsynapses, no reduction of synaptic puncta was observable one month p.i. However, a substantial reduction of postsynaptic puncta could be seen three months p.i., compared to control. Interestingly, the synapse loss in both synaptic compartments was not restricted to the astrocytic territory but was also evident in neighboring areas not occupied by mKate2 astrocytes.

These results suggest a significant excitatory synapse loss in somatosensory cortical brain areas in Aldh1l1/P301S mice three months p.i. These results are in good agreement with the loss of excitatory synapses observed in post mortem brains of tauopathy patients [164]. The substantial excitatory synapse loss in this astrocytic tauopathy model may be a consequence of the aberrant Ca^{2+} signals as previously shown. Elevated Ca^{2+} transients in hyperactive astrocytes possibly trigger excess release of glutamate that may act on NMDA receptors on excitatory neuronal synapses which leads to excitotoxicity. Astrocyte derived glutamate can activate pre- and postsynaptic NMDA receptors in several diseases, including AD, leading to enhanced excitatory synaptic transmission and hyperexcitability and thus presumably trigger increased network excitation and neuronal cell death [243]. Further, increased astrocyte Ca^{2+} signals are correlated with elevated extracellular glutamate levels, which contribute to excitotoxicity, as seen in a stroke model [248]. Astrocytes in tauopathies may also lose their function to protect neurons from glutamate neurotoxicity [165]. These studies further strengthen the obtained results.

The fact that synapse loss was also observed in adjacent areas not occupied by mKate2 astrocytes may be explained by an extension of compromised function to neighboring astrocytes. Astrocytes are interconnected through gap junctions formed by hemichannels. Those gap junctions enable a rapid communication and ion exchange between cells [249], [250]. Intracellular Ca^{2+} can spread to neighboring astrocytes via those gap junctions, inducing Ca^{2+} waves that can activate a large astrocyte population [251], [252]. One hypothesis on why synapse loss in the Aldh1l1/P301S model extends to adjacent areas is that hyperactive astrocytes propagate large amounts of Ca^{2+} to neighboring astrocytes. In turn, this may activate pathological downstream cascades also in those neighboring cells, which possibly lead to synapse loss in that areas.

Further, glutamate release from connexin hemichannels could be involved in that whole process. Connexin 43 is a major gap junction protein subunit in astrocytes and connexin hemichannels control the extracellular release of gliotransmitters like glutamate or ATP [249]. Connexin 43 is implicated to play a role in certain neurodegenerative diseases [253], [254]. Under pathological conditions, those hemichannels show an increased activity. One study showed that treatment of cultured mouse astrocytes with Aβ increases glial connexin hemichannel activity and promotes the release of glutamate, inducing neuronal cell death by triggering neuronal hemichannel activity [255]. Possibly a similar mechanism may be responsible for neuronal death in the Aldh1l1/P301S model, but induced by astrocytic tau. It is postulated that increased opening of hemichannels can be triggered by high levels of intracellular Ca^{2+}, resulting in excessive release of glutamate that is toxic to neighboring cells [249], [256], which ultimately further supports those findings.

4.6 Conclusion

Taken together, the results obtained in this thesis suggest a role of pathological tau in astrocytes for the contribution to neurodegenerative processes. Previously thought of as mere bystanders in neurodegenerative diseases, newer findings provide more and more insights that astrocytes are directly involved in pathological changes. Although tau is expressed to a high extent in neurons and only to a limited amount in astrocytes, accumulated pathological tau in astrocytes can affect cell internal processes that may expand to neighboring cells. The results of this thesis provide new insights into pathological mechanisms caused by tau in astrocytes. The obtained results show that phospho-tau can be found in cortical astrocytes in the Aldh1l1/P301S model, which can form star-like structures, similar to what is seen in PSP brains. Further, *in vivo* astrocytic Ca^{2+} imaging revealed that astrocytes in this mouse model acquire a hyperactive profile three months post injection, as seen by an increased firing frequency of Ca^{2+} transients. The elevated firing rate was observed at the level of microdomains, where PAPs are intimately in contact with synapses. By using an immunofluorescence approach, a substantial excitatory synapse loss three months post injection could be observed in both pre- and postsynaptic compartments, which was found among the astrocyte domain and also outside. The increased frequency of Ca^{2+} transients may lead to elevated excitatory gliotransmitter release and therefore to neuronal cell death. Given the fact that synapse loss was also observed in areas not governed by mKate2 astrocytes, the hyperactivity of astrocytes may spread to neighboring cells as high frequency Ca^{2+} waves, which possibly triggers similar pathological cascades in that cells and contacting synapses. However, this may not be the exclusive mechanism for synapse loss in that model. Other mechanisms leading to synapse loss that are not related to Ca^{2+} dependent gliotransmitter release could be involved but remain to be elucidated in future studies.

4.7 Limitations

This mouse model provided insights into tau related pathomechanisms within astrocytes and their synaptic partners. However, for *in vivo* astrocytic Ca^{2+} imaging lightly anesthetized animals were used, which received minimal amounts of isoflurane (0,5 %). Even though the anesthesia state was kept to a minimum, and breath as well as heart rate was measured throughout imaging sessions to make the obtained results comparable between the animals, studies showed that astrocytic Ca^{2+} signals may be suppressed in their functional state during general anesthesia [189], [257]. Therefore, astrocytes may show alterations in Ca^{2+} responses depending on anesthesia depth and type of anesthesia used. Performing Ca^{2+} imaging in completely awake mice may clarify this issue.

4.8 Future aspects

For this thesis, a virus-inducible astrocytic tau mouse model was developed that expresses tau in astrocytes of the whole CNS via systemic transgene delivery. This study focused mainly on pathological aspects in somatosensory cortical regions. Further studies may use this virus approach to study tau mediated pathological changes in astrocytes in other brain regions. Astrocytes are known to be highly heterogeneous in their morphology [258] and expression profiles, which could make them more vulnerable in selected brain regions to degenerative processes [115]. Changes in astrocytic reactivity could be observed region specific in different neurodegenerative diseases [259]–[261]. Further, different brain regions are affected by tau pathology in different tauopathies [262]. Thus, specific brain regional effects of astrocytic tau could be a subject for future research. Further studies are also needed to understand the molecular mechanisms underlying astrocytic hyperactivity in this mouse model and the contribution to synapse loss.

5 Abbreviations

aa	Amino acid
AAV	Adeno-associated virus
AD	Alzheimer's disease
AGD	Argyrophilic grain disease
ALDH1l1	Aldehyde dehydrogenase 1 family member L1
AMPAR	α-amino-3-hydroxy-5-methyl-4-isoxazolepropionic acid receptor
Aβ	Amyloid beta
APP	Amyloid precursor protein
ATP	Adenosine triphosphate
BBB	Blood-brain barrier
bp	Base pair
bpm	Beats per minute
brpm	Breaths per minute
Ca^{2+}	Calcium
CaM	Calmodulin
CBD	Corticobasal degeneration
CBh	Hybrid chicken β-actin
Cdk5	Cycline-dependent kinase 5
CNS	Central nervous system
Cre	Causes recombination
DIO	Double-floxed inverted open reading frame
DNA	Deoxyribonucleic acid
eGFP	Enhanced green fluorescent protein
EtOH	Ethanol
fs	Femtosecond
FTD	Frontotemporal dementia
FTLD	Frontotemporal lobar degeneration
GABA	Gamma-aminobutyric acid
GECI	Genetically encoded calcium indicator

GFAP	Glial fibrillary acidic protein
GGT	Globular glial tauopathy
hMAPT	Human microtubule-associated protein tau
Hz	Hertz
i.p.	Intraperitoneal
KO	Knock out
MHz	Megahertz
MTBR	Microtubule binding region
NA	Numerical aperture
NFT	Neurofibrillary tangles
NMDAR	N-methy-D-aspartate receptor
NaCl	Sodium chloride
NaN_3	Sodium azide
Nl	Nanoliter
PAP	Peripheral astrocytic process
PHF	Paired helical filament
PBS	Phosphate buffered saline
PCR	Polymerase chain reaction
PFA	Paraformaldehyde
p.i.	Post injection
PiD	Pick’s disease
PSP	Progressive supranuclear palsy
ROI	Region of interest
s.c.	Subcutaneous
SEM	Standard error of the mean
SOPF	Specific and opportunistic pathogen free
TA	Tufted astrocyte
V	Volt
vg	Vector genomes
WT	Wild type

6 List of figures & tables

7 References

[1] M. D. Weingarten, A. H. Lockwood, S. Y. Hwo, and M. W. Kirschner, “A protein factor essential for microtubule assembly,” *Proc. Natl. Acad. Sci.*, vol. 72, no. 5, pp. 1858–1862, May 1975, doi: 10.1073/pnas.72.5.1858.

[2] R. L. Neve, P. Harris, K. S. Kosik, D. M. Kurnit, and T. A. Donlon, “Identification of cDNA clones for the human microtubule-associated protein tau and chromosomal localization of the genes for tau and microtubule-associated protein 2,” *Mol. Brain Res.*, vol. 1, no. 3, pp. 271–280, Dec. 1986, doi: 10.1016/0169-328X(86)90033-1.

[3] Y. Wang and E. Mandelkow, “Tau in physiology and pathology,” *Nat. Rev. Neurosci.*, vol. 17, no. 1, pp. 22–35, Jan. 2016, doi: 10.1038/nrn.2015.1.

[4] P. Barbier *et al.*, “Role of tau as a microtubule-associated protein: structural and functional aspects,” *Front. Aging Neurosci.*, vol. 11, p. 204, Aug. 2019, doi: 10.3389/fnagi.2019.00204.

[5] M. Goedert, M. G. Spillantini, R. Jakes, D. Rutherford, and R. A. Crowther, “Multiple isoforms of human microtubule-associated protein tau: sequences and localization in neurofibrillary tangles of Alzheimer’s disease,” *Neuron*, vol. 3, no. 4, pp. 519–526, 1989, doi: 10.1016/0896-6273(89)90210-9.

[6] J. - P Brion, C. Smith, A. - M Couck, J. - M Gallo, and B. H. Anderton, “Developmental changes in τ phosphorylation: fetal τ is transiently phosphorylated in a manner similar to paired helical filament- τ characteristic of Alzheimer’s disease,” *J. Neurochem.*, vol. 61, no. 6, pp. 2071–2080, 1993, doi: 10.1111/j.1471-4159.1993.tb07444.x.

[7] M. G. Spillantini, R. A. Crowther, W. Kamphorst, P. Heutink, and J. C. van Swieten, “Tau pathology in two dutch families with mutations in the microtubule-binding region of tau,” *Am. J. Pathol.*, vol. 153, no. 5, pp. 1359–1363, Nov. 1998, doi: 10.1016/S0002-9440(10)65721-5.

[8] P. Poorkaj *et al.*, “A genomic sequence analysis of the mouse and human microtubule-associated protein tau,” *Mamm. Genome*, vol. 12, no. 9, pp. 700–712, Sep. 2001, doi: 10.1007/s00335-001-2044-8.

[9] F. Hernández and J. Avila, “Tauopathies,” *Cell. Mol. Life Sci.*, vol. 64, no. 17, pp. 2219–2233, Sep. 2007, doi: 10.1007/s00018-007-7220-x.

[10] L. Buée, T. Bussière, V. Buée-Scherrer, A. Delacourte, and P. R. Hof, “Tau protein isoforms, phosphorylation and role in neurodegenerative disorders,” *Brain Res. Rev.*, vol. 33, no. 1, pp. 95–130, Aug. 2000, doi: 10.1016/S0165-0173(00)00019-9.

[11] N. V. Shults *et al.*, “Tau protein in lung smooth muscle cells,” *J. Respir.*, vol. 1, no. 1, pp. 30–39, Nov. 2020, doi: 10.3390/jor1010003.

[12] P. LoPresti, S. Szuchet, S. C. Papasozomenos, R. P. Zinkowski, and L. I. Binder, “Functional implications for the microtubule-associated protein tau: localization in oligodendrocytes,” *Proc. Natl. Acad. Sci.*, vol. 92, no. 22, pp. 10369–10373, Oct. 1995, doi: 10.1073/pnas.92.22.10369.

[13] R. Müller, M. Heinrich, S. Heck, D. Blohm, and C. Richter-Landsberg, “Expression of microtubule-associated proteins MAP2 and tau in cultured rat brain oligodendrocytes,” *Cell Tissue Res.*, vol. 288, no. 2, pp. 239–249, Apr. 1997, doi: 10.1007/s004410050809.

[14] M. A. Kahlson and K. J. Colodner, “Glial tau pathology in tauopathies: functional consequences,” *J. Exp. Neurosci.*, vol. 9, no. S2, pp. 43–50, Jan. 2015, doi: 10.4137/JEN.S25515.

[15] L. A. Ezerskiy *et al.*, “Astrocytic 4R tau expression drives astrocyte reactivity and dysfunction,” *JCI Insight*, vol. 7, no. 1, p. e152012, Jan. 2022, doi: 10.1172/jci.insight.152012.
[16] S. Jeganathan, M. von Bergen, H. Brutlach, H.-J. Steinhoff, and E. Mandelkow, “Global hairpin folding of tau in solution,” *Biochemistry*, vol. 45, no. 7, pp. 2283–2293, Feb. 2006, doi: 10.1021/bi0521543.
[17] J. Chen, Y. Kanai, N. J. Cowan, and N. Hirokawa, “Projection domains of MAP2 and tau determine spacings between microtubules in dendrites and axons,” *Nature*, vol. 360, no. 6405, pp. 674–677, Dec. 1992, doi: 10.1038/360674a0.
[18] T. Guo, W. Noble, and D. P. Hanger, “Roles of tau protein in health and disease,” *Acta Neuropathol.*, vol. 133, no. 5, pp. 665–704, 2017, doi: 10.1007/s00401-017-1707-9.
[19] D. B. Murphy, K. A. Johnson, and G. G. Borisy, “Role of tubulin-associated proteins in microtubule nucleation and elongation,” *J. Mol. Biol.*, vol. 117, no. 1, pp. 33–52, Nov. 1977, doi: 10.1016/0022-2836(77)90021-3.
[20] D. G. Drubin and M. W. Kirschner, “Tau protein function in living cells,” *J. Cell Biol.*, vol. 103, no. 6, pp. 2739–2746, Dec. 1986, doi: 10.1083/jcb.103.6.2739.
[21] T. Crowther, M. Goedert, and C. M. Wischik, “The repeat region of microtubule-associated protein tau forms part of the core of the paired helical filament of Alzheimer’s disease,” *Ann. Med.*, vol. 21, no. 2, pp. 127–132, Jan. 1989, doi: 10.3109/07853898909149199.
[22] N. Gustke, B. Trinczek, J. Biernat, E. M. Mandelkow, and E. Mandelkow, “Domains of τ protein and interactions with microtubules,” *Biochemistry*, vol. 33, no. 32, pp. 9511–9522, 1994, doi: 10.1021/bi00198a017.
[23] A. Venkatramani and D. Panda, “Regulation of neuronal microtubule dynamics by tau: implications for tauopathies,” *Int. J. Biol. Macromol.*, vol. 133, pp. 473–483, Jul. 2019, doi: 10.1016/j.ijbiomac.2019.04.120.
[24] J. Gilley *et al.*, “Age-dependent axonal transport and locomotor changes and tau hypophosphorylation in a ‘P301L’ tau knockin mouse,” *Neurobiol. Aging*, vol. 33, no. 3, pp. 621.e1-621.e15, Mar. 2012, doi: 10.1016/j.neurobiolaging.2011.02.014.
[25] K. Stamer, R. Vogel, E. Thies, E. Mandelkow, and E.-M. Mandelkow, “Tau blocks traffic of organelles, neurofilaments, and APP vesicles in neurons and enhances oxidative stress,” *J. Cell Biol.*, vol. 156, no. 6, pp. 1051–1063, Mar. 2002, doi: 10.1083/jcb.200108057.
[26] Q. Chen *et al.*, “Tau protein is involved in morphological plasticity in hippocampal neurons in response to BDNF,” *Neurochem. Int.*, vol. 60, no. 3, pp. 233–242, Feb. 2012, doi: 10.1016/j.neuint.2011.12.013.
[27] M. L. Frandemiche *et al.*, “Activity-dependent tau protein translocation to excitatory synapse is disrupted by exposure to amyloid-beta oligomers,” *J. Neurosci.*, vol. 34, no. 17, pp. 6084–6097, Apr. 2014, doi: 10.1523/JNEUROSCI.4261-13.2014.
[28] R. Velazquez *et al.*, “Acute tau knockdown in the hippocampus of adult mice causes learning and memory deficits,” *Aging Cell*, vol. 17, no. 4, p. e12775, Aug. 2018, doi: 10.1111/acel.12775.
[29] J. L. Cantero, E. Hita-Yañez, B. Moreno-Lopez, F. Portillo, A. Rubio, and J.

Avila, “Tau protein role in sleep-wake cycle,” *J. Alzheimer’s Dis.*, vol. 21, no. 2, pp. 411–421, Aug. 2010, doi: 10.3233/JAD-2010-100285.
[30] J. L. Cantero, B. Moreno-Lopez, F. Portillo, A. Rubio, E. Hita-Yañez, and J. Avila, “Role of tau protein on neocortical and hippocampal oscillatory patterns,” *Hippocampus*, vol. 21, no. 8, pp. 827–834, 2010, doi: 10.1002/hipo.20798.
[31] J. K. Holth *et al.*, “The sleep-wake cycle regulates brain interstitial fluid tau in mice and CSF tau in humans,” *Science (80-.).*, vol. 363, no. 6429, pp. 880–884, Feb. 2019, doi: 10.1126/science.aav2546.
[32] C.-W. Chang, E. Shao, and L. Mucke, “Tau: Enabler of diverse brain disorders and target of rapidly evolving therapeutic strategies,” *Science (80-.).*, vol. 371, no. 6532, p. eabb8255, Feb. 2021, doi: 10.1126/science.abb8255.
[33] J. Avila, J. J. Lucas, M. Pérez, and F. Hernández, “Role of tau protein in both physiological and pathological conditions,” *Physiol. Rev.*, vol. 84, no. 2. pp. 361–384, Apr. 2004, doi: 10.1152/physrev.00024.2003.
[34] D. P. Hanger, B. H. Anderton, and W. Noble, “Tau phosphorylation: the therapeutic challenge for neurodegenerative disease,” *Trends Mol. Med.*, vol. 15, no. 3, pp. 112–119, 2009, doi: 10.1016/j.molmed.2009.01.003.
[35] T. Kimura, K. Ishiguro, and S. Hisanaga, “Physiological and pathological phosphorylation of tau by Cdk5,” *Front. Mol. Neurosci.*, vol. 7, p. 65, Jul. 2014, doi: 10.3389/fnmol.2014.00065.
[36] L. Martin *et al.*, “Tau protein kinases: involvement in Alzheimer’s disease,” *Ageing Res. Rev.*, vol. 12, no. 1, pp. 289–309, Jan. 2013, doi: 10.1016/j.arr.2012.06.003.
[37] W. Noble, D. P. Hanger, C. C. J. Miller, and S. Lovestone, “The importance of tau phosphorylation for neurodegenerative diseases,” *Front. Neurol.*, vol. 4, p. 83, 2013, doi: 10.3389/fneur.2013.00083.
[38] T. F. Gendron and L. Petrucelli, “The role of tau in neurodegeneration,” *Mol. Neurodegener.*, vol. 4, p. 13, 2009, doi: 10.1186/1750-1326-4-13.
[39] S. L. Morris *et al.*, “Defined tau phosphospecies differentially inhibit fast axonal transport through activation of two independent signaling pathways,” *Front. Mol. Neurosci.*, vol. 13, p. 610037, Jan. 2021, doi: 10.3389/fnmol.2020.610037.
[40] K. Shahpasand *et al.*, “Regulation of mitochondrial transport and inter-microtubule spacing by tau phosphorylation at the sites hyperphosphorylated in Alzheimer’s disease,” *J. Neurosci.*, vol. 32, no. 7, pp. 2430–2441, Feb. 2012, doi: 10.1523/JNEUROSCI.5927-11.2012.
[41] M. Goedert, R. Jakes, and E. Vanmechelen, “Monoclonal antibody AT8 recognises tau protein phosphorylated at both serine 202 and threonine 205,” *Neurosci. Lett.*, vol. 189, no. 3, pp. 167–170, 1995, doi: 10.1016/0304-3940(95)11484-E.
[42] H. Zempel, E. Thies, E.-M. Mandelkow, and E.-M. Mandelkow, “Amyloid-beta oligomers cause localized Ca2+ elevation, missorting of endogenous tau into dendrites, tau phosphorylation, and destruction of microtubules and spines,” *J. Neurosci.*, vol. 30, no. 36, pp. 11938–11950, Sep. 2010, doi: 10.1523/JNEUROSCI.2357-10.2010.
[43] T. Kimura, G. Sharma, K. Ishiguro, and S. Hisanaga, “Phospho-tau bar

code: analysis of phosphoisotypes of tau and its application to tauopathy," *Front. Neurosci.*, vol. 12, p. 44, Feb. 2018, doi: 10.3389/fnins.2018.00044.
[44] M. Goedert, "Tau gene mutations and their effects," *Mov. Disord.*, vol. 20, no. SUPPL. 12, pp. 45–52, 2005, doi: 10.1002/mds.20539.
[45] P. Heutink *et al.*, "Hereditary frontotemporal dementia is linked to chromosome 17q21-q22: a genetic and clinicopathological study of three dutch families," *Ann. Neurol.*, vol. 41, no. 2, pp. 150–159, Feb. 1997, doi: 10.1002/ana.410410205.
[46] P. Poorkaj *et al.*, "Tau is a candidate gene for chromosome 17 frontotemporal dementia," *Ann. Neurol.*, vol. 43, no. 6, pp. 815–825, Jun. 1998, doi: 10.1002/ana.410430617.
[47] M. Hutton *et al.*, "Association of missense and 5′-splice-site mutations in tau with the inherited dementia FTDP-17," *Nature*, vol. 393, pp. 702–705, Jun. 1998, doi: 10.1038/31508.
[48] C. V. Greaves and J. D. Rohrer, "An update on genetic frontotemporal dementia," *J. Neurol.*, vol. 266, no. 8, pp. 2075–2086, 2019, doi: 10.1007/s00415-019-09363-4.
[49] R. Shafei *et al.*, "Two pathologically confirmed cases of novel mutations in the MAPT gene causing frontotemporal dementia," *Neurobiol. Aging*, vol. 87, pp. 141.e15-141.e20, Mar. 2020, doi: 10.1016/j.neurobiolaging.2019.11.009.
[50] D. C. Chung, S. Roemer, L. Petrucelli, and D. W. Dickson, "Cellular and pathological heterogeneity of primary tauopathies," *Mol. Neurodegener.*, vol. 16, no. 1, p. 57, Dec. 2021, doi: 10.1186/s13024-021-00476-x.
[51] B. Ghetti, A. L. Oblak, B. F. Boeve, K. A. Johnson, B. C. Dickerson, and M. Goedert, "Invited review: frontotemporal dementia caused by microtubule-associated protein tau gene (MAPT) mutations: a chameleon for neuropathology and neuroimaging," *Neuropathol. Appl. Neurobiol.*, vol. 41, no. 1, pp. 24–46, Feb. 2015, doi: 10.1111/nan.12213.
[52] K. A. Josephs, "Current understanding of neurodegenerative diseases associated with the protein tau," *Mayo Clin. Proc.*, vol. 92, no. 8, pp. 1291–1303, Aug. 2017, doi: 10.1016/j.mayocp.2017.04.016.
[53] M. S. Forman, "Genotype-phenotype correlations in FTDP-17: does form follow function?," *Exp. Neurol.*, vol. 187, no. 2, pp. 229–234, Jun. 2004, doi: 10.1016/j.expneurol.2004.01.031.
[54] G. G. Kovacs, "Tauopathies," in *Handbook of Clinical Neurology*, vol. 145, 2018, pp. 355–368.
[55] M.-L. Caillet-Boudin, L. Buée, N. Sergeant, and B. Lefebvre, "Regulation of human MAPT gene expression," *Mol. Neurodegener.*, vol. 10, p. 28, Dec. 2015, doi: 10.1186/s13024-015-0025-8.
[56] A. J. Myers *et al.*, "The MAPT H1c risk haplotype is associated with increased expression of tau and especially of 4 repeat containing transcripts," *Neurobiol. Dis.*, vol. 25, no. 3, pp. 561–570, Mar. 2007, doi: 10.1016/j.nbd.2006.10.018.
[57] P. M. Stanford, "Mutations in the tau gene that cause an increase in three repeat tau and frontotemporal dementia," *Brain*, vol. 126, no. 4, pp. 814–826, Apr. 2003, doi: 10.1093/brain/awg090.
[58] T. Arendt, J. T. Stieler, and M. Holzer, "Tau and tauopathies," *Brain Res.*

Bull., vol. 126, pp. 238–292, Sep. 2016, doi: 10.1016/j.brainresbull.2016.08.018.
[59] S. Barghorn *et al.*, “Structure, microtubule interactions, and paired helical filament aggregation by tau mutants of frontotemporal dementias,” *Biochemistry*, vol. 39, no. 38, pp. 11714–11721, Sep. 2000, doi: 10.1021/bi000850r.
[60] K. H. Strang, T. E. Golde, and B. I. Giasson, “MAPT mutations, tauopathy, and mechanisms of neurodegeneration,” *Lab. Investig.*, vol. 99, no. 7, pp. 912–928, Jul. 2019, doi: 10.1038/s41374-019-0197-x.
[61] C. E. G. Leyns and D. M. Holtzman, “Glial contributions to neurodegeneration in tauopathies,” *Mol. Neurodegener.*, vol. 12, no. 1, p. 50, Dec. 2017, doi: 10.1186/s13024-017-0192-x.
[62] E. Iseki *et al.*, “Familial frontotemporal dementia and parkinsonism with a novel N296H mutation in exon 10 of the tau gene and a widespread tau accumulation in the glial cells,” *Acta Neuropathol.*, vol. 102, no. 3, pp. 285–292, Sep. 2001, doi: 10.1007/s004010000333.
[63] T. Hashimoto *et al.*, “Abnormal activity in the globus pallidus in off-period dystonia,” *Ann. Neurol.*, vol. 49, no. 2, pp. 242–245, Feb. 2001, doi: 10.1002/1531-8249(20010201)49:2<242::AID-ANA44>3.0.CO;2-G.
[64] I. D’Souza and G. D. Schellenberg, “Regulation of tau isoform expression and dementia,” *Biochim. Biophys. Acta - Mol. Basis Dis.*, vol. 1739, no. 2–3, pp. 104–115, Jan. 2005, doi: 10.1016/j.bbadis.2004.08.009.
[65] M. Cruts, J. Theuns, and C. Van Broeckhoven, “Locus-specific mutation databases for neurodegenerative brain diseases,” *Hum. Mutat.*, vol. 33, no. 9, pp. 1340–1344, Sep. 2012, doi: 10.1002/humu.22117.
[66] C. M. Karch *et al.*, “A comprehensive resource for induced pluripotent stem cells from patients with primary tauopathies,” *Stem Cell Reports*, vol. 13, no. 5, pp. 939–955, Nov. 2019, doi: 10.1016/j.stemcr.2019.09.006.
[67] R. Dayanandan *et al.*, “Mutations in tau reduce its microtubule binding properties in intact cells and affect its phosphorylation,” *FEBS Lett.*, vol. 446, no. 2–3, pp. 228–232, Mar. 1999, doi: 10.1016/S0014-5793(99)00222-7.
[68] M. Hasegawa, M. J. Smith, and M. Goedert, “Tau proteins with FTDP-17 mutations have a reduced ability to promote microtubule assembly,” *FEBS Lett.*, vol. 437, no. 3, pp. 207–210, 1998, doi: 10.1016/S0014-5793(98)01217-4.
[69] M. Goedert, R. Jakes, and R. A. Crowther, “Effects of frontotemporal dementia FTDP-17 mutations on heparin-induced assembly of tau filaments,” *FEBS Lett.*, vol. 450, no. 3, pp. 306–311, 1999, doi: 10.1016/S0014-5793(99)00508-6.
[70] A. D. Sperfeld *et al.*, “FTDP-17: an early-onset phenotype with parkinsonism and epileptic seizures caused by a novel mutation,” *Ann. Neurol.*, vol. 46, no. 5, pp. 708–715, Nov. 1999, doi: 10.1002/1531-8249(199911)46:5<708::AID-ANA5>3.0.CO;2-K.
[71] O. Bugiani *et al.*, “Frontotemporal dementia and corticobasal degeneration in a family with a P301S mutation in tau,” *J. Neuropathol. Exp. Neurol.*, vol. 58, no. 6, pp. 667–677, Jun. 1999, doi: 10.1097/00005072-199906000-00011.

[72] A. Lossos *et al.*, “Frontotemporal dementia and parkinsonism with the P301S tau gene mutation in a jewish family,” *J. Neurol.*, vol. 250, no. 6, pp. 733–740, Jun. 2003, doi: 10.1007/s00415-003-1074-4.
[73] B. Allen *et al.*, “Abundant tau filaments and nonapoptotic neurodegeneration in transgenic mice expressing human P301S tau protein,” *J. Neurosci.*, vol. 22, no. 21, pp. 9340–9351, Nov. 2002, doi: 10.1523/JNEUROSCI.22-21-09340.2002.
[74] Y. Yoshiyama *et al.*, “Synapse loss and microglial activation precede tangles in a P301S tauopathy mouse model,” *Neuron*, vol. 53, no. 3, pp. 337–351, Feb. 2007, doi: 10.1016/j.neuron.2007.01.010.
[75] H. Takeuchi *et al.*, “P301S mutant human tau transgenic mice manifest early symptoms of human tauopathies with dementia and altered sensorimotor gating,” *PLoS One*, vol. 6, no. 6, p. e21050, Jun. 2011, doi: 10.1371/journal.pone.0021050.
[76] A. Lathuilière *et al.*, “Motifs in the tau protein that control binding to microtubules and aggregation determine pathological effects,” *Sci. Rep.*, vol. 7, no. 1, p. 13556, Dec. 2017, doi: 10.1038/s41598-017-13786-2.
[77] J. M. McCarthy *et al.*, “Development of P301S tau seeded organotypic hippocampal slice cultures to study potential therapeutics,” *Sci. Rep.*, vol. 11, no. 1, p. 10309, Dec. 2021, doi: 10.1038/s41598-021-89230-3.
[78] M. Goedert, D. S. Eisenberg, and R. A. Crowther, “Propagation of tau aggregates and neurodegeneration,” *Annu. Rev. Neurosci.*, vol. 40, pp. 189–210, 2017, doi: 10.1146/annurev-neuro-072116-031153.
[79] J. A. Macdonald *et al.*, “Assembly of transgenic human P301S tau is necessary for neurodegeneration in murine spinal cord,” *Acta Neuropathol. Commun.*, vol. 7, no. 1, p. 44, Dec. 2019, doi: 10.1186/s40478-019-0695-5.
[80] I. Ferrer *et al.*, “Familial behavioral variant frontotemporal dementia associated with astrocyte-predominant tauopathy,” *J. Neuropathol. Exp. Neurol.*, vol. 74, no. 4, pp. 370–379, Apr. 2015, doi: 10.1097/NEN.0000000000000180.
[81] R. Virchow, “Die Cellularpathologie in Ihrer Begruendung auf Physiologische und Pathologische Gewebelehre (ed. Hirschwald, A.),” *Berlin*, 1858.
[82] C. Golgi, “Sulla sostanza grigia del cervello,” *Gazz. Med. Ital. Lomb.*, vol. 6, pp. 244–246, 1873.
[83] M. von Lenhossek, “Zur Kenntnis der Neuroglia des menschlichen Rückenmarkes.,” *Verh. Anat. Ges.*, vol. 5, pp. 193–221, 1891.
[84] W. L. Andriezen, “The neuroglia elements in the human brain,” *BMJ*, vol. 2, no. 1700, pp. 227–230, Jul. 1893, doi: 10.1136/bmj.2.1700.227.
[85] N. A. Oberheim, S. A. Goldman, and M. Nedergaard, “Heterogeneity of astrocytic form and function,” in *Methods in Molecular Biology*, vol. 814, 2012, pp. 23–45.
[86] A. Verkhratsky and M. Nedergaard, “Physiology of astroglia,” *Physiol. Rev.*, vol. 98, no. 1, pp. 239–389, Jan. 2018, doi: 10.1152/physrev.00042.2016.
[87] B. S. Khakh and B. Deneen, “The emerging nature of astrocyte diversity,” *Annu. Rev. Neurosci.*, vol. 42, no. 1, pp. 187–207, Jul. 2019, doi: 10.1146/annurev-neuro-070918-050443.

[88] C.-C. John Lin *et al.*, “Identification of diverse astrocyte populations and their malignant analogs,” *Nat. Neurosci.*, vol. 20, no. 3, pp. 396–405, Mar. 2017, doi: 10.1038/nn.4493.
[89] M. Y. Batiuk *et al.*, “Identification of region-specific astrocyte subtypes at single cell resolution,” *Nat. Commun.*, vol. 11, no. 1, p. 1220, Dec. 2020, doi: 10.1038/s41467-019-14198-8.
[90] E. A. Bushong, M. E. Martone, Y. Z. Jones, and M. H. Ellisman, “Protoplasmic astrocytes in CA1 stratum radiatum occupy separate anatomical domains,” *J. Neurosci.*, vol. 22, no. 1, pp. 183–192, Jan. 2002, doi: 10.1523/JNEUROSCI.22-01-00183.2002.
[91] H. K. Kimelberg, “Functions of mature mammalian astrocytes: a current view,” *Neurosci.*, vol. 16, no. 1, pp. 79–106, Feb. 2010, doi: 10.1177/1073858409342593.
[92] W.-S. Chung *et al.*, “Astrocytes mediate synapse elimination through MEGF10 and MERTK pathways,” *Nature*, vol. 504, no. 7480, pp. 394–400, Dec. 2013, doi: 10.1038/nature12776.
[93] L. P. Diniz, I. C. P. Matias, M. N. Garcia, and F. C. A. Gomes, “Astrocytic control of neural circuit formation: highlights on TGF-beta signaling,” *Neurochem. Int.*, vol. 78, pp. 18–27, Dec. 2014, doi: 10.1016/j.neuint.2014.07.008.
[94] W. Chung, N. J. Allen, and C. Eroglu, “Astrocytes control synapse formation, function, and elimination,” *Cold Spring Harb. Perspect. Biol.*, vol. 7, no. 9, p. a020370, Sep. 2015, doi: 10.1101/cshperspect.a020370.
[95] W. Walz, “Role of glial cells in the regulation of the brain ion microenvironment,” *Prog. Neurobiol.*, vol. 33, no. 4, pp. 309–333, Jan. 1989, doi: 10.1016/0301-0082(89)90005-1.
[96] M. E. Hatten and C. A. Mason, “Mechanisms of glial-guided neuronal migration in vitro and in vivo,” *Experientia*, vol. 46, no. 9, pp. 907–916, Sep. 1990, doi: 10.1007/BF01939383.
[97] J. Su *et al.*, “Retinal inputs signal astrocytes to recruit interneurons into visual thalamus,” *Proc. Natl. Acad. Sci.*, vol. 117, no. 5, pp. 2671–2682, Feb. 2020, doi: 10.1073/pnas.1913053117.
[98] M. Lavialle, G. Aumann, E. Anlauf, F. Pröls, M. Arpin, and A. Derouiche, “Structural plasticity of perisynaptic astrocyte processes involves ezrin and metabotropic glutamate receptors,” *Proc. Natl. Acad. Sci.*, vol. 108, no. 31, pp. 12915–12919, Aug. 2011, doi: 10.1073/pnas.1100957108.
[99] Y. Bernardinelli, D. Muller, and I. Nikonenko, “Astrocyte-synapse structural plasticity,” *Neural Plast.*, vol. 2014:23210, 2014, doi: 10.1155/2014/232105.
[100] E. Bindocci, I. Savtchouk, N. Liaudet, D. Becker, G. Carriero, and A. Volterra, “Three-dimensional Ca 2+ imaging advances understanding of astrocyte biology,” *Science (80-.).*, vol. 356, no. 6339, p. eaai8185, May 2017, doi: 10.1126/science.aai8185.
[101] M. R. Witcher, Y. D. Park, M. R. Lee, S. Sharma, K. M. Harris, and S. A. Kirov, “Three-dimensional relationships between perisynaptic astroglia and human hippocampal synapses,” *Glia*, vol. 58, no. 5, pp. 572–587, 2010, doi: 10.1002/glia.20946.
[102] J. P. Heller and D. A. Rusakov, “The Nanoworld of the tripartite synapse:

insights from super-resolution microscopy," *Front. Cell. Neurosci.*, vol. 11, p. 374, Nov. 2017, doi: 10.3389/fncel.2017.00374.
[103] A. Semyanov and A. Verkhratsky, "Astrocytic processes: from tripartite synapses to the active milieu," *Trends Neurosci.*, vol. 44, no. 10, pp. 781–792, Oct. 2021, doi: 10.1016/j.tins.2021.07.006.
[104] J. Hirrlinger, S. Hulsmann, and F. Kirchhoff, "Astroglial processes show spontaneous motility at active synaptic terminals in situ," *Eur. J. Neurosci.*, vol. 20, no. 8, pp. 2235–2239, Oct. 2004, doi: 10.1111/j.1460-9568.2004.03689.x.
[105] A. Araque, V. Parpura, R. P. Sanzgiri, and P. G. Haydon, "Tripartite synapses: glia, the unacknowledged partner," *Trends Neurosci.*, vol. 22, no. 5, pp. 208–215, May 1999, doi: 10.1016/S0166-2236(98)01349-6.
[106] G. Perea, M. Navarrete, and A. Araque, "Tripartite synapses: astrocytes process and control synaptic information," *Trends Neurosci.*, vol. 32, no. 8, pp. 421–431, Aug. 2009, doi: 10.1016/j.tins.2009.05.001.
[107] N. A. Oberheim, X. Wang, S. Goldman, and M. Nedergaard, "Astrocytic complexity distinguishes the human brain," *Trends Neurosci.*, vol. 29, no. 10, pp. 547–553, Oct. 2006, doi: 10.1016/j.tins.2006.08.004.
[108] A. Volterra and J. Meldolesi, "Astrocytes, from brain glue to communication elements: the revolution continues," *Nat. Rev. Neurosci.*, vol. 6, no. 8, pp. 626–640, Aug. 2005, doi: 10.1038/nrn1722.
[109] A. Verkhratsky and M. Nedergaard, "Astroglial cradle in the life of the synapse," *Philos. Trans. R. Soc. B Biol. Sci.*, vol. 369, no. 1654, p. 20130595, Oct. 2014, doi: 10.1098/rstb.2013.0595.
[110] P. J. Magistretti, "Neuron–glia metabolic coupling and plasticity," *J. Exp. Biol.*, vol. 209, no. 12, pp. 2304–2311, Jun. 2006, doi: 10.1242/jeb.02208.
[111] I. Allaman, M. Bélanger, and P. J. Magistretti, "Astrocyte–neuron metabolic relationships: for better and for worse," *Trends Neurosci.*, vol. 34, no. 2, pp. 76–87, Feb. 2011, doi: 10.1016/j.tins.2010.12.001.
[112] J. D. Rothstein *et al.*, "Localization of neuronal and glial glutamate transporters," *Neuron*, vol. 13, no. 3, pp. 713–725, Sep. 1994, doi: 10.1016/0896-6273(94)90038-8.
[113] J. Kang, L. Jiang, S. A. Goldman, and M. Nedergaard, "Astrocyte-mediated potentiation of inhibitory synaptic transmission," *Nat. Neurosci.*, vol. 1, no. 8, pp. 683–692, Dec. 1998, doi: 10.1038/3684.
[114] M. Navarrete and A. Araque, "Endocannabinoids potentiate synaptic transmission through stimulation of astrocytes," *Neuron*, vol. 68, no. 1, pp. 113–126, Oct. 2010, doi: 10.1016/j.neuron.2010.08.043.
[115] I. Matias, J. Morgado, and F. C. A. Gomes, "Astrocyte heterogeneity: impact to brain aging and disease," *Front. Aging Neurosci.*, vol. 11, p. 59, Mar. 2019, doi: 10.3389/fnagi.2019.00059.
[116] C. R. Rose, L. Felix, A. Zeug, D. Dietrich, A. Reiner, and C. Henneberger, "Astroglial glutamate signaling and uptake in the hippocampus," *Front. Mol. Neurosci.*, vol. 10, p. 451, Jan. 2018, doi: 10.3389/fnmol.2017.00451.
[117] T. Abe, H. Sugihara, H. Nawa, R. Shigemoto, N. Mizuno, and S. Nakanishi, "Molecular characterization of a novel metabotropic glutamate receptor mGluR5 coupled to inositol phosphate/Ca2+ signal transduction," *J. Biol. Chem.*, vol. 267, no. 19, pp. 13361–13368, 1992, doi: 10.1016/s0021-

9258(18)42219-3.
[118] L. Pasti, A. Volterra, T. Pozzan, and G. Carmignoto, “Intracellular calcium oscillations in astrocytes: a highly plastic, bidirectional form of communication between neurons and astrocytes in situ,” *J. Neurosci.*, vol. 17, no. 20, pp. 7817–7830, Oct. 1997, doi: 10.1523/JNEUROSCI.17-20-07817.1997.
[119] S. J. Bradley and R. A. J. Challiss, “G protein-coupled receptor signalling in astrocytes in health and disease: A focus on metabotropic glutamate receptors,” *Biochem. Pharmacol.*, vol. 84, no. 3, pp. 249–259, Aug. 2012, doi: 10.1016/j.bcp.2012.04.009.
[120] C. González-Arias and G. Perea, *Gliotransmission at tripartite synapses*. Springer International Publishing, 2019.
[121] M. M. Halassa, T. Fellin, and P. G. Haydon, “The tripartite synapse: roles for gliotransmission in health and disease,” *Trends Mol. Med.*, vol. 13, no. 2, pp. 54–63, 2007, doi: 10.1016/j.molmed.2006.12.005.
[122] S. Koizumi, “Synchronization of Ca2+ oscillations: involvement of ATP release in astrocytes,” *FEBS J.*, vol. 277, no. 2, pp. 286–292, Jan. 2010, doi: 10.1111/j.1742-4658.2009.07438.x.
[123] B.-E. Yoon and C. J. Lee, “GABA as a rising gliotransmitter,” *Front. Neural Circuits*, vol. 8, p. 141, Dec. 2014, doi: 10.3389/fncir.2014.00141.
[124] S. Lee *et al.*, “Channel-mediated tonic GABA release from glia,” *Science (80-.).*, vol. 330, no. 6005, pp. 790–796, Nov. 2010, doi: 10.1126/science.1184334.
[125] N. B. Hamilton and D. Attwell, “Do astrocytes really exocytose neurotransmitters?,” *Nat. Rev. Neurosci.*, vol. 11, no. 4, pp. 227–238, 2010, doi: 10.1038/nrn2803.
[126] M. Santello, C. Calì, and P. Bezzi, “Gliotransmission and the tripartite synapse,” in *Advances in Experimental Medicine and Biology*, vol. 970, 2012, pp. 307–331.
[127] H. R. Parri, T. M. Gould, and V. Crunelli, “Spontaneous astrocytic Ca2+ oscillations in situ drive NMDAR-mediated neuronal excitation,” *Nat. Neurosci.*, vol. 4, no. 8, pp. 803–812, Aug. 2001, doi: 10.1038/90507.
[128] T. Fellin, O. Pascual, S. Gobbo, T. Pozzan, P. G. Haydon, and G. Carmignoto, “Neuronal synchrony mediated by astrocytic glutamate through activation of extrasynaptic NMDA receptors,” *Neuron*, vol. 43, no. 5, pp. 729–743, Sep. 2004, doi: 10.1016/j.neuron.2004.08.011.
[129] M. C. Angulo, “Glutamate released from glial cells synchronizes neuronal activity in the hippocampus,” *J. Neurosci.*, vol. 24, no. 31, pp. 6920–6927, Aug. 2004, doi: 10.1523/JNEUROSCI.0473-04.2004.
[130] P. Jourdain *et al.*, “Glutamate exocytosis from astrocytes controls synaptic strength,” *Nat. Neurosci.*, vol. 10, no. 3, pp. 331–339, Mar. 2007, doi: 10.1038/nn1849.
[131] N. Bazargani and D. Attwell, “Astrocyte calcium signaling: the third wave,” *Nat. Neurosci.*, vol. 19, no. 2, pp. 182–189, Feb. 2016, doi: 10.1038/nn.4201.
[132] A. H. Cornell-Bell, P. G. Thomas, and J. M. Caffrey, “Ca2+ and filopodial responses to glutamate in cultured astrocytes and neurons,” *Can. J. Physiol. Pharmacol.*, vol. 70, p. Suppl:S206-S218, May 1992, doi:

10.1139/y92-264.
[133] A. H. Cornell-Bell, S. M. Finkbeiner, M. S. Cooper, and S. J. Smith, “Glutamate induces calcium waves in cultured astrocytes: long-range glial signaling,” *Science (80-.).*, vol. 247, no. 4941, pp. 470–473, Jan. 1990, doi: 10.1126/science.1967852.
[134] J. T. Porter and K. D. McCarthy, “Hippocampal astrocytes in situ respond to glutamate released from synaptic terminals,” *J. Neurosci.*, vol. 16, no. 16, pp. 5073–5081, Aug. 1996, doi: 10.1523/JNEUROSCI.16-16-05073.1996.
[135] V. Parpura, T. A. Basarsky, F. Liu, K. Jeftinija, S. Jeftinija, and P. G. Haydon, “Glutamate-mediated astrocyte–neuron signalling,” *Nature*, vol. 369, no. 6483, pp. 744–747, Jun. 1994, doi: 10.1038/369744a0.
[136] E. Shigetomi *et al.*, “Imaging calcium microdomains within entire astrocyte territories and endfeet with GCaMPs expressed using adeno-associated viruses,” *J. Gen. Physiol.*, vol. 141, no. 5, pp. 633–647, 2013, doi: 10.1085/jgp.201210949.
[137] A. Agarwal *et al.*, “Transient opening of the mitochondrial permeability transition pore induces microdomain calcium transients in astrocyte processes,” *Neuron*, vol. 93, no. 3, pp. 587-605.e7, Feb. 2017, doi: 10.1016/j.neuron.2016.12.034.
[138] B. S. Khakh and K. D. McCarthy, “Astrocyte calcium signaling: from observations to functions and the challenges therein,” *Cold Spring Harb. Perspect. Biol.*, vol. 7, no. 4, p. a020404, Apr. 2015, doi: 10.1101/cshperspect.a020404.
[139] A. Lia *et al.*, “Calcium signals in astrocyte microdomains, a decade of great advances,” *Front. Cell. Neurosci.*, vol. 15, p. 673433, Jun. 2021, doi: 10.3389/fncel.2021.673433.
[140] J. L. Stobart *et al.*, “Cortical circuit activity evokes rapid astrocyte calcium signals on a similar timescale to neurons,” *Neuron*, vol. 98, no. 4, pp. 726-735.e4, May 2018, doi: 10.1016/j.neuron.2018.03.050.
[141] N. Ahmadpour, M. Kantroo, and J. L. Stobart, “Extracellular calcium influx pathways in astrocyte calcium microdomain physiology,” *Biomolecules*, vol. 11, no. 10, p. 1467, Oct. 2021, doi: 10.3390/biom11101467.
[142] C. Giaume and L. Venance, “Intercellular calcium signaling and gap junctional communication in astrocytes.,” *Glia*, vol. 24, no. 1, pp. 50–64, Sep. 1998, [Online]. Available: http://www.ncbi.nlm.nih.gov/pubmed/9700489.
[143] S. Finkbeiner, “Calcium waves in astrocytes-filling in the gaps,” *Neuron*, vol. 8, no. 6, pp. 1101–1108, 1992, doi: 10.1016/0896-6273(92)90131-V.
[144] K. S. Christopherson *et al.*, “Thrombospondins are astrocyte-secreted proteins that promote CNS synaptogenesis,” *Cell*, vol. 120, no. 3, pp. 421–433, Feb. 2005, doi: 10.1016/j.cell.2004.12.020.
[145] E. V. Jones, Y. Bernardinelli, Y. C. Tse, S. Chierzi, T. P. Wong, and K. K. Murai, “Astrocytes control glutamate receptor levels at developing synapses through SPARC-β-integrin interactions,” *J. Neurosci.*, vol. 31, no. 11, pp. 4154–4165, Mar. 2011, doi: 10.1523/JNEUROSCI.4757-10.2011.
[146] C. C. Steinmetz and G. G. Turrigiano, “Tumor necrosis factor alpha signaling maintains the ability of cortical synapses to express synaptic

scaling," *J. Neurosci.*, vol. 30, no. 44, pp. 14685–14690, Nov. 2010, doi: 10.1523/JNEUROSCI.2210-10.2010.
[147] N. Takata *et al.*, "Astrocyte calcium signaling transforms cholinergic modulation to cortical plasticity in vivo," *J. Neurosci.*, vol. 31, no. 49, pp. 18155–18165, Dec. 2011, doi: 10.1523/JNEUROSCI.5289-11.2011.
[148] M. Navarrete *et al.*, "Astrocytes mediate in vivo cholinergic-induced synaptic plasticity," *PLoS Biol.*, vol. 10, no. 2, p. e1001259, Feb. 2012, doi: 10.1371/journal.pbio.1001259.
[149] J. Grosche, V. Matyash, T. Möller, A. Verkhratsky, A. Reichenbach, and H. Kettenmann, "Microdomains for neuron–glia interaction: parallel fiber signaling to Bergmann glial cells," *Nat. Neurosci.*, vol. 2, no. 2, pp. 139–143, Feb. 1999, doi: 10.1038/5692.
[150] M. M. Halassa *et al.*, "Astrocytic modulation of sleep homeostasis and cognitive consequences of sleep loss," *Neuron*, vol. 61, no. 2, pp. 213–219, 2009, doi: 10.1016/j.neuron.2008.11.024.Astrocytic.
[151] T. Fellin *et al.*, "Endogenous nonneuronal modulators of synaptic transmission control cortical slow oscillations in vivo," *Proc. Natl. Acad. Sci.*, vol. 106, no. 35, pp. 15037–15042, Sep. 2009, doi: 10.1073/pnas.0906419106.
[152] R. J. Thompson *et al.*, "Activation of pannexin-1 hemichannels augments aberrant bursting in the hippocampus," *Science (80-.).*, vol. 322, no. 5907, pp. 1555–1559, Dec. 2008, doi: 10.1126/science.1165209.
[153] M. Eddleston and L. Mucke, "Molecular profile of reactive astrocytes — implications for their role in neurologic disease," *Neuroscience*, vol. 54, no. 1, pp. 15–36, May 1993, doi: 10.1016/0306-4522(93)90380-X.
[154] N. J. Maragakis and J. D. Rothstein, "Mechanisms of disease: astrocytes in neurodegenerative disease," *Nat. Clin. Pract. Neurol.*, vol. 2, no. 12, pp. 679–689, Dec. 2006, doi: 10.1038/ncpneuro0355.
[155] M. V. Sofroniew, "Molecular dissection of reactive astrogliosis and glial scar formation," *Trends Neurosci.*, vol. 32, no. 12, pp. 638–647, Dec. 2009, doi: 10.1016/j.tins.2009.08.002.
[156] T. Wyss-Coray and L. Mucke, "Inflammation in neurodegenerative disease—a double-edged sword," *Neuron*, vol. 35, no. 3, pp. 419–432, Aug. 2002, doi: 10.1016/S0896-6273(02)00794-8.
[157] R. M. Ransohoff, "How neuroinflammation contributes to neurodegeneration," *Science (80-.).*, vol. 353, no. 6301, pp. 777–783, Aug. 2016, doi: 10.1126/science.aag2590.
[158] I. Ferrer, "Astrogliopathy in tauopathies," *Neuroglia*, vol. 1, no. 1, pp. 126–150, Jul. 2018, doi: 10.3390/neuroglia1010010.
[159] I. Ferrer *et al.*, "Glial and neuronal tau pathology in tauopathies," *J. Neuropathol. Exp. Neurol.*, vol. 73, no. 1, pp. 81–97, Jan. 2014, doi: 10.1097/NEN.0000000000000030.
[160] K. Schindowski *et al.*, "Alzheimer's disease-like tau neuropathology leads to memory deficits and loss of functional synapses in a novel mutated tau transgenic mouse without any motor deficits," *Am. J. Pathol.*, vol. 169, no. 2, pp. 599–616, Aug. 2006, doi: 10.2353/ajpath.2006.060002.
[161] A. Maté de Gérando *et al.*, "Neuronal tau species transfer to astrocytes and induce their loss according to tau aggregation state," *Brain*, vol. 144, no. 4,

pp. 1167–1182, May 2021, doi: 10.1093/brain/awab011.
[162] S. Narasimhan *et al.*, “Pathological tau strains from human brains recapitulate the diversity of tauopathies in nontransgenic mouse brain,” *J. Neurosci.*, vol. 37, no. 47, pp. 11406–11423, Nov. 2017, doi: 10.1523/JNEUROSCI.1230-17.2017.
[163] S. Narasimhan *et al.*, “Human tau pathology transmits glial tau aggregates in the absence of neuronal tau,” *J. Exp. Med.*, vol. 217, no. 2, p. e20190783, Feb. 2020, doi: 10.1084/jem.20190783.
[164] N. Briel, K. Pratsch, S. Roeber, T. Arzberger, and J. Herms, “Contribution of the astrocytic tau pathology to synapse loss in progressive supranuclear palsy and corticobasal degeneration,” *Brain Pathol.*, vol. 31, no. 4, p. e12914, Jul. 2021, doi: 10.1111/bpa.12914.
[165] M. Sidoryk-Wegrzynowicz, Y. N. Gerber, M. Ries, M. Sastre, A. M. Tolkovsky, and M. G. Spillantini, “Astrocytes in mouse models of tauopathies acquire early deficits and lose neurosupportive functions,” *Acta Neuropathol. Commun.*, vol. 5, no. 1, p. 89, Dec. 2017, doi: 10.1186/s40478-017-0478-9.
[166] M. S. Forman, “Transgenic mouse model of tau pathology in astrocytes leading to nervous system degeneration,” *J. Neurosci.*, vol. 25, no. 14, pp. 3539–3550, Apr. 2005, doi: 10.1523/JNEUROSCI.0081-05.2005.
[167] M. J. Booth and T. Wilson, “Refractive-index-mismatch induced aberrations in single-photon and two-photon microscopy and the use of aberration correction,” *J. Biomed. Opt.*, vol. 6, no. 3, pp. 266–272, 2001, doi: 10.1117/1.1382808.
[168] F. Helmchen and W. Denk, “Deep tissue two-photon microscopy,” *Nat. Methods*, vol. 2, no. 12, pp. 932–940, Dec. 2005, doi: 10.1038/nmeth818.
[169] R. K. P. Benninger and D. W. Piston, “Two-photon excitation microscopy for the study of living cells and tissues,” *Curr. Protoc. Cell Biol.*, vol. Chapter 4, Jun. 2013, doi: 10.1002/0471143030.cb0411s59.
[170] M. Oheim, D. J. Michael, M. Geisbauer, D. Madsen, and R. H. Chow, “Principles of two-photon excitation fluorescence microscopy and other nonlinear imaging approaches,” *Adv. Drug Deliv. Rev.*, vol. 58, no. 7, pp. 788–808, Oct. 2006, doi: 10.1016/j.addr.2006.07.005.
[171] W. Denk, J. H. Strickler, and W. W. Webb, “Two-photon laser scanning fluorescence microscopy,” *Science (80-.).*, vol. 248, no. 4951, pp. 73–76, Apr. 1990, doi: 10.1126/science.2321027.
[172] M. Rubart, “Two-photon microscopy of cells and tissue,” *Circ. Res.*, vol. 95, no. 12, pp. 1154–1166, Dec. 2004, doi: 10.1161/01.RES.0000150593.30324.42.
[173] K. Takasaki, R. Abbasi-Asl, and J. Waters, “Superficial bound of the depth limit of two-photon imaging in mouse brain,” *eneuro*, vol. 7, no. 1, p. ENEURO.0255-19.2019, Jan. 2020, doi: 10.1523/ENEURO.0255-19.2019.
[174] H. Tanaka and T. Ikegami, “Social exclusion and disengagement of covert attention from social signs: the moderating role of fear of negative evaluation,” *Jpn. Psychol. Res.*, vol. 61, no. 2, pp. 133–141, Apr. 2019, doi: 10.1111/jpr.12197.
[175] V. E. Centonze and J. G. White, “Multiphoton excitation provides optical sections from deeper within scattering specimens than confocal imaging,”

Biophys. J., vol. 75, no. 4, pp. 2015–2024, Oct. 1998, doi: 10.1016/S0006-3495(98)77643-X.
[176] X. Wang *et al.*, “Astrocytic Ca2+ signaling evoked by sensory stimulation in vivo,” *Nat. Neurosci.*, vol. 9, no. 6, pp. 816–823, Jun. 2006, doi: 10.1038/nn1703.
[177] H. Hirase, L. Qian, P. Barthó, and G. Buzsáki, “Calcium dynamics of cortical astrocytic networks in vivo,” *PLoS Biol.*, vol. 2, no. 4, pp. 494–499, Apr. 2004, doi: 10.1371/journal.pbio.0020096.
[178] V. A. Romoser, P. M. Hinkle, and A. Persechini, “Detection in living cells of Ca2+-dependent changes in the fluorescence emission of an indicator composed of two green fluorescent protein variants linked by a calmodulin-binding sequence,” *J. Biol. Chem.*, vol. 272, no. 20, pp. 13270–13274, May 1997, doi: 10.1074/jbc.272.20.13270.
[179] A. Miyawaki *et al.*, “Fluorescent indicators for Ca2+based on green fluorescent proteins and calmodulin,” *Nature*, vol. 388, no. 6645, pp. 882–887, Aug. 1997, doi: 10.1038/42264.
[180] J. Nakai, M. Ohkura, and K. Imoto, “A high signal-to-noise Ca2+ probe composed of a single green fluorescent protein,” *Nat. Biotechnol.*, vol. 19, no. 2, pp. 137–141, Feb. 2001, doi: 10.1038/84397.
[181] Q. Wang, B. Shui, M. I. Kotlikoff, and H. Sondermann, “Structural basis for calcium sensing by GCaMP2,” *Structure*, vol. 16, no. 12, pp. 1817–1827, Dec. 2008, doi: 10.1016/j.str.2008.10.008.
[182] G. S. Baird, D. A. Zacharias, and R. Y. Tsien, “Circular permutation and receptor insertion within green fluorescent proteins,” *Proc. Natl. Acad. Sci.*, vol. 96, no. 20, pp. 11241–11246, Sep. 1999, doi: 10.1073/pnas.96.20.11241.
[183] T. Knöpfel, “Genetically encoded optical indicators for the analysis of neuronal circuits,” *Nat. Rev. Neurosci.*, vol. 13, no. 10, pp. 687–700, Oct. 2012, doi: 10.1038/nrn3293.
[184] M. Ohkura *et al.*, “Genetically encoded green fluorescent Ca2+ indicators with improved detectability for neuronal Ca2+ signals,” *PLoS One*, vol. 7, no. 12, p. e51286, Dec. 2012, doi: 10.1371/journal.pone.0051286.
[185] T.-W. Chen *et al.*, “Ultrasensitive fluorescent proteins for imaging neuronal activity,” *Nature*, vol. 499, no. 7458, pp. 295–300, Jul. 2013, doi: 10.1038/nature12354.
[186] R. Srinivasan *et al.*, “Ca2+ signaling in astrocytes from Ip3r2−/− mice in brain slices and during startle responses in vivo,” *Nat. Neurosci.*, vol. 18, no. 5, pp. 708–717, May 2015, doi: 10.1038/nn.4001.
[187] G. Ji *et al.*, “Ca2+-sensing transgenic mice,” *J. Biol. Chem.*, vol. 279, no. 20, pp. 21461–21468, May 2004, doi: 10.1074/jbc.M401084200.
[188] R. Srinivasan *et al.*, “New transgenic mouse lines for selectively targeting astrocytes and studying calcium signals in astrocyte processes in situ and in vivo,” *Neuron*, vol. 92, no. 6, pp. 1181–1195, Dec. 2016, doi: 10.1016/j.neuron.2016.11.030.
[189] M. Paukert, A. Agarwal, J. Cha, V. A. Doze, J. U. Kang, and D. E. Bergles, “Norepinephrine controls astroglial responsiveness to local circuit activity,” *Neuron*, vol. 82, no. 6, pp. 1263–1270, Jun. 2014, doi: 10.1016/j.neuron.2014.04.038.

[190] Y. Oe *et al.*, “Distinct temporal integration of noradrenaline signaling by astrocytic second messengers during vigilance,” *Nat. Commun.*, vol. 11, no. 1, p. 471, Dec. 2020, doi: 10.1038/s41467-020-14378-x.
[191] E. Shigetomi, S. Kracun, M. V Sofroniew, and B. S. Khakh, “A genetically targeted optical sensor to monitor calcium signals in astrocyte processes,” *Nat. Neurosci.*, vol. 13, no. 6, pp. 759–766, Jun. 2010, doi: 10.1038/nn.2557.
[192] K. Kanemaru *et al.*, “In vivo visualization of subtle, transient, and local activity of astrocytes using an ultrasensitive Ca2+ indicator,” *Cell Rep.*, vol. 8, no. 1, pp. 311–318, Jul. 2014, doi: 10.1016/j.celrep.2014.05.056.
[193] K. E. Poskanzer and R. Yuste, “Astrocytes regulate cortical state switching in vivo,” *Proc. Natl. Acad. Sci.*, vol. 113, no. 19, pp. E2675–E2684, May 2016, doi: 10.1073/pnas.1520759113.
[194] Y. Otsu *et al.*, “Calcium dynamics in astrocyte processes during neurovascular coupling,” *Nat. Neurosci.*, vol. 18, no. 2, pp. 210–218, Feb. 2015, doi: 10.1038/nn.3906.
[195] L. Ye, M. A. Haroon, A. Salinas, and M. Paukert, “Comparison of GCaMP3 and GCaMP6f for studying astrocyte Ca2+ dynamics in the awake mouse brain,” *PLoS One*, vol. 12, no. 7, p. e0181113, Jul. 2017, doi: 10.1371/journal.pone.0181113.
[196] A. Battefeld, M. A. Popovic, S. I. de Vries, and M. H. P. Kole, “High-frequency microdomain Ca2+ transients and waves during early myelin internode remodeling,” *Cell Rep.*, vol. 26, no. 1, pp. 182-191.e5, Jan. 2019, doi: 10.1016/j.celrep.2018.12.039.
[197] E. A. Pnevmatikakis and A. Giovannucci, “NoRMCorre: An online algorithm for piecewise rigid motion correction of calcium imaging data,” *J. Neurosci. Methods*, vol. 291, pp. 83–94, Nov. 2017, doi: 10.1016/j.jneumeth.2017.07.031.
[198] Y. Wang *et al.*, “FASP: a machine learning approach to functional astrocyte phenotyping from time-lapse calcium imaging data,” in *2016 IEEE 13th International Symposium on Biomedical Imaging (ISBI)*, Apr. 2016, pp. 351–354, doi: 10.1109/ISBI.2016.7493281.
[199] S. J. Guzman, A. Schlögl, and C. Schmidt-Hieber, “Stimfit: quantifying electrophysiological data with Python,” *Front. Neuroinform.*, vol. 8, p. 16, 2014, doi: 10.3389/fninf.2014.00016.
[200] Y. Wang *et al.*, “SynQuant: an automatic tool to quantify synapses from microscopy images,” *Bioinformatics*, vol. 36, no. 5, pp. 1599–1606, Mar. 2020, doi: 10.1093/bioinformatics/btz760.
[201] T. Ishihara *et al.*, “Age-dependent emergence and progression of a tauopathy in transgenic mice overexpressing the shortest human tau isoform,” *Neuron*, vol. 24, no. 3, pp. 751–762, Nov. 1999, doi: 10.1016/S0896-6273(00)81127-7.
[202] J.-P. Brion, G. Tremp, and J.-N. Octave, “Transgenic expression of the shortest human tau affects its compartmentalization and its phosphorylation as in the pretangle stage of Alzheimer’s disease,” *Am. J. Pathol.*, vol. 154, no. 1, pp. 255–270, Jan. 1999, doi: 10.1016/S0002-9440(10)65272-8.
[203] E. Dassie *et al.*, “Focal expression of adeno-associated viral-mutant tau

induces widespread impairment in an APP mouse model," *Neurobiol. Aging*, vol. 34, no. 5, pp. 1355–1368, May 2013, doi: 10.1016/j.neurobiolaging.2012.11.011.
[204] S. Wegmann *et al.*, "Removing endogenous tau does not prevent tau propagation yet reduces its neurotoxicity," *EMBO J.*, vol. 34, no. 24, pp. 3028–3041, Dec. 2015, doi: 10.15252/embj.201592748.
[205] K. Eckermann *et al.*, "The β-propensity of tau determines aggregation and synaptic loss in inducible mouse models of tauopathy," *J. Biol. Chem.*, vol. 282, no. 43, pp. 31755–31765, Oct. 2007, doi: 10.1074/jbc.M705282200.
[206] S. Maeda *et al.*, "Expression of A152T human tau causes age-dependent neuronal dysfunction and loss in transgenic mice," *EMBO Rep.*, vol. 17, no. 4, pp. 530–551, Apr. 2016, doi: 10.15252/embr.201541438.
[207] Z. He *et al.*, "Transmission of tauopathy strains is independent of their isoform composition," *Nat. Commun.*, vol. 11, no. 1, p. 7, 2020, doi: 10.1038/s41467-019-13787-x.
[208] K. Richetin *et al.*, "Tau accumulation in astrocytes of the dentate gyrus induces neuronal dysfunction and memory deficits in Alzheimer's disease," *Nat. Neurosci.*, vol. 23, no. 12, pp. 1567–1579, Dec. 2020, doi: 10.1038/s41593-020-00728-x.
[209] P. Wang and Y. Ye, "Astrocytes in neurodegenerative diseases: a perspective from tauopathy and α-synucleinopathy," *Life*, vol. 11, no. 9, p. 938, Sep. 2021, doi: 10.3390/life11090938.
[210] K. Y. Chan *et al.*, "Engineered AAVs for efficient noninvasive gene delivery to the central and peripheral nervous systems," *Nat. Neurosci.*, vol. 20, no. 8, pp. 1172–1179, Aug. 2017, doi: 10.1038/nn.4593.
[211] R. C. Challis *et al.*, "Systemic AAV vectors for widespread and targeted gene delivery in rodents," *Nat. Protoc.*, vol. 14, no. 2, pp. 379–414, Feb. 2019, doi: 10.1038/s41596-018-0097-3.
[212] K. V Kuchibhotla, C. R. Lattarulo, B. T. Hyman, and B. J. Bacskai, "Synchronous hyperactivity and intercellular calcium waves in astrocytes in Alzheimer mice," *Science (80-.).*, vol. 323, no. 5918, pp. 1211–1215, Feb. 2009, doi: 10.1126/science.1169096.
[213] T. Takano, H. X, D. R, Z. B, and M. Nedergaard, "Two-photon imaging of astrocytic Ca2+ signaling and the microvasculature in experimental mice models of Alzheimer's disease," *Ann. N. Y. Acad. Sci.*, vol. 1097, no. 1, pp. 40–50, Feb. 2007, doi: 10.1196/annals.1379.004.
[214] L. Brambilla, F. Martorana, and D. Rossi, "Astrocyte signaling and neurodegeneration," *Prion*, vol. 7, no. 1, pp. 28–36, Jan. 2013, doi: 10.4161/pri.22512.
[215] R. Piacentini *et al.*, "Reduced gliotransmitter release from astrocytes mediates tau-induced synaptic dysfunction in cultured hippocampal neurons," *Glia*, vol. 65, no. 8, pp. 1302–1316, Aug. 2017, doi: 10.1002/glia.23163.
[216] E. H. Bigio *et al.*, "Cortical synapse loss in progressive supranuclear palsy," *J. Neuropathol. Exp. Neurol.*, vol. 60, no. 5, pp. 403–410, May 2001, doi: 10.1093/jnen/60.5.403.
[217] B. R. Hoover *et al.*, "Tau mislocalization to dendritic spines mediates synaptic dysfunction independently of neurodegeneration," *Neuron*, vol. 68,

no. 6, pp. 1067–1081, Dec. 2010, doi: 10.1016/j.neuron.2010.11.030.
[218] J. S. Jackson *et al.*, “Altered synapse stability in the early stages of tauopathy,” *Cell Rep.*, vol. 18, no. 13, pp. 3063–3068, Mar. 2017, doi: 10.1016/j.celrep.2017.03.013.
[219] B. Dejanovic *et al.*, “Changes in the synaptic proteome in tauopathy and rescue of tau-induced synapse loss by C1q antibodies,” *Neuron*, vol. 100, no. 6, pp. 1322–1336, Dec. 2018, doi: 10.1016/j.neuron.2018.10.014.
[220] W. R. Bevan-Jones *et al.*, “Neuroinflammation and protein aggregation co-localize across the frontotemporal dementia spectrum,” *Brain*, vol. 143, no. 3, pp. 1010–1026, Mar. 2020, doi: 10.1093/brain/awaa033.
[221] Y.-R. Zhang *et al.*, “Peripheral immunity is associated with the risk of incident dementia,” *Mol. Psychiatry*, pp. 10.1038/s41380-022-01446–5, Jan. 2022, doi: 10.1038/s41380-022-01446-5.
[222] S. Köglsberger *et al.*, “Gender-specific expression of ubiquitin-specific peptidase 9 modulates tau expression and phosphorylation: possible implications for tauopathies,” *Mol. Neurobiol.*, vol. 54, no. 10, pp. 7979–7993, Dec. 2017, doi: 10.1007/s12035-016-0299-z.
[223] I. Farhy-Tselnicker and N. J. Allen, “Astrocytes, neurons, synapses: a tripartite view on cortical circuit development,” *Neural Dev.*, vol. 13, no. 1, p. 7, Dec. 2018, doi: 10.1186/s13064-018-0104-y.
[224] E. M. Ullian, S. K. Sapperstein, K. S. Christopherson, and B. A. Barres, “Control of synapse number by glia,” *Science (80-.).*, vol. 291, no. 5504, pp. 657–661, Jan. 2001, doi: 10.1126/science.291.5504.657.
[225] W. C. Risher *et al.*, “Astrocytes refine cortical connectivity at dendritic spines,” *Elife*, vol. 3, pp. 1–24, Dec. 2014, doi: 10.7554/eLife.04047.
[226] H. Kucukdereli *et al.*, “Control of excitatory CNS synaptogenesis by astrocyte-secreted proteins Hevin and SPARC,” *Proc. Natl. Acad. Sci.*, vol. 108, no. 32, pp. E440–E449, Aug. 2011, doi: 10.1073/pnas.1104977108.
[227] N. Haruyama, A. Cho, and A. B. Kulkarni, “Overview: engineering transgenic constructs and mice,” *Curr. Protoc. Cell Biol.*, vol. Chapter 19, Mar. 2009, doi: 10.1002/0471143030.cb1910s42.
[228] J. Götz *et al.*, “Somatodendritic localization and hyperphosphorylation of tau protein in transgenic mice expressing the longest human brain tau isoform,” *EMBO J.*, vol. 14, no. 7, pp. 1304–1313, 1995, doi: 10.1002/j.1460-2075.1995.tb07116.x.
[229] M. Ramsden, “Age-dependent neurofibrillary tangle formation, neuron loss, and memory impairment in a mouse model of human tauopathy (P301L),” *J. Neurosci.*, vol. 25, no. 46, pp. 10637–10647, Nov. 2005, doi: 10.1523/JNEUROSCI.3279-05.2005.
[230] K. SantaCruz *et al.*, “Tau suppression in a neurodegenerative mouse model improves memory function,” *Science (80-.).*, vol. 309, no. 5733, pp. 476–481, Jul. 2005, doi: 10.1126/science.1113694.
[231] S. Oddo *et al.*, “Triple-transgenic model of Alzheimer’s disease with plaques and tangles,” *Neuron*, vol. 39, no. 3, pp. 409–421, Jul. 2003, doi: 10.1016/S0896-6273(03)00434-3.
[232] F. Denk and R. Wade-Martins, “Knock-out and transgenic mouse models of tauopathies,” *Neurobiol. Aging*, vol. 30, no. 1, pp. 1–13, Jan. 2009, doi: 10.1016/j.neurobiolaging.2007.05.010.

[233] R. L. Klein, R. D. Dayton, J. B. Tatom, C. G. Diaczynsky, and M. F. Salvatore, “Tau expression levels from various adeno-associated virus vector serotypes produce graded neurodegenerative disease states,” *Eur. J. Neurosci.*, vol. 27, no. 7, pp. 1615–1625, Apr. 2008, doi: 10.1111/j.1460-9568.2008.06161.x.
[234] T. Vogels, G. Vargova, P. Majerova, and T. Hromadka, “AAV vectors to study the functional consequences of neuronal and astrocytic tau pathology using in vivo 2-photon imaging,” *Alzheimer’s Dement.*, vol. 16, no. S3, pp. 1–2, Dec. 2020, doi: 10.1002/alz.042199.
[235] D. Shcherbo *et al.*, “Far-red fluorescent tags for protein imaging in living tissues,” *Biochem. J.*, vol. 418, no. 3, pp. 567–574, Mar. 2009, doi: 10.1042/BJ20081949.
[236] G. Šimić *et al.*, “Tau protein hyperphosphorylation and aggregation in Alzheimer’s disease and other tauopathies, and possible neuroprotective strategies,” *Biomolecules*, vol. 6, no. 1, p. 6, Jan. 2016, doi: 10.3390/biom6010006.
[237] T. J. Malia *et al.*, “Epitope mapping and structural basis for the recognition of phosphorylated tau by the anti-tau antibody AT8,” *Proteins Struct. Funct. Bioinforma.*, vol. 84, no. 4, pp. 427–434, Apr. 2016, doi: 10.1002/prot.24988.
[238] C. Kersaitis, G. M. Halliday, and J. J. Kril, “Regional and cellular pathology in frontotemporal dementia: relationship to stage of disease in cases with and without Pick bodies,” *Acta Neuropathol.*, vol. 108, no. 6, pp. 515–523, Dec. 2004, doi: 10.1007/s00401-004-0917-0.
[239] H. Asai *et al.*, “Depletion of microglia and inhibition of exosome synthesis halt tau propagation,” *Nat. Neurosci.*, vol. 18, no. 11, pp. 1584–1593, Nov. 2015, doi: 10.1038/nn.4132.
[240] S. Saman *et al.*, “Exosome-associated tau is secreted in tauopathy models and is selectively phosphorylated in cerebrospinal fluid in early Alzheimer disease,” *J. Biol. Chem.*, vol. 287, no. 6, pp. 3842–3849, Feb. 2012, doi: 10.1074/jbc.M111.277061.
[241] M. S. Fiandaca *et al.*, “Identification of preclinical Alzheimer’s disease by a profile of pathogenic proteins in neurally derived blood exosomes: a case-control study,” *Alzheimer’s Dement.*, vol. 11, no. 6, pp. 600–607, Jun. 2015, doi: 10.1016/j.jalz.2014.06.008.
[242] J. E. Simpson *et al.*, “Microarray analysis of the astrocyte transcriptome in the aging brain: relationship to Alzheimer’s pathology and APOE genotype,” *Neurobiol. Aging*, vol. 32, no. 10, pp. 1795–1807, Oct. 2011, doi: 10.1016/j.neurobiolaging.2011.04.013.
[243] E. Shigetomi, K. Saito, F. Sano, and S. Koizumi, “Aberrant calcium signals in reactive astrocytes: a key process in neurological disorders,” *Int. J. Mol. Sci.*, vol. 20, no. 4, p. 996, Feb. 2019, doi: 10.3390/ijms20040996.
[244] A. Araque, G. Carmignoto, P. G. Haydon, S. H. R. Oliet, R. Robitaille, and A. Volterra, “Gliotransmitters travel in time and space,” *Neuron*, vol. 81, no. 4, pp. 728–739, Feb. 2014, doi: 10.1016/j.neuron.2014.02.007.
[245] M. Arizono *et al.*, “Structural basis of astrocytic Ca2+ signals at tripartite synapses,” *Nat. Commun.*, vol. 11, no. 1, p. 1906, Dec. 2020, doi: 10.1038/s41467-020-15648-4.

[246] P. Bezzi *et al.*, “Astrocytes contain a vesicular compartment that is competent for regulated exocytosis of glutamate,” *Nat. Neurosci.*, vol. 7, no. 6, pp. 613–620, Jun. 2004, doi: 10.1038/nn1246.
[247] M. Santello and A. Volterra, “Synaptic modulation by astrocytes via Ca2+-dependent glutamate release,” *Neuroscience*, vol. 158, no. 1, pp. 253–259, Jan. 2009, doi: 10.1016/j.neuroscience.2008.03.039.
[248] C. Rakers and G. C. Petzold, “Astrocytic calcium release mediates peri-infarct depolarizations in a rodent stroke model,” *J. Clin. Invest.*, vol. 127, no. 2, pp. 511–516, Dec. 2016, doi: 10.1172/JCI89354.
[249] L. Xing, T. Yang, S. Cui, and G. Chen, “Connexin hemichannels in astrocytes: role in CNS disorders,” *Front. Mol. Neurosci.*, vol. 12, no. February, pp. 1–10, Feb. 2019, doi: 10.3389/fnmol.2019.00023.
[250] A. S. Lapato and S. K. Tiwari-Woodruff, “Connexins and pannexins: at the junction of neuro-glial homeostasis & disease,” *J. Neurosci. Res.*, vol. 96, no. 1, pp. 31–44, Jan. 2018, doi: 10.1002/jnr.24088.
[251] Y. Fujii, S. Maekawa, and M. Morita, “Astrocyte calcium waves propagate proximally by gap junction and distally by extracellular diffusion of ATP released from volume-regulated anion channels,” *Sci. Rep.*, vol. 7, no. 1, p. 13115, Dec. 2017, doi: 10.1038/s41598-017-13243-0.
[252] M. O. K. Enkvist and K. D. McCarthy, “Activation of protein kinase C blocks astroglial gap junction communication and inhibits the spread of calcium waves,” *J. Neurochem.*, vol. 59, no. 2, pp. 519–526, Aug. 1992, doi: 10.1111/j.1471-4159.1992.tb09401.x.
[253] J. I. Nagy, W. Li, E. L. Hertzberg, and C. A. Marotta, “Elevated connexin43 immunoreactivity at sites of amyloid plaques in Alzheimer’s disease,” *Brain Res.*, vol. 717, no. 1–2, pp. 173–178, Apr. 1996, doi: 10.1016/0006-8993(95)01526-4.
[254] A. Kawasaki *et al.*, “Modulation of connexin 43 in rotenone-induced model of Parkinson’s disease,” *Neuroscience*, vol. 160, no. 1, pp. 61–68, 2009, doi: 10.1016/j.neuroscience.2009.01.080.
[255] J. A. Orellana *et al.*, “Amyloid-induced death in neurons involves glial and neuronal hemichannels,” *J. Neurosci.*, vol. 31, no. 13, pp. 4962–4977, Mar. 2011, doi: 10.1523/JNEUROSCI.6417-10.2011.
[256] E. Decrock *et al.*, “Calcium and connexin-based intercellular communication, a deadly catch?,” *Cell Calcium*, vol. 50, no. 3, pp. 310–321, Sep. 2011, doi: 10.1016/j.ceca.2011.05.007.
[257] A. S. Thrane *et al.*, “General anesthesia selectively disrupts astrocyte calcium signaling in the awake mouse cortex,” *Proc. Natl. Acad. Sci.*, vol. 109, no. 46, pp. 18974–18979, Nov. 2012, doi: 10.1073/pnas.1209448109.
[258] N. A. Oberheim *et al.*, “Uniquely hominid features of adult human astrocytes,” *J. Neurosci.*, vol. 29, no. 10, pp. 3276–3287, Mar. 2009, doi: 10.1523/JNEUROSCI.4707-08.2009.
[259] H. Phatnani and T. Maniatis, “Astrocytes in neurodegenerative disease,” *Cold Spring Harb. Perspect. Biol.*, vol. 7, no. 6, p. a020628, Jun. 2015, doi: 10.1101/cshperspect.a020628.
[260] M. Olabarria, H. N. Noristani, A. Verkhratsky, and J. J. Rodríguez, “Concomitant astroglial atrophy and astrogliosis in a triple transgenic animal model of Alzheimer’s disease,” *Glia*, vol. 58, no. 7, pp. 831–838,

2010, doi: 10.1002/glia.20967.
[261] H. Braak, M. Sastre, and K. Del Tredici, “Development of α-synuclein immunoreactive astrocytes in the forebrain parallels stages of intraneuronal pathology in sporadic Parkinson’s disease,” *Acta Neuropathol.*, vol. 114, no. 3, pp. 231–241, Aug. 2007, doi: 10.1007/s00401-007-0244-3.
[262] A. Duquette, C. Pernègre, A. Veilleux Carpentier, and N. Leclerc, “Similarities and differences in the pattern of tau hyperphosphorylation in physiological and pathological conditions: impacts on the elaboration of therapies to prevent tau pathology,” *Front. Neurol.*, vol. 11, p. 607680, Jan. 2021, doi: 10.3389/fneur.2020.607680.

8 Publications

List of Publications

Briel N, Ruf Viktoria C, **Pratsch K**, Roeber S, Mielke J, Dorostkar MM, Windl O, Arzberger T, Herms J, Struebing F L. Single-Nucleus Chromatin Accessibility profiling Highlights Distinct Astrocyte Signatures in Progressive Supranuclear Palsy and Corticobasal Degeneration. *Acta Neuropathol.* 144(4):615-635 (2022)

Briel N, **Pratsch K**, Roeber S, Arzberger T, Herms J. Contribution of the astrocytic tau pathology to synapse loss in progressive supranuclear palsy and corticobasal degeneration. *Brain Pathol.* 31(4):e12914 (2021)

Peters F, Salihoglu H, **Pratsch K**, Herzog E, Pigoni M, Sgobio C, Lichtenthaler SF, Neumann U, Herms J. Tau deletion reduces plaque-associated BACE1 accumulation and decelerates plaque formation in a mouse model of Alzheimer's disease. *EMBO J.* 38(23):e102345 (2019)

Manuscripts in preparation

Pratsch K, Unemura C, Ito M, Horiguchi N, Herms J. Novel BACE1 selective Inhibitor does not affect synaptic plasticity *in vivo*. (*in preparation*)

Conference poster participation

Briel N, **Pratsch K**, Roeber S, Arzberger T, Herms J. Synapse Loss in Progressive Supranuclear Palsy and Corticobasal Degeneration and the Role of Astrocytic Tau. *XV European Meeting on Glial Cells in Health and Disease 2021, Marseille, France.*

Pratsch K, Peters F, Slapakova L, Arzberger T, Dorostkar M, Herms J. The role of plaque associated axonal pathology for the progression of Alzheimer's disease. *ADPD 2018, Lisbon, Portugal.*

Batawi A, **Pratsch K**., Hummel T. Development and plasticity of the Drosophila CO_2 circuitry. *Axon 2015, IST Klosterneuburg, Austria.*

9 Curriculum Vitae

Der Lebenslauf wurde aus der elektronischen Fassung entfernt

10 Acknowledgements

First of all, I would like to cordially thank Prof. Dr. Jochen Herms, for constantly supporting me throughout my journey as a doctoral student. I am very grateful for his guidance, scientific advice and discussions that have raised new interesting research ideas.

Further, I want to thank my doctoral father Prof. Dr. Heinrich Leonhardt, for fruitful discussions during the TAC meetings and for agreeing to represent this thesis at the faculty of biology. I also want to thank Dr. Sabina Tahirovic for being part of the TAC and her interest in my research topic and all members of the thesis defense committee for their time and effort.

Another thanks goes to some colleagues of AG Herms and DZNE that helped and supported me in all aspects: Dr. Paul Feyen, who was always a great motivator and supporter, and who came up with new ideas to further push this interesting research topic. Gian Marco Calandra, who helped a lot with the Ca^{2+} analysis and his expertise. Tanja, Rachele, Carmelo, Severin, Nils, Anna, Laura SM, Laura TG, Pri, Fumi, and Tharshika for their friendship, nice coffee breaks, our barbeque parties, chats, laughter and a positive environment. A special thanks to Jose, my lab mate and partner in crime. I am very grateful to have met you from the beginning. We could bond our friendship in a very special way, it was always fun with you, in the lab and also outside. Thank you for always being there for me in all those times, for our jokes and insiders, our spanish conversations and special songs from our “favorite” singers.

I am grateful for all fellow Marie Curie colleagues of SYNDEGEN. It was a very nice and positive experience with you, which involved gaining a lot of new expertise, exploring other laboratories, having nice chats and going out together, but especially for creating a positive network environment. I further want to thank all animal caretakers from the ZNP as well as Gerda and Hannah, for their veterinary expertise and nice discussions.

During my time here in Munich I am truly blessed to have met many fantastic people and made new friends. I am especially grateful for Tanja, Martin and Julia from the Austrian in Munich expats, for having very nice evenings together and helping me to get settled in a foreign country. Without you, this city would be different. A big thanks goes to my friends Elli, Berndi, Agnes and Sarah. You are such amazing people, I am happy to have you in my life. Thank you for always cheering me up in hard times, for finding new motivation and for your true friendship. Simon, I am very grateful to have met you. Thank you for always being there for me, supporting me in all needs and sharing your knowledge how to get through all ups and downs of PhD life.

Finally, I want to express my deepest gratitude to my parents and my brother, for their constant support and their unconditional love. I am really happy to have such a supporting family, thank you for always believing in me.